An analysis on the circuit breaking phenomenon of High-Temperature Superconductor Circuit Breaker (HTSCB)

Muhammad Aasim Ullah

A thesis submitted to

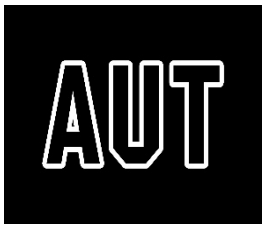

School of Engineering, Computer & Mathematical Sciences,

Auckland University of Technology (AUT), Auckland,

New Zealand.

In fulfilment of the requirements for the degree of

Doctor of Philosophy (PhD)

February 2018

School of Engineering

TABLE OF CONTENTS

LIST OF FIGURES

LIST OF TABLES

ATTESTATION OF AUTHORSHIP

"I hereby declare that this report is my sole work and to the top of my belief and knowledge, it comprises no material formerly published or composed by another individual (with the exception of where explicitly defined in the text and acknowledgements), nor material which to significant extent has been submitted for the award of any other degree or diploma of a university or other institution of higher learning.

I understand that my thesis may be available to others electronically."

……

(Muhammad Aasim Ullah)

February' 2018

ACKNOWLEDGEMENTS

In the name of Allah, the Most Merciful, the Most Beneficent

"*He who does not thank people, does not thank Allah*" – this a saying from beloved Prophet (peace be upon him). As I am closing the chapter of my PhD life, I humbly remember all those teachers who taught me even a word in my entire student life. I am very grateful to many people and organisations for their generous support and encouragement that has made it possible for me to undertake this work.

I would like to exhibit my first appreciation, debt and gratitude to my supervisors, Prof. Tek Tjing Lie, Dr. Kosala Gunawardane, and Associate Professor N.K.C. Nair for their caring direction, patience, kind assistance and ceaseless support all over my study period at AUT. I would also like to express my thanks to my colleagues and lab technicians for their technical and moral support throughout the journey. The research at AUT opens for me a new professional contacts and friends worldwide in academia. I am grateful for providing me this wonderful opportunity.

Brothers in same faith from home and abroad whose ceaseless prayer always has given me more than my expectation. Special thanks to all my friends at the department for their assistance and support for proof reading. Two names are worthy to be mentioned: Dr. Miftah and Sayedus Salehin. The accompany of AUT Chaplain- Sheikh Rafat Najm and his teams: New Muslim Projects and Al-Hikmah Boys from AUT Masjid was a complete new experience for me. The wonderful faces, places and time will greatly be missed.

Last but most importantly, I am inexpressibly thankful to my wonderful family for everything. The unconditional love and support of my dearest wife: Mashreka Binte Shams and the coming of ‘little 3 weeks kid’ Aisha Mabrura has always been the driven force to submit my thesis in 2 year 8 months. Heartfelt gratefulness also goes to my mother, deceased father and to my in laws’ parents

and family. You all make me who I am. Finally, to my family, spread far and wide, I express my deep-felt thanks and love to you all for your unfailing love and support, not only during this project, but during my staying in Auckland these past years. Thousand thanks and gratitude to all of you for taking care of my tons of responsibility back in home for past 3 years.

On the very last line, I remember my deceased elder brother, who returned to another world ten years back. Its him who always taught me to think bigger.

July 2018, Auckland. **Muhammad Aasim Ullah**

ABSTRACT

Development of High-Temperature Superconductor (HTS) materials in recent years has raised interest in carrying out novel research work of HTS application in power technology. Despite HTS solutions are said to provide better power system stability benefits, the integrity and operation of HTSCB yet need to be well investigated and validated by means of its appropriate modelling in power system distribution network. In this research, the technical characteristics of HTSCB is determined by one of the basic arc model theories. The further experiments are designated to analyze the performance of future HTSCB.

The performance of HTSCB is designed by developing an HTS arc model. This is the most complex, challenging and important aspect of this research. The parameters of arc model should precisely be set before any effort is carried out to analyze its behaviour in a distribution network under a variety of fault circumstances. Simulation studies are conducted to show the electrical arc characteristics of HTSCB under the high current condition. The arc model can then be inserted in different network models and analyzed for numerous system loading with over current situations and for different HTS applications. The modelling is executed on a single-phase distribution network model. The limitations of the conventional arc models for HTS application are briefly discussed in this study from the simulation study. The scope of further development of HTS arc model is also identified.

The developed arc model is later used to mitigate the residual flux problem of HTS Transformer. The inrush current of an HTS transformer can rise ten times

higher than the rated current. The inrush current also exist a longer period of time comparing to short-circuit current. The repeated switching of HTS transformer is a big concern for its superconductivity. HTS arc model with HTS transformer is investigated for different fault interruption methods. During the process, the residual flux of HTS transformer is mitigated at the minimum operating time.

Finally, the design and experimental validation of arcing phenomenon in cryogenic arc chamber is investigated. A comprehensive analysis of flow field and numerical solution in cryogenic arc chamber is analyzed to observe the magnetic field in cryogenic arc chamber. The results of HTSCB and its arc model promises a novel circuit breaking phenomenon. The simulation results show the benefits of less pre-striking effect to use in HTS machines in Alternative Current (AC) applications and experimental result validate the result of arc model. The overall investigations show that the significant geometrical parameters of arc chamber and breaker contacts need to be optimized to improve the performance of HTSCB. The detailed analysis of flow separation, losses, its origin and minimized electrical field strength in short circuit condition help the design to improve its flow field and efficiency.

LIST OF SYMBOLS AND ABBREVIATIONS

θ	- Voltage-phase
	- Arc time constant
$\emptyset$	Power factor angle during short-circuit situation
$\emptyset_L$	Core flux
$\emptyset_m$	Maximum flux
$\emptyset_r$	Residual flux
Ψ	Electron system order
σ	Electrical conductivity
σ_B	Stefan Bolzmann's constant
$\sigma_{i,j}(T,P)$	Cold medium conductivity
γ	Phase angle on phase voltage when fault initiated
τ_1	Arc-time constant
τ_c, τ_m	Time constant of Cassie and Mayr model
ω (t)	Window function
α ,β	Constants of the arcs
η, η_l	Molecular and turbulent viscosity correspondingly
ρ	Cold medium density
ρ_{arc}	Mass density
υ	Reluctivity
a,b	Dependency of power loss and arc time constant on the arc conductance
f	Power system (fundamental) frequency
g	Arc conductance (Siemens) of the electric arc

h_{enth1}, h_{enth2}	Enthalpy of inner and outer surface of arc chamber
h_0	Total enthalpy
i(t)	- Arc current (Ampere)
	-Instant interrupting current
i_φ	Magnetize current
k_t	Turbulent thermal conductivity
l_{arc}	Arc length
p_{arc}	Arc pressure
r_{arc}	Arc radius
t	Time constant (seconds)
t_{pk}	Time when TRV grows as first peak
V	Radial velocity
Cs, C_L	Capacitence of source and load side respectively
$G_{i,j}$	Conductivity value of HTS
$\sum_{k=1}^{n} G_{i,k}$	Total conductivity value
I_{SC1},I_{SC2}	Fault currents
I_{HTS}/I_{SC}	Rated breaking
I_F	Steady-state fault current
I_{ss}	Total fault current
J	Current density of exciting current
K	- Kelvin
	- Ratio of fault current to rated short circuit current
K_3	Correction factor inrush-decay

L	Fault inductance
L_1	Inductance in primary side
L_s	Inductance in source side
N	Finite rate of energy loss
N1	Number of turn
P	- Arc power loss (Watts) - Pressure
Q	Energy storage capacity
P_{axial}	Power loss for axial mass flow
P_{in}	Supplied power
P_{loss}	Power loss due to turbulence of arcing
P_{net}	Net power of the arc
P_{out}	Transported power by radiation and cooling
P_{rad}	Power loss due to radiation or radial mass flow
P_0	Dissipated power at current passing through zero
R	- Arc/Fault resistance - Total resistance of system resistance and transformer winding resistance
Rs	Resistance of source
T_{arc}	Arc temperature
T_d	TRV-time delay
T_d	Time to reach to peak
T1 ,T2	Oscillation period of the capacitor voltage in the source side
U_{pk}	Peak voltage

U_{rms}	Root mean square (rms) value of voltage
U_s	Source power
u	- Arc voltage
	-Axial velocity
u_{avg_arc}	Average arc voltage in high current range
Vz ,Vr	represents the axial and radial velocity respectively
v(t)	Arc voltage (kV)
V_{arc}	Volume of the arc
W_{con}	Convection value
X(τ,ω)	Fundamental for Fourier Transform
ABB	Asea Brown Boveri Ltd
AC	Alternating current
BCS	Bardeen–Cooper–Schrieffer theory
CBs	Circuit breakers
CFD	Computational Fluid Dynamics
DC	Direct current
EMF	Electromotive force
FCL	Fault Current Limiter
FEM	Finite Element Method
HTS	High-Temperature Superconductor
HTSCB	High-Temperature Superconductor Circuit breaker
HVDC	High voltage direct current
LN	Liquid Nitrogen
LTE	Local Thermodynamic Equilibrium
MMF	Magneto-Motive Force

MTTF	Mean Time to Failure
MTTM	Mean Time to Maintenance
MTTR	Mean Time to Repair
RMS	Root mean square
RRRV	Rate of Rise of Recovery Voltage
SCCB	Superconducting Cable embedded high power Circuit Breaker
SCCL	Superconducting Current Limiters
SLF	Short Line Fault
TCR	Thermal Contact Resistance
TMF	Transverse magnetic field
TRV	Transient recovery voltage
VCB	Vacuum circuit breaker

CHAPTER 1- INTRODUCTION

This introductory chapter presents a brief overview of the thesis, motivation, scope, and numerous contributions.

1.1 CONTEXT

The physics behind High-Temperature Superconductivity (HTS) technology in power industry was mainly explored during 21st century. HTS has the prospect to convey fundamental change to electric power advances. Currently, the transmission and distribution of electricity are on course of its stunning advancement. Superconductivity is replacing copper electrical conductors with a ceramic superconducting alternative. The rationale is its significant efficiency of eliminating resistive losses. HTS based cables, transformers, wind turbine generators and Fault Current Limiters (FCL) are reported to be well developed and precisely validated in last few years. A potential research of a circuit breaker for HTS application is therefore highly relevant and impactful in the context of additional development of HTS implementation pathway.

Superconducting solutions have encountered challenges since its very beginning. It has always been a complicated process with AC applications. Disconnecting the breaker section quickly and isolating the problem is possibly the simplified solution of a high voltage breaker. Otherwise, the rest of the superconductors of different machines might be badly damaged.

1.2 BACKGROUND AND MOTIVATION

1.2.1 The Trend of HTS research in New Zealand

HTS based research has extensive historical record of executing successful projects in New Zealand. The research follows HTS applications development with the $Bi_2Sr_2Ca_2Cu_3O_{10+x}$ (Bi-2223) or first generation (1G) HTS material [1,2] and existing commercial delivery of HTS magnets, methods, strategies, techniques and components through the superconducting companies (General Cable Superconductors Ltd, HTS-110 Ltd etc.) supported by a comprehensive local supply chain. Since 1987 to date several significant research on HTS technologies in New Zealand are being led by Industrial Research Ltd. (IRL) and Robinson Research Institute of Victoria University of Wellington [3].

1.2.2 The need of a potential HTS breaker

HTS was introduced first by Alex Muller and Georg Bednorz in 1986 [4]. Since then it has been used for several innovative prospects. The practical application of superconductivity is reported to be applied in numerous electrical power machines like transformers [5-6], wind generators [7-8], cables [9-10], current limiters [11-12], etc. In high current condition, the superconductivity of these HTS machines is damaged. The damage happens due to the re-strike (pre-strike and post arc) effect during arcing. Semiconductors based breaker can be used for these HTS machines. However, it generates a large transfer loss.

A breaker made of HTS material can bring the advantage of similar material contact resistance for other HTS machines. In this thesis, the feasibility of HTSCB is investigated with high critical current and low AC loss. The coolant arc medium liquid nitrogen is proposed as electrical insulation. Liquid nitrogen in these cases

is used as effective as the insulation oil in HTS application [13]. The HTS contact properties of reduced refrigeration cost and greater reliability overcomes the constraints in many HTS application, especially for the transformer [14].

To control a breaker in AC application is a big challenge. Moreover, when the period of arcing is longer it harms the superconductivity of HTS equipment very easily. For HTS equipment issue, the point of maintenance and disconnection are more crucial for cryogenic concern. Basically, this is where the concept of HTS breakers come in either as hybrid or non-hybrid breaker. The breaker may combine to redirect any surge in current and then shut it off which can be a series of mechanical and electronic circuit breaking devices as well. The unit should be capable of stopping a surge equivalent to the form that the breaking time should significantly less than the blink of an eye.

It is found that large AC loss is generated for HTS machines. It demands of time to think of a smart solution in order to overcome these boundaries. Only HTS breaker can easily overcome the contact-resistance obstacle. If it is hybrid HTS breaker then the conduction losses are expected to be much marginal. A successful research for HTS Ultra-fast current interruption possibly can lead to future company production.

Functionally, the HTSCB can combine with the functions of superconducting cables, FCL and circuit breakers to form a Superconducting Cable embedded high power Circuit Breaker (SCCB). The SCCB will thereby offer zero to near zero resistance to the flow of electrical current, which can reduce losses to the minimum (almost no loss) improving the overall system efficiency and also ensure

that it will effectively break during circuit emergencies. The arc in breaker usually starts from its conducting surface. The usage of Liquid Nitrogen (LN) can reduce the temperature of arcing region of HTS breaker. Unlike existing circuit breakers technologies, HTSCB is expected to make the interruption at millisecond range in cold medium. It has the usual feature of overcoming the limitations of operating speed for HTS applications. One of the downsides of this technology is its AC loss. For the losses in an HTS machine more energy is essential in order to preserve the required temperature of the cryostat. The magnetic field in an HTS machine increases the superconductor losses in addition to reducing the critical current [15]. However, for a hybrid HTS breaker, the conduction losses are expected to be marginal. Thereby, the possibility of realizing an HTS ultra-fast current interruption has a higher potential for future applications.

1.3 RATIONALE AND SIGNIFICANCE

The physics of HTS has been extensively studied and used as commercial prototypes during the 21st century. Recently, there has been growing interest amongst researchers on the use of HTS for power system equipment developments. The major difficulty in design and development of HTSCB is its short circuit withstand capability of the contacts, especially during fault recovery and during arcing for high current endurance. Emergency detection and its immediate solution are crucial to ensure quality control of sound protection-scheme. The HTSCB can be an emerging technology which can reduce the quenching to a great extent for any short, medium and high range transmissions. It can be a solution not only for HTS equipment but also can replace other conventional breakers including automated real-time interruption. Therefore, it is a new research area with enormous possibilities.

The thesis utilizes standard design parameters for a developed HTS arc model. The research evolves with the development of the prescribed arc model. The variation of electrical characteristics of the HTS arc model for different condition and scenarios is simulated in order to establish its efficacy. The HTS arc model is mainly investigated in this thesis for a simple distribution network. Investigations are executed further to inspect the efficiency of the HTS arc model for an HTS transformer in high current endurance condition. The performance is validated by a small-scale test bed scheme. During the preliminary simulation process, several situations are monitored under cryogenic environment. The simulation results showed the proposed HTSCB has immense potential to be implemented for numerous applications.

1.4 THESIS OBJECTIVES

Based on the research and literature review, the main focus of the entire research is based on the analysis of the circuit breaking phenomenon of HTSCB. Therefore, the objectives can be summarized as follows:

- To find a solution of protection for different HTS applications.
- To investigate the arcing behaviour in Liquid Nitrogen (LN) environment.
- To develop an existing method of arc modelling for HTS equipment protection.
- To investigate different circuit-breaking condition of HTSCB under Finite Element Method (FEM) computation.
- To mitigate the residual flux of HTS transformer with the switching of HTS arc model.

1.5 THESIS SUMMARY

The key concentration of this thesis is to find an HTS based possible solution of protection for HTS application. Corresponding simulations and experiments are performed on this holistic perspective. The initial results are then put into practice with further simulations and experiments. To conclude the introduction, an overview of the structure of the entire research work is enclosed in Figure 1.

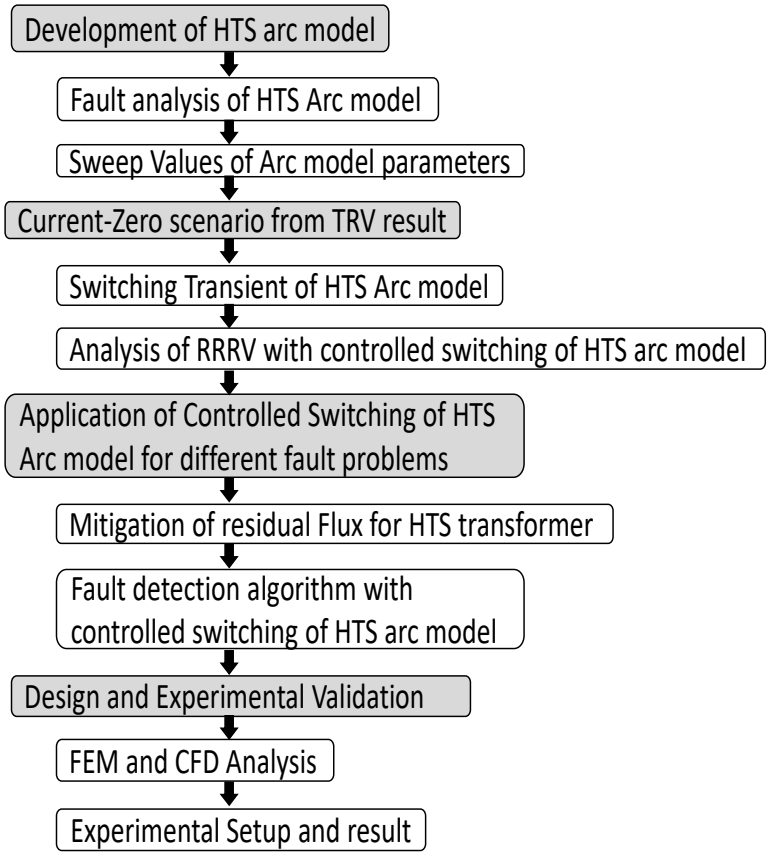

Figure 1: Basic framework of the thesis

This thesis is structured as follows:

Chapter 1: This chapter is the current introductory chapter. It highlights the background of research, motivation, relevancy, the rationale of executing the study and the objectives of the work. Finally, the chapter presents a summary of the structure of this thesis.

Chapter 2: This chapter provides a holistic description of the HTS research, the research gap and also about numerous theories of arc equations and mechanism of the HTSCB.

Chapter 3: One of the most important parts of the research: HTS arc model with Browne's theory is developed in this chapter. The arc current along with arc voltage for the HTS arc model is investigated in this chapter.

Chapter 4: In this chapter, the analysis of Rate of Rise of Recovery Voltage (RRRV) for an HTS arc model is investigated with Normal and Controlled Fault Interruption (CFI). It is found that Pre-striking voltage can be reduced for HTS application with CFI method.

Chapter 5: In this chapter, two applications of controlled switching of HTS arc model are discussed. Firstly, the residual flux of HTS transformer is mitigated at minimum operating time of CFI method. Then, a fault detection algorithm is developed with the CFI method.

Chapter 6: In this chapter, design and experimental validation of arcing phenomenon in cryogenic arc chamber is investigated with Finite Element Method (FEM) and Computational Fluid Dynamics (CFD).

Chapter 7: A summary of the major findings and proposals on potential future research works are suggested in this conclusive chapter.

1.6 CONTRIBUTIONS

The research undertaken in this thesis has made the following contributions to advance the current state of the research.

- The idea of HTS contact within liquid nitrogen arc chamber shows good

potentiality to replace the existing breaker technologies for HTS applications.

- The simulation results from HTS arc model show improved pre-striking and post arcing effect especially for HTS application during high fault current condition.

The following list of publication has been published as part of this research work.

Journal Paper

[J1] **A. Ullah**, T. T. Lie, K. Gunawardane and N. K. C. Nair, " Analysis of Rate of Rise of Recovery Voltage (RRRV) effect of a High-Temperature Superconductor (HTS) Arc Model" IET Journal of Transmission, Generation, Distribution. (Provisionally accepted- April'2018)

Conference papers

[C1]. **A. Ullah**, T. T. Lie, K. Gunawardane, N. K. C. Nair, "Development of Browne's Arc model for HTS Application" in *Power System Technology (POWERCON), 2016 IEEE International Conference*, Wollongong, NSW, Australia. *on*, pp. 1-4. IEEE, 2016.

[C2]. **A. Ullah**, T. T. Lie, K. Gunawardane and N. K. C. Nair, "The improvement of Rate of Rise of Recovery Voltage (RRRV) for an HTS breaker," *2017 IEEE Manchester PowerTech*, Manchester, United Kingdom, 2017, pp. 1-6.

[C3]. **A. Ullah**, T. T. Lie, K. Gunawardane and N. K. C. Nair, " Mitigation of Residual Flux for High-Temperature Superconductor (HTS) Transformer by Controlled Switching of HTS Breaker Arc Model" *2017 IEEE ISGT Asia*, Auckland, 2017, pp. 1-6.

[C4]. **A. Ullah**, T. T. Lie, K. Gunawardane and N. K. C. Nair, " Arcing Behaviour of A Potential High-Temperature Superconductor (HTS) Circuit Breaker Arc Model" in *2018 IEEE IESES*, Waikato, New Zealand, (2018).

[C5]. **A. Ullah**, T. T. Lie, K. Gunawardane and N. K. C. Nair, " Failure Detection Algorithm for High-Temperature Superconductor (HTS) Breaker Arc Model" in *2018 IEEE ISGT North America*, Washington DC, USA.

CHAPTER 2- SUPERCONDUCTIVITY AND ARC MODEL THEORIES

Research and development concerning HTS applications have been developed in the world very recently. Apart from the rated current capability of HTS material, this is crucial as well to establish applicable and accurate performance test for protection systems of HTS Machines. The HTS breaker combines the functions of superconducting cables, fault current limiters and circuit breakers to form a Superconducting Cable embedded high power Circuit Breaker (SCCB). The superconducting SCCB offers zero to near zero resistance to the flow of electrical current, which can reduce losses to the minimum (almost no loss) and improve the overall system efficiency to great extent.

2.1 DISCOVERY AND DEVELOPMENT

In 1911, a researcher from Netherlands named H. Onnes Kamerlingh experienced superconductivity accidentally in mercury. The temperature was under the helium's usual boiling point when noticing its association concerning temperature and electrical resistance. Earlier in 1908, the same researcher liquefied helium that was used in his research in Leiden. It was observed that under 4.2 Kelvin (K) temperatures mercury's resistivity decreased to zero very unexpectedly [16,17]. Nonetheless, the decrease of resistance was not constant. A unique zero resistance state of a few materials was founded from the idea. This changeover stage was defined as the superconducting condition. The temperature where the event took place is named as the transition temperature.

Superconductivity was also identified in several other metals such as tin and lead within a few years [18]. Therefore, erratic speculation arose from this remarkable invention. The researchers believed heavy electric machinery and large field

magnets could be operated without loss. Although, this expectation was encountered with numerous challenges. Furthermore, it was believed in the earlier stage that the characteristic and numerous features of electric machines can be damaged by incompatible magnetic fields and leakage currents.

Onnes analyzed an experiment with Nickel (Ni) alloy covered with Lead (Pb) based superconducting solder in 1913. During the test, superconductivity was not found in the material at magnetic fields under 50 milli- Tesla (mT) [19]. In 1933, Meissner and Ochsenfeld identified that the magnetic field decreased to zero when a superconductor material cooled down under the critical temperature (Tc) in a weak magnetic field of a value smaller than the critical value (Hc) [20]. This is the fundamental theory of a superconductor that is referred to as Meissner effect.

Afterward researchers observed that not only magnetic field and temperature, but also current density is required to be maintained below critical values as a way to keep the superconductivity [21]. After all these findings, HTS equipment are conducted under Liquid Nitrogen (LN) temperature of 77K. In the meantime, the current density values have also been developed to beneficial levels of 105 to 106 A/cm^2.

From 1911, several superconducting materials were investigated. A number of inspiring possibilities, theories and hypothesis were suggested. Comprehensive studies were conducted on electromagnetic properties of these materials. In 1957, Bardeen, Cooper and Schrieffer [22] unveiled their investigation about superconductivity's microscopic theory. The hypothesis was also named as superconductivity's BCS theory (named after John Bardeen, Leon Cooper, and John Robert Schrieffer). This theory delivered an explanation of the microscopic

actions of superconductors in low temperature. The theory clarified numerous uncertainties and ambiguities of the superconductivity characteristics.

Kunzler [23] discovered a new class of superconducting alloys at the same time period with others. The alloy could withstand large current densities and very high magnetic fields. After 1970, High performance superconducting wires became commercially available. The new technology established pulsed field magnets and high DC. As a result, the applications on high power AC could be looked into a great extent as well.

2.2 SUPERCONDUCTING THEORY AND ZERO RESISTANCE

Superconductivity is a state of material which loses its resistance due to cooling in very low temperature. The temperature needs to be lower than the material's transition temperature [24]. The in depth search for new superconducting materials was successful with the finding of superconductivity characteristic at 77 K. The temperature is also found higher than liquid nitrogen's boiling point. The superconductors are then manufactured in the forms of tapes, wires and bulk materials for very high-current applications. The superconductors are fabricated in thin and thick type film forms for different electrical power and electronic applications. A detailed discussion on the general theory of HTS and its possible application in protection industry is discussed in [25]. Twenty years after the discovery of HTS, practical superconducting wires are now being implemented on a trial basis to a number of electrical and industrial applications such as transmission lines, a ship's engine, transformers and many other devices.

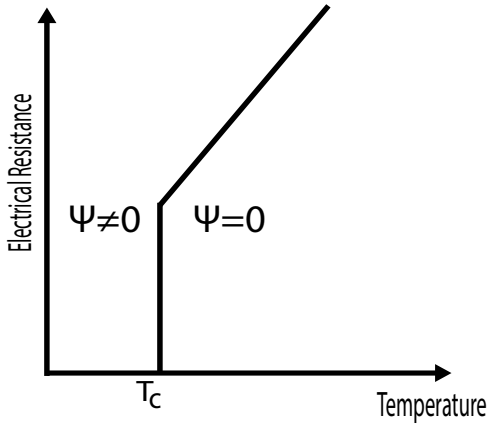

Figure 2: A standard temperature dependence scenario of superconductor's electrical resistance

Figure 2 shows the relation of a superconductor's temperature dependence for the electrical resistance. The curve drops gradually as the superconductor is cooled down to the point until it disappears abruptly. The temperature recording point where this incident happens is known as the critical temperature Tc [25]. It is shown in Figure 2 when T>Tc and electron system order, Ψ=0 the material refers to the normal conducting state. Similarly when T<Tc and Ψ ≠ 0 the material corresponds to the superconducting state of the material. This is a basic theory of superconductor and zero resistance that to be used in prospective HTS breaker research. The biggest issue for an HTS breaker is its electrical resistance and temperature during quenching.

2.3 THEORY OF AC CIRCUIT BREAKING AND ARCING

Circuit breakers are key equipment in power systems. High voltage circuit breakers play a significant function in distribution and transmission systems. Its basic function is to separate faulted areas of a network and to disrupt the fault currents. In a circuit breaker when current carrying contacts open, the medium close to opening contacts grows highly ionized. The disrupted current obtains low resistive path, then proceeds to flow through this area even though the

contacts are physically not connected. Throughout the flowing of disrupting current from one contact to other, the path gets extremely high heat and it glows. This phenomenon is known as arc.

The arc continues within the contacts until the current is disrupted. Since arc alone is a conductive route of electricity. It is crucial to quench the arc in a quickest possible way. Hence, the principal designing condition of a circuit breaker is to offer the best-suited system of arc quenching.

The mechanism of current interruption in an AC breaker is however completely different from that of DC. In DC, the arc continues until it is finally suppressed. While in AC, at each half-cycle the current flows through a natural zero. The arc extinguishes itself twice every cycle of current, re-striking each time until it is no longer able to do so.

In AC, an immediate disruption of current induces huge switching voltage in circuit breaker. Consequently, it stresses the system's insulation and breaker contacts. The breaker contacts receive a progressive but speedy, transition from the arc.

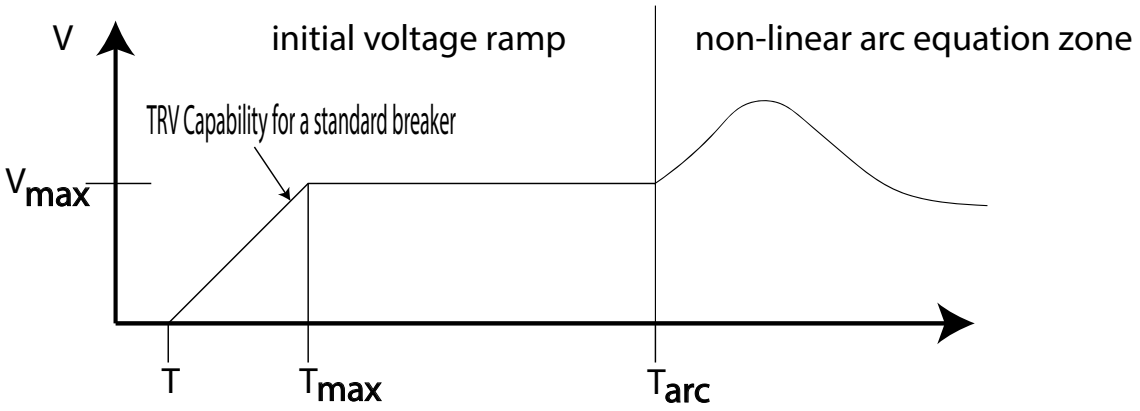

Figure 3: Breaker sequence in circuit breaker

The time series of current carrying to the current breaking states during circuit breaker's opening situation are shown in Figure 3 [26]. Here, the initial contact

parting action is followed by the nonlinear arc equation zone. Transient Recovery Voltage (TRV) capability for standard breaker is also shown.

The highlighted features of a solid circuit breaker are listed as follows:

- It should work as a perfect conductor when closed and perfect insulator when opened.
- Less pre-striking or post arcing effect of the breaker.
- It should have quick switching capabilities.
- It should not produce over-voltages when operating.

The HTS material shows a high prospect to meet these important aspects of a sound circuit breaker.

2.4 CONVENTIONAL ARC MODELS & ITS LIMITATION FOR HTS APPLICATION

The purpose of arc model study is to explain the physical phenomena of arc breaking with complex mathematics. It is used for the simulation of arc-circuit interaction to describe the actions of the arc. It gives the relation between the circuit variable and the arc conductance. Its different parameters are mostly acquired from complex arc equations.

There are basically two kinds of numerical arc models:

i) Physical arc model: It explains the physical phenomena of the arc by means of complicated mathematical terms.

ii) **Black box arc model:** It demonstrates the behaviour of the arc by presenting the relationship between the circuit variables and arc conductance [27]. It is mostly applied in order to simulate the arc-circuit interaction.

The arcing phenomenon in a circuit breaker is quite complex. For AC and HTS applications, there will be a flow of both heat and mass. Plasma consisting of positive ions is also involved [28]. Hence, it is difficult to precisely predict the behaviour of the arc. There are a few theories for Arc Modelling as discussed in [29], the main theories of arc interruption are as follows:

i. Slepian's theory
ii. Prince's theory
iii. Cassie's theory
iv. Mayr's theory
v. Browne's combined theory

Joseph Slepian released an arc interruption theory in 1928 [30]. The hypothesis is also acknowledged as "race theory". In this theory, the criteria for successful interruption is effectively described. It states that the rate of dielectric strength for the arc gap should rise quicker as compared to the rate at which the system voltage develops. The race theory was utilized to demonstrate the arc behaviour in the interruption of AC circuits although it is not completely appropriate for HTS application. It is anticipated that the build-up of dielectric strength is independent of the rate of increase in re-striking voltage. This is true especially for any cryogenic environment [31].

D. C. Prince [32] from U.S. and F. Kesselring [33] from Germany endorsed a new theory referred to as the wedge or the shifting or theory. It's known mostly as Prince Theory. This theory addresses the situation where if there is an interruption in a circuit and the recovery voltage is not adequately large to provide a breakdown. It happens only when the span of the gas release path brought into the arc increases during the timeframe of interruption. At current zero Prince [32]

proposed a simple wedge model in contrary to Slepian's theory. This also does not appear to be the best match for HTS applications. The current zero scenario is the concern here as at current zero, there should be no electrical power input. For HTS applications, the arc is cut by a wedge of cold medium (either cryogenic or cold gas) entering the upstream location between the electrodes. Hence, for HTS application whether an electrical current continued after current zero or not has a bigger possibility than relying on its breakdown. In a cryogenic environment when the circuit voltage is applied after current zero, the electrical breakdown is expected to take place through this wedge of the cold medium.

A. M. Cassie proposed another theory for the development of an arc in 1939 [34].This theory resulted in developing a useful differential equation for the conductivity of the arc. It was assumed that a high current arc is influenced by convection loss throughout the high current time span. According to this conjecture, a roughly steady temperature over the arc diameter was preserved. It was noticed that when the current varies, the arc cross section also changes accordingly. But the heat range inside the arc column is not likely to be adjusted with the change. Cassie's theory states that the convective flow is regularly reduced by the arc area. Once again, the modification of the column due to the cold medium (either gas or cryogenic) flow has its own limitation. Hence, Cassie's theory also does appear to be applicable for HTS applications. This is because a piece of stretchy elastic of circular section fixed at one end has the effect of the cold medium. The other end is made to move at a speed equal to that of sound in the cold medium at arc temperature.

O. Mayr published his theory in 1943 [35]. He considered a different approach than Cassie. He took an arc column of constant arc diameter. He varied the arc

temperature as a function of time. It was also assumed that i) the conductivity of the arc was reliant on temperature ii) the decay of the arc happened because of the thermal conduction. The theory at current zero period is generally accepted. Many researchers successfully applied the Mayr's model at current zero. The reason is the radial losses in this region which is a significant controlling issue. Mayr's theory with some addition of experimental constant would give an extra feature for practical implementation of HTS. Actually, it is witnessed that, the arc heat range is usually over 6000 Kelvin which was presumed previously by Mayr.

T. E. Browne identified the limitation of Mayr's theory in 1948 [36]. A model was developed making use of an equation like the equation of Cassie. It determined arc which was current controlled and incorporated into the equation of Mayr. It was basically used in order to control the temperature. In case the interruption does not happen at the expected current zero, there is a choice to represent using the Cassie representation. In 1958, Browne tried to expand the application of the combined model [37]. It included the investigation of thermal re-ignitions. This work successfully analysed the first few microseconds following the post current zero period.

Browne's arc model is designed according to the Cassie's and Mayr's differential arc equations combination. The primary benefit of the model for HTS application is that it can be applied in arrangement with various complex networks. It gives the large-scale option of using both active and passive parameters of the equivalent circuit. For the high-current time interval, arc conductance's behaviour is studied in different ranges for different models. For Cassie's model, arc conductance behaviour is studied at temperatures above 8000 Kelvin or more. On the other hand, Mayr's arc modelling in the area of current zero operates at

temperatures below 8000 Kelvin. The Browne's combined theory hence has an advantage of addressing a wide range of temperature variance for HTS application.

Experimental research shows that Browne's model is a beneficial tool that has a practical use [38]. Browne computed the model from the assessments of gas blast interrupters. He discovered a constant in the order of one microsecond that is acceptable with the generally acknowledged range identified by other researchers [39]. Among many other types of research, there were different opinions about the requirement of re-ignition.

At equal conductance points, Amsinck [40] considers the parameters to be equal (therefore, a re-ignition is essential to find the parameters). While Hochrainer [41] thinks the parameters should be of identical values at points of equal current. Hence, re-ignition is essential to find the parameters. Zückler [42] thinks the parameters to be equal in two following time steps (therefore, no re-ignition is essential).

2.5 ARC EQUATIONS

Arc conductance usually works as a function of three outputs in arc equation. The expression can be written as:

$$g = F\,(P_{in}, P_{out}, t) = \frac{i_{arc}}{u_{arc}} = \frac{1}{R} \tag{2.1}$$

Where P_{in} is supplied power, P_{out} is transported power by radiation and cooling and t is time.

If the transported power and the supplied power vary with the arc conductance, the stored energy channel is then expressed as:

$$Q = \int_0^t (P_{in} - P_{out})dt \tag{2.2}$$

The instantaneous arc conductance can be defined as

$$g = F(Q) = F[\int_0^t (P_{in} - P_{out})dt] \tag{2.3}$$

The arc conductance's rate of change gets a new expression when it is divided by the instantaneous arc conductance value:

$$\frac{1}{g}\frac{dg}{dt} = \frac{1}{g}\frac{dF(Q)}{dQ}\frac{d(Q)}{dt} \tag{2.4}$$

Some adjustment of the equations above gives the general arc equation as equation (2.5)

$$\frac{d(\ln(g))}{dt} = \frac{F'(Q)}{F(Q)}\ (P_{in} - P_{out}) \tag{2.5}$$

Solution to this equation requires assumption, arc models and solutions to the equation. From equation (2.4) and (2.5) Mayr arc model is presented by the following equation.

$$\frac{1}{g_m}\frac{dg_m}{dt} = \frac{1}{\tau_m}\ (\frac{u_i}{P_0} - 1) \tag{2.6}$$

In equation (2.6) Mayr arc model is investigated for the electric arc in the area of current passing through zero [43].

Similarly, Cassie's arc model is investigated for the high current in equation (2.7)

$$\frac{1}{g_c}\frac{dg_c}{dt} = \frac{1}{\tau_c}\ (\frac{u^2}{U_{arc}^2} - 1) \tag{2.7}$$

Where, u and i are the arc voltage and current correspondingly dependent upon time values; g represents the conductance of the electric arc, τ_m and τ_c denote the time constants of the Mayr and Cassie arc models U_{arc} is the average arc voltage in high current range and P_0 is the dissipated power at the time when current passes through zero.

The other recent modern models are mostly complied with the basic roles of Cassie and Mayr arc models. Like Browne used the Mayr's equation for current zero and Cassie's equation for the high current interval. Habedank used almost similar idea to design his model. This model is the combination of Mayr and Cassie models. It is considered to cover both high current range and the zero-crossing together [44].

$$\frac{1}{g} = \frac{1}{g_c} + \frac{1}{g_m} \tag{2.8}$$

Habedank arc model consists of one algebraic as equation (2.8) and two differential equations as equation (2.6) and (2.7).

Schavemaker arc model is a modified Mayr arc model with a constant time parameter τ and the cooling power that is a function of the electrical power input. The differential equation for this model is shown as follows:

$$\frac{1}{g}\frac{dg}{dt} = \frac{1}{\tau}\left(\frac{ui}{\max(U_{arc})\,|i|, P_0 + P_1 ui} - 1\right) \tag{2.9}$$

In equation (2.9), the term P_0 dominates for low current and the resulting equation is similar to the Mayr model. At a high current, the term $U_{arc}|i|$ still dominates and the model reduces to that of Cassie arc model [45].

In the Schwarz arc model [46] is almost similar to Mayr arc model. In this model extra parameters *a* and *b* are used as the dependency of power loss and arc time constant on the arc conductance as expressed in equation (2.10).

$$\frac{1}{g}\frac{dg}{dt} = \frac{1}{\tau g^{a}}\left(\frac{ui}{Pg^{b}} - 1\right) \tag{2.10}$$

The KEMA arc model [47] is derived from three Mayr arc models in series and is shown in [45]. By assigning different values to λ_i , a model more like the Mayr or the Cassie model can be considered. λ=1 defines the Mayr arc model and λ=2 points out to Cassie arc model:

$$\frac{1}{g} = \frac{1}{g_1} + \frac{1}{g_2} + \frac{1}{g_3}, \frac{dg_i}{dt} = \frac{1}{P_i\tau_i} g_i^{\lambda_i} u_i^2 - \frac{1}{\tau_i} g_i \tag{2.11}$$

Here $\tau_2 = \frac{\tau_1}{k_1}$, $\tau_3 = \frac{\tau_2}{k_2}$ and $P_2 = \frac{P_3}{k_3}$. For the arc models, dissipated power and arc time constant are expected to get the effect on arc voltage behavior during current zero-crossing. Consequently, there will be the impact on the ignition voltage, Transient Recovery Voltage (TRV), and Rate of Rise of Re-striking Voltage (RRRV) [48]. This will be really interesting to investigate different cases and scenarios. The research on TRV and RRRV is continued in following chapters of this thesis.

2.6 THE MECHANISM OF HTS BREAKER

The method of arc control in perspective of HTS breaker will differ from oil, vacuum or air-break circuit-breakers. The oil breaker performs by flushing out the 'combustion' products of the arc while vacuum breaker works by controlling the arc medium and the air-breaker operates by controlling the re-striking voltage wave.

HTS breaker is likely to function in very cold space. The moving contact can move only a short space from the fixed contact while opening. When the contacts first separate in mid-cycle, an arc is driven and the current continues to flow.

When the re-striking voltage is found across the open contacts, for HTS environment there should be no gas dielectric to break down. Therefore the chance of growing a new arc should be less. The arc consequently should not restrike. HTS breaker contacts will likely be suitable for repeated use as contactors.

The Vacuum Circuit Breaker (VCB) is very common, particularly for medium ranges of voltage, due to its excellent efficiency. At VCB when the operating linkage reaches a certain level specified by the manufacturer, the whole vacuum interrupter element must be replaced. HTS breaker offers the advantage of replacement of its cold medium.

Moreover, liquid nitrogen can work as an insulator as it is not electrically conductive. Nitrogen is a non-polar gas and thus it is likely to be non-conductive. The same theory is used by using liquid nitrogen in computer cooling.

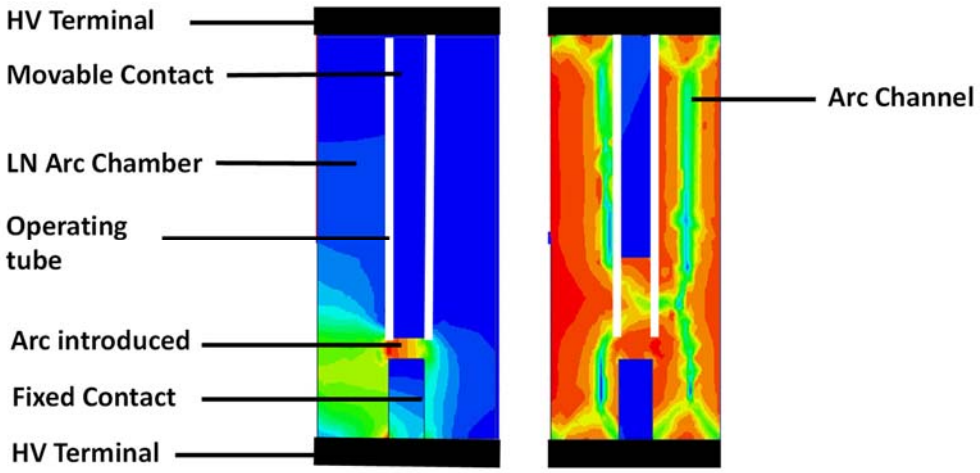

(a) (b)

Figure 4: Arcing stages for HTS breaker (a) during arcing in mid-cycle (b) during current-zero arc extinguish

In Figure 4 structure and arcing stage of HTSCB is shown. Figure 4(a) shows the proposed internal structure of HTSCB and the arc introduced in mid cycle. Figure 4(b) demonstrates the development of arc channel in HTSCB.

2.7 NUMEROUS CHALLENGES

Few disadvantages of distribution systems of high voltage AC systems area appears as challenges for any type of breakers. Some of other challenges are summarized and briefly explained as follows:

i. Complex and expensive System: Operating and designing of HTS equipment are complex and expensive. For HVAC substations the converters are complex as well. Stations expenditure can be offset in this case, but offsets require power lines of considerable length as well. The power flow management in HTS systems demands steady communication among the terminals. Few downsides of related transmission systems such as links with high voltage systems area appear as

challenges for breakers. Building the HTSCB from these perspectives is obviously challenging.

ii. Harmonics: It's natural for current and voltage harmonics to occur in prompt disconnection areas with HTS machine. The process is associated with the consumption of reactive power. Consequently, the system demands the installation of compensation units of reactive power and pricy filter-compensation sections.

iii. Size and capacities: The concern for breaker sizes is a big challenge for protection study, it becomes even more challenging with cryogenic condition. The problem of breaker contact and LN arc chamber size optimization of HTSCB is outlined in Chapter 6 of this thesis.

iv. Difficult grounding installation: HVAC transmission for HTS machine grounding requires a difficult and complicated installation. It develops long lasting and efficient grounding.

v. Corona loss: The electric field can grow from the surface of breaker contact during arcing. There is a chance to develop corona loss in this case. The charges on the contact surface often create leakage current and wastes energy [49].

vi. Ohmic loss: The ohmic loss of the breaker contact is also a concern. As the electric charge carriers inside the bulk contacts experience resistance as a sort of friction.

CHAPTER 3- DEVELOPMENT OF HTS ARC MODEL

Current interruption of a Circuit Breaker (CB) can be identified as a statistical approach. The characteristic of a novel circuit breaker can only be investigated by a series of simulation and laboratory experiments. A great range of tests should be executed in order to find appropriate outcomes. On the contrary, the expenditures of CB experiments are reasonably higher and time-consuming. Consequently, there is the benefit to get the results from the simulation of the breaker arc model as a way to supplement the essential tests [50]. The behaviour of HTS arc model and its characteristics in electrical power networks meets the same purpose.

An arc model of HTSCB is developed with MATLAB® Simulink [51] in this chapter. The model is developed as a combination of the famous Cassie's and Mayr's differential arc equations. HTS arc model's simulation study and the behaviour of HTSCB describes a complex breaker model that is inserted into a simple equivalent network. From the model elements the following issues are investigated in this chapter:

- *The breaker efficiency of current interruption.*
- *Characteristics of breaker in the network under different specific conditions.*

The chapter is based on the following articles:

[1] **A. Ullah**, T. T. Lie, K. Gunawardane, N. K. C. Nair, “Development of Browne’s Arc model for HTS Application” in *Power System Technology (POWERCON), 2016 International Conference* on, Wollongong, NSW, Australia. (2016)
[2] **A. Ullah**, T. T. Lie, K. Gunawardane and N. K. C. Nair, " Arcing Behaviour of A Potential High-Temperature Superconductor (HTS) Circuit Breaker Arc Model" in *2018 IEEE IESES*, Waikato, New Zealand, (2018).

3.1 Development of Browne's Arc Modelling for HTS

The theories of Arc Modelling and its limitation from HTS arcing perspective are discussed in Section 2.3 of this thesis. Arc characteristic under high current shows some useful results. Browne's combined theory is considered as a preliminary solution for the development of HTS arc model.

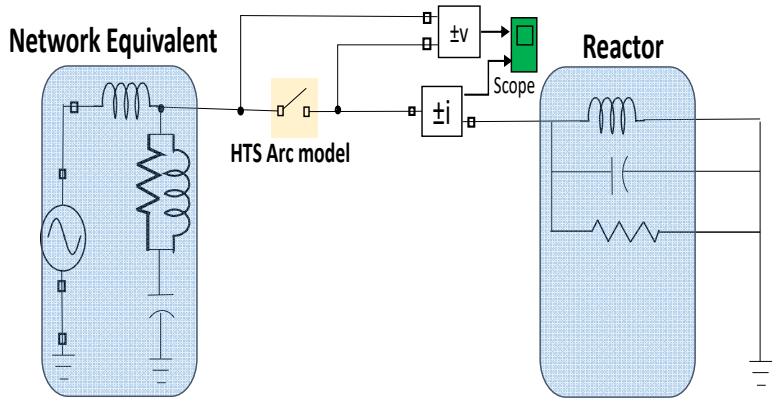

(a)

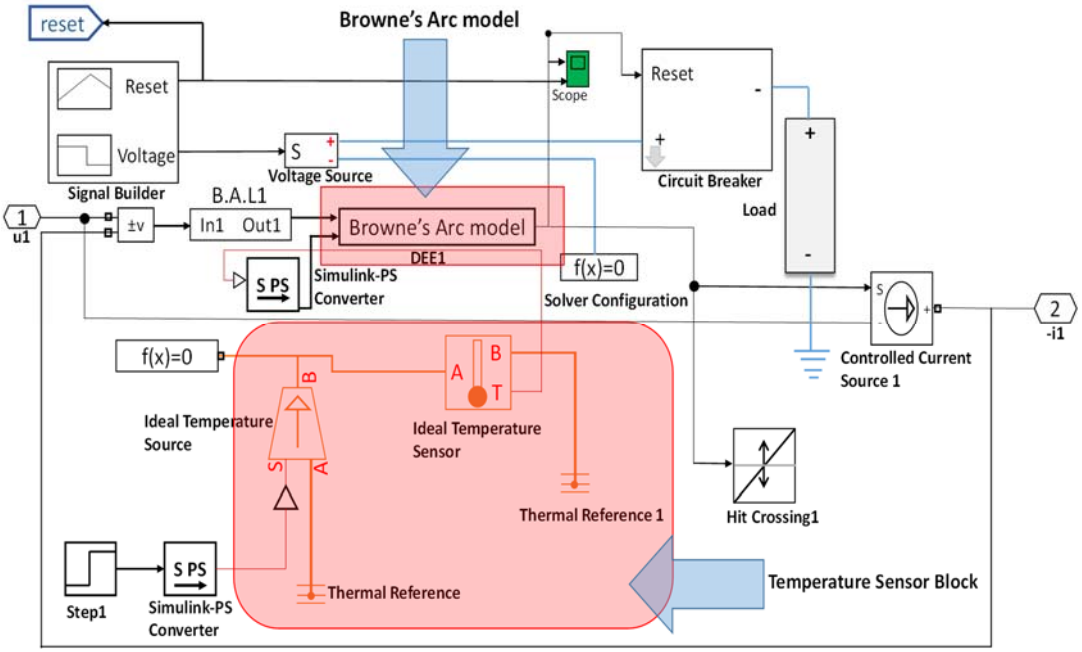

(b)

Figure 5: (a) HTS arc model with network equivalent (b) HTS arc model theoretical structure: Browne's Combined Arc modelling for HTS Application

The theoretical structure in network equivalent and the inside framework of the arc model are shown in Figure 5 . The model is firstly prepared on a sample of simulated arc voltage and current results. In Figure 5, HTS arc model with network equivalent and the inside of HTS arc model is shown. The arcing experiment of the HTS arc model is demonstrated in Chapter 6.

Arc is extinguished for each current zero in AC. In the Browne's arc models current sources are used control the voltage in order to investigate the arcing situation. The differential equations are modeled in MATLAB® Simulink for prior and around current zero. If *i* is the current that passes through prior to the opening of breaker contact and *L* is the inductance of the system, then the expression for switching over voltage during opening of contacts is $V = L.(di/dt).$ where *di/dt* is the rate of change of current with respect to time.

In this proposed model the HTS breaker mechanism is maintained with a time constant of first order. The setup is modelled as a frequency dependent model. When 11 kV supply is applied, it results in a high current that exceeds the circuit breaker current rating and hence the breaker trips. The reset is then pressed, and the voltage is ramped up. The breaker then trips just beyond the circuit breaker current rating. This is the simple mechanism for the HTS arc model. A device block is used as well to switch the differential into physical measurement signals pressure, *P* and temperature, *T*. In order to use the breaker especially for other HTS applications, the Matlab model assumes an ideal pressure and temperature sensor. The pressure and temperature are assessed across two ports of the HTS breaker arc model.

The controlled current source and measurement block of Figure 5 work as links between electrical signals and Simulink blocks. The transfer function for the

simulation block measures the voltages across elements and the currents through breaker contacts and transmission line. The function of numerous components of the Brown arc model is clarified in the following section. The important block parameters of Browne's arc model are used as:

Temperature Sensor Block: The operation of breaker contact is controlled by the temperature control and a current controlled source. The contacts are separated for any temperature rise about set tolerant cooling temperature of 90 K during arcing or any arc current beyond rated current.

DEE (Differential Equation Editor): Browne arc model's equations have been designed by means of the Simulink Differential Equation Editor (DEE) block. As discussed in section 2.3, Browne's combined arc model consists of a Cassie and Mayr arc model in series. That is *dlng/dt=1/tau_m*((ui/P0)-1)* and *dlng/dt=1/tau_c*((u^2/Uc^2)-1)* respectively for the equations (2.6) and (2.7). The function block is set for four free parameters: *tau_m* is the Mayr time constant, P_0 is the Mayr cooling power, *tau_c* is the Cassie time constant and *Uc* is the Cassie arc voltage.

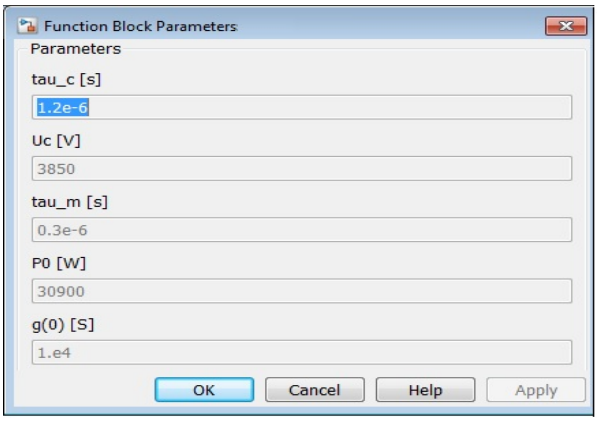

(a)

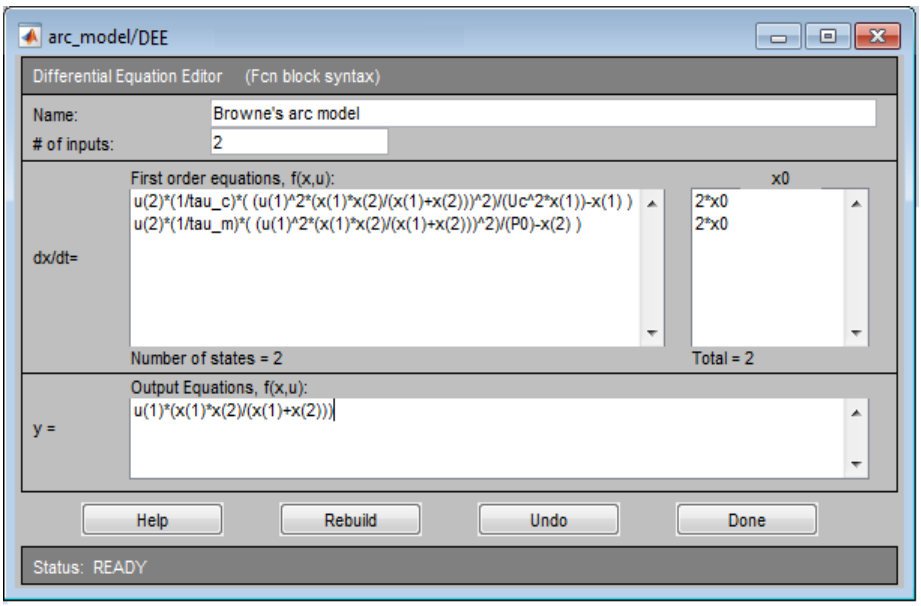

(b)

Figure 6: (a) Function Block Parameter and (b) DEE block of Browne's Arc model

In Figure 6, *u(1)* and *u(2)* are two inputs of the DEE block. *u(1)* equals the arc voltage: *u. u(2)* symbolise the separation of the HTSCB's contacts. If *u(2) = 1* the contacts are being opened and *u(2) = 0* when the contacts are closed. *x0* is the initial value of the state variable, i.e. the initial value of the arc conductance: *g(0). x(1), x(2)* are the state variables of the differential equation. In this case it is natural logarithm of the arc conductance: *ln(g).* Finally, *y* is the output of the DEE block and the arc current is *i*.

Hit crossing: The Simulink 'Hit crossing' block registers the data when input data crosses the zero value. For this simulation it is used for current. For this reason, this block assures that the simulation locates the zero crossing point by adjusting the step size. This is worth addressing that the current and voltage zero crossing of the HTSCB reacts as a non-linear resistance. This is regarded as a significant moment for interruption technique. The more accurate the interruption is close to current-zero, the better it is for the interruption process.

Step: The Simulink 'Step' block controls contact separation of the proposed HTSCB. A step is developed from zero-value to one for the particular contact separation time. Differential equation 3.1 is solved for the condition when the contacts are closed.

$$\frac{d\ln g}{dt} = 0 \tag{3.1}$$

The arc model acts as a conductance with the value g(0). For the time on of contact separation, the Mayr equation can be resolved as:

$$\frac{d\ln g}{dt} = \frac{1}{\tau}\left(\frac{gu^2}{P} - 1\right) \tag{3.2}$$

Controlling the Arc conductivity and model resistance: Mayr's and Cassie's models are only appropriate in current zero area. HTS arc model has a distinctive advantage for this current zero as well. The complete HTS arc model adjusts the conductivity of resistors from both models. It works as like as the real circuit breaker. Prior to the breaker is disconnected, its resistance is kept constant and very small. For both models, the value of 10^{-5} Ω is used.

The electric arc burns in the breaker as soon as contact disconnection takes place. In the HTS model, a constant voltage for the arc is considered with the pre-set values for either sections of the model. The overall resistance of the model is measured in accordance with the pre-set values. The current passes via the arc determine this resistance. This is carried out by one part of the model and the part sets the early conditions of the calculation.

The arc time is assumed for few microseconds in the simulation. The resistance of the model is transferred and controlled in accordance with both differential equations. This is a significant section of the simulation prior to current zero point. The resistance is determined based on the differential equations till successful

arc is extinguished. In this instance, the resistance of both sections of the model is placed to a high value (10^{+5} Ω). If arc extinguishing is not recognized, the differential equations are used to determine arc resistance until end of the simulation. The results are claimed realistic results following the same process in [45] .

3.2 ARC MODEL COMPUTATION

3.2.1 Arc current and arc voltage

This study will use a precise mathematical model to identify and summarize the particular behavior of HTS switch arc. The electromechanical HTS breaker mechanism is approximated with a first-order time constant, and it is assumed that the mechanical force is proportional to load current.

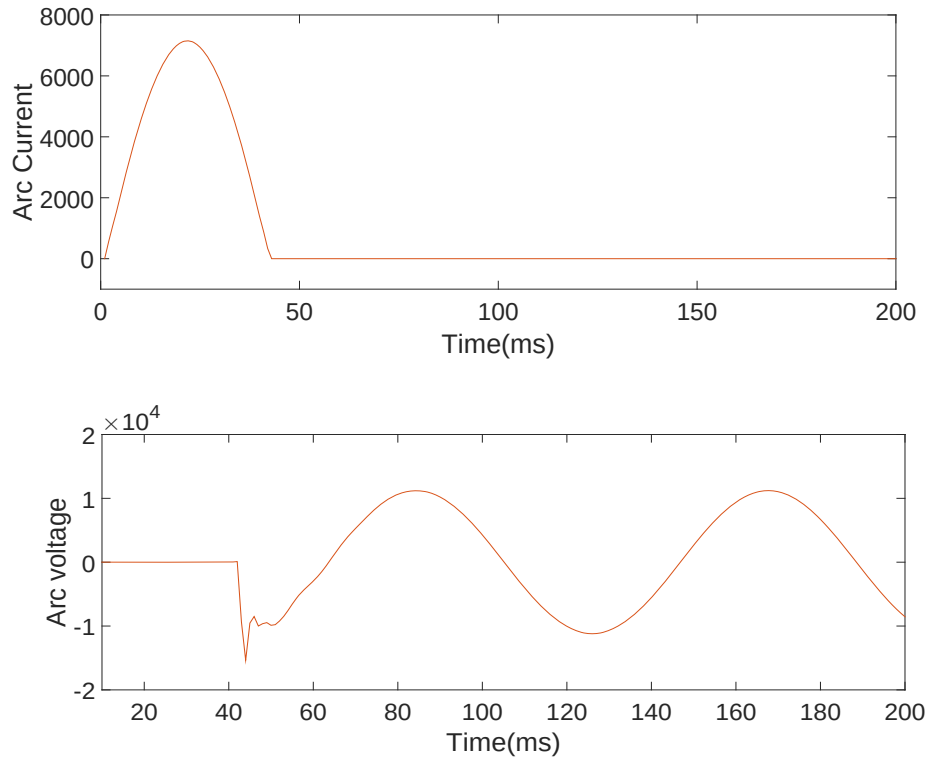

Figure 7: Arc voltage and current for Browne's Arc model for HTS application

When 11kV supply is applied, it results in a high current that exceeds the circuit breaker current rating, and hence the breaker trips. The reset is then pressed, and the voltage is ramped up. The breaker then trips just beyond the circuit breaker current rating.

From the simulation the findings are as follows:

- The arc acts as a non-linear resistance.
- The power input into the arc channel is zero.
- The arc voltage is constant in the high current period.

It is assumed that a typical arc can exist after current zero because the arc temperature exceeds a certain value for cryogenic. The equation for energy can be integrated from $r=0$ to the arc radius and yields another equation, which is accurate enough for the realistic application purpose so it is not necessary to include the other equations anymore. As suggested in [31] the simplified equation is used as in MATLAB function. This is applicable to more general cases with respect to the circuit breaker and can be modified to match the test data for different cases.

In the case of interruption of very high current, it can be considered as an extreme case study for the arc model. In that case, there is the possibility of the air breakdown. The arc is regarded as a non-linear resistance too. However, the arc has no re-striking. It tends to keep conducting through the arc path under this high current, which makes the arc extinction impossible.

Switch voltage shows the periodical steady state at one stage as shown in Figure 7. The simulation result reflects that the arc under the high current tends to last for a longer time which is absolutely intolerable in system operation. Although the arc length will not enlarge significantly when compared with that under low current, the long-lasting time of the arc may cause the other switches or breakers to be opened by the control signals coming from the relay protection system.

3.2.2 Sweep values of parameters

It is frequently required to execute multiple iterations of an arc circuit to recover its faulty features. A parameter sweep of a complex circuit like arc model can be executed for a different variation of analysis frequencies. It can be used in order to estimate unknown model parameters, tune control parameters or to examine the effectiveness of an algorithm. The problem of minimizing the arcing time of HTS arc model with a parameter sweep is discussed in this section. A standalone executable MATLAB® based program is performed in this regard. Steps to perform parameter sweep in MATLAB are as follows:

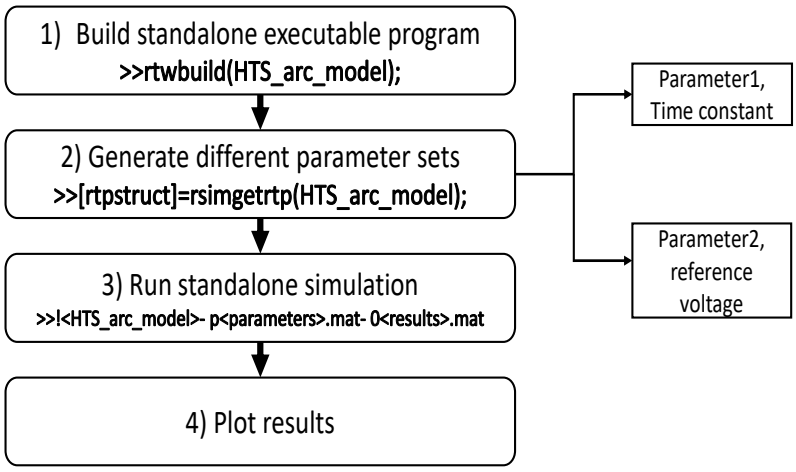

Figure 8: Parameter sweep steps of HTS arc model

In Figure 8, the steps of parameter sweep are shown. First, a standalone executable program is built for the HTS arc model. Then, the parameter set for

the arc model is generated for the parameters like the time constant and the reference voltage. The iteration process shifts the dimensions of the parameters of arc model. The optimized value of parameterization provides the best results for minimum arc timing within a user-defined range. Finally, the results are shown by running the standalone simulation. The results are then analysed and compared with each run. In order to repeatedly change the value of black box parameter, a separate variable needs to be created in MATLAB workspace.

According to interruption theory, arc voltage above reference voltage decrease the current. If arcing voltage is higher than the reference voltage, the value of arc current is cut down to zero. The simulation result of Browne's arc model can validate this theory. In this section, arcing voltage time is decided by a time constant. It ensures the dependency of fault time on selected parameters. Two parameters of Browne's arc model: reference voltage and time constant is selected for parameter sweeping calculation. Several values are chosen for each parameter as stated in Table 1 and the result is shown against arc voltage and current. One default value is chosen for the parameter, whereas the others are varied.

Table 1. Iterative simulation of chosen Sweep values

Parameters	Default value	Sweep value
τ [µs]	100	50,80,110,140,170
Uc [kV]	11	9,11,13,15,17

Figure 9 shows that arc voltage and current grows with the variation of reference voltage and time constant. It is found that if the time constant increases, the

voltage generation slows down. Consequently, current interruption time slows down as well.

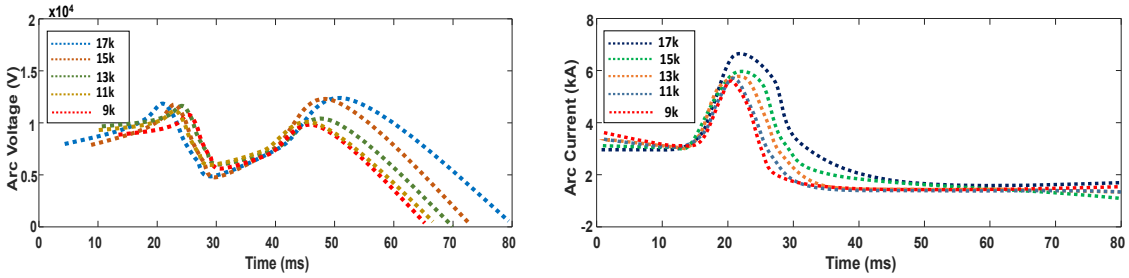

(a)

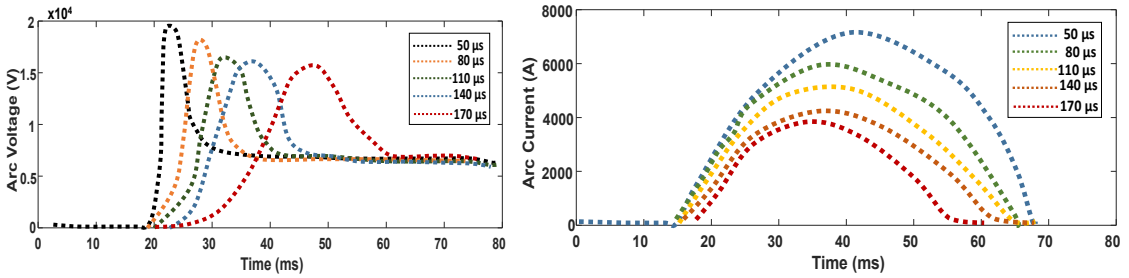

(b)

Figure 9: Browne's model transient response with respect to (a) reference voltage (b) time constant

In Figure 9 (a), it is shown that when rated voltage U_c is grown, the arc peak voltage also grows. If the reference voltage develops, the slope of voltage increases as well. The ignition becomes steeper to ensure arc current can reach zero instantly. It is noticeable, time constant influence the arc voltage and current. If time constant increases, voltage graph stretches with the transition and current graph becomes broader. Arc voltage influences the voltage graph as well. Voltage graph follows an upward trend with the rise of the value. In general, for all the cases the initial and ending transient point is identified within the range of 20-80ms. The values are used in the following calculations.

3.2.3 Arc resistance

HTS materials for electrical machines rely significantly for its critical current densities at temperatures to the point when cryogenic losses are tolerable. Among the HTS materials MgB_2, $(Bi,Pb)_2Sr_2Ca_2Cu_3O_x$ and $YBa_2Cu_3O_x$ operates within the temperature range 30K to 120K. In Table 2, Classification of different critical temperature of HTS compounds is enlisted [52]. HTS power cables, generators, leads, transformers, motors, energy-storage devices and fault current limiters are using Bi-series HTS material in great extent.

Table 2. Classification of different critical temperature of HTS compounds

HTS Family	Compounds	Highest, T_c
Bi-HTS	Bi-1212	102K
	Bi-2201	34K
	Bi-2234	110K
Pb-HTS	Pb-1212	70K
	Pb-1223	122K
Hg-HTS	Hg-1201	95K
	Hg-1234	127K
	Hg-2234	114K
123-HTS	Y-123, YBCO	92K
	Yb-123	89k
B-HTS	B-1223	75K
	B-1245	85K

The arc originates from the contacts or from the transition of high voltage discharge. For steady state situation, the rate of arc current changes very little. Electric arcing is self-sustained discharge. The arc originates from the contacts or from the transition of high voltage discharge. For steady state situation, the rate of arc current changes very little. The increased arc current flow increases the ionization in liquid nitrogen arc chamber. Arc possesses negative resistance characteristics. Applied voltage and arc resistance may vary to calculate the property of arcing length.

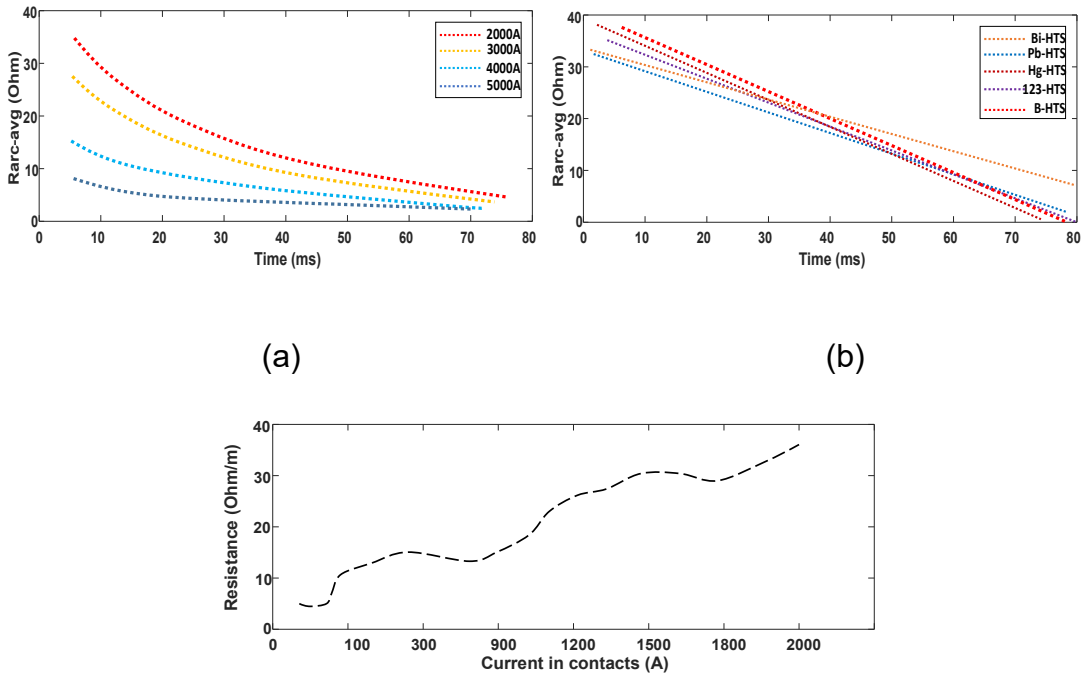

Figure 10: (a) The change rate of average arc resistance for different arc current and (b) The change rate of average arc resistance for different critical temperature of different materials of HTS family (c) The change of resistance for breaker contacts

Figure 10(a) demonstrates the average arc resistance for various current ranges. Arc resistance is calculated by dividing arc voltage with arc current at each data point. As a result arc's dynamic characteristic, the arc resistance is found as constant as a standard resistor. The graph is obtained by averaging the arc resistance for several gap lengths at described load current level. It is found that the arcing current has an impact on arc resistance. When the current is low, the load current shows a significant impact on the arc resistance. Figure 10 (b) demonstrates the change rate of average arc resistance for critical temperature of different materials of HTS family. All of the curves from different HTS families show a downward trend of arc resistance characteristics in Figure 10 (b). Figure

10 (c) shows the relationship for resisance of supercondcting contact and the current passes through it. As the resistance increases linearly for increasing current through the contacts, it means it will resist the current during arcing.

3.4 CONCLUDING REMARKS

The primary benefit of the arc model is that it can be straightaway utilized in numerous machine models and complex network. Similarly, this HTS arc model can also be applied in order to identify the current interruption performance of HTSCB for particular conditions determined by different machines and networks.

The sweep value of parameters and the average arc resistance show the advantage of dealing with the non-linear arc models. In the high current interval, the arc-circuit interaction changes slowly. The effect of the parameters is investigated within the limited number of ranges. Large computational steps can be taken for future investigations as well. Around current zero, the arc characteristics are expected to be changed faster. Figure 9 and Figure 10 shows the characteristics result of the Browne's HTS arc model. The arc model therefore needs to investigate TRV of HTS arc model during the short time of arcing before current zero. In Chapter 4, the HTS arc model is used to find the characteristic of TRV for different current zero scenarios.

CHAPTER 4- CURRENT-ZERO SCENARIO OF HTS ARC MODEL

In this chapter, the HTS arc model is used to find the characteristic of TRV for current zero scenarios. After the current interruption in HTSCB, the arcing medium around the contacts is stressed due to the Rate of Rise of Recovery Voltage (RRRV). The existing charged particles begin to drift and trigger post-arc current. Consequently, large amount of energy is produced in the arc channel. Current interruption problem then converts towards quenching issue of discharging particle. The stage of this quench elimination of electric power input starts from the thermal losses and the recovery voltage of electric arc. The phenomenon is named as the thermal recovery phase which lasts for few microseconds only. For HTS machine it is very important to control the quenching current within miliseconds to maintain its superconductivity. The study and controlling of RRRV for any breaker therefore very important.

In this chapter, two different types of switching: normal and controlled have been used in order to analyze the RRRV of HTSCB.

This chapter is based on the following articles:

[1] **A. Ullah**, T. T. Lie, K. Gunawardane, and N. K. C. Nair. "The improvement of Rate of Rise of Recovery Voltage (RRRV) for an HTS breaker " In 12th IEEE PES Powertech Conference, IEEE, 2017.

[2] **A. Ullah**, T. T. Lie, K. Gunawardane and N. K. C. Nair, " Analysis of Rate of Rise of Recovery Voltage (RRRV) effect of a High-Temperature Superconductor (HTS) Arc Model" IET Journal of Transmission, Generation, Distribution. (Provisionally accepted-April 2018)

4.1 NORMAL SWITCHING OF HTS ARC MODEL

The implementation of arcing phenomenon of a circuit breaker in a network is quite complex. The steps for this experiment are shown in Figure 11. In this particular study, it is assumed that the fault is located at the circuit-breaker terminal.

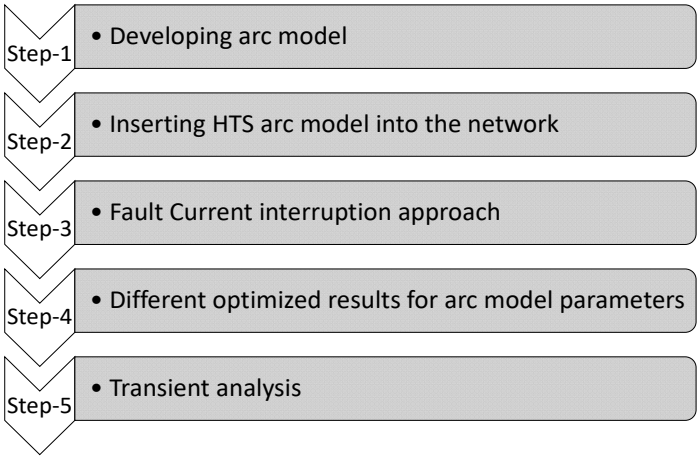

Figure 11. Different steps of RRRV improvement of an HTS breaker

4.1.1 Developing arc model

A Browne's model for HTS application and its calculation of power system transients is investigated earlier in section 3.1. The proposed model of the HTS breaker is maintained with a time constant of the first order for any distribution network. For 11kV supply when it results in a high current that exceeds the circuit breaker current rating and the breaker trips. It is also assumed that a typical arc can appear after current zero because the arc temperature exceeds a certain value for the cryogenic condition. The equation for energy can be integrated from r=0 to the arc radius which is accurate enough for the realistic application purpose. The simplified equations are used as in MATLAB function. These are more general cases with respect to the circuit breaker and can be modified to match the test data for different cases.

Browne simplified the equation of Cassie and the Mayr [29] . The theory of Cassie before current zero is represented as:

$$\frac{d}{dx}\left(\frac{1}{R^2}\right)+\frac{2}{\theta}\left(\frac{1}{R^2}\right)=\frac{2}{\theta}\left(\frac{1}{E_0}\right)^2 \quad (4.1)$$

The theory of Mayr around current zero as:

$$\frac{dR}{dt}-\frac{R}{\theta}=-\frac{e^2}{\theta N_0} \quad (4.2)$$

4.1.2 Inserting HTS arc model into the network

HTS arc model is used in this section to investigate the interrupting short-circuit currents or for the current interruption. For this analysis, the HTS arc model is inserted in this step into a distribution network along with an HTS transformer as shown in Figure 12.

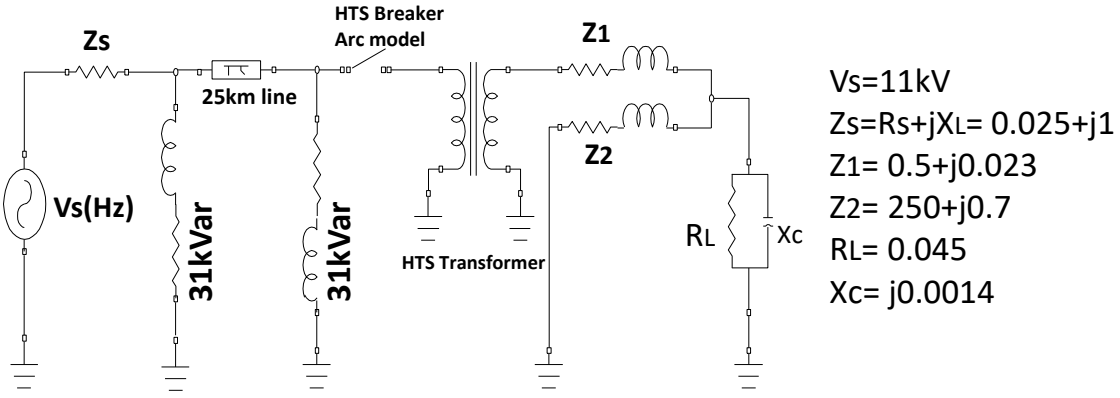

Figure 12. Equivalent circuit of a distribution network for HTS arc model with HTS transformer

The HTS transformers are claimed to be very efficient which are developed to meet the mechanical reliability of insulation and windings system. The most common high-temperature superconductors used for HTS transformers are $Bi_2Sr_2Ca_2Cu_3O_x$ (Bi-2223), $YBa_2Cu_3O_x$ (Y-123 or YBCO) and $Bi_2Sr_2Ca_1Cu_2O_x$

(Bi-2212). Such products established superconducting actions at the temperature below 105, 90 and 80K correspondingly and work nicely in cryogenic condition [53-54]. Usual linear transformer block with HTS transformer specification is used here. Several studies are performed to investigate the operation of HTS power transformers in real life [55- 56]. HTS transformer performs pretty well in distribution network from technical and economic aspects [57-58].

4.1.3 Fault Current interruption approach

For fault line case, the circuit breaker arc model behavior is analysed through RRRV characteristics. Usually, the medium voltage circuit breaker is used in order to meet the requirements for terminal fault. The simulation is performed for 11kV HTS circuit breaker arc model in order to examine the arc model ability to interrupt a fault in that connected to a faulty system. The circuit breaker arc model efficiency is highly impacted by the early part of TRV which is an accumulation of several saw-tooth waves. Typically, the application of medium voltage circuit breakers is chosen in order to meet the requirements for terminal fault. The simulation is performed in order to examine the HTS arc model ability to interrupt a fault that is connected to an HTS transformer.

The short circuit current I_{sc} is a line breaker current for a fault applied near HTS transformer line. It appears that an adequately huge voltage of arcing can drive the disrupted current with a perfect HTS arc model. This step presents the numerical method of interruption applied in the simultaneous solution of electrical network and arc equations.

Very high RRRV grows around the circuit breaker arc model when fault occurs in the network. For this study, the fault is considered straight away after the HTS transformer. Consequently, extreme TRV situations may affect the network.

Hence the value of the capacitance between HTS circuit breaker and HTS transformer is vital to compensate the peak TRV values.

4.1.4 Different optimized results for arc parameters

The arc equation and the characteristic is determined earlier as a non-linear function in section 3.2.1 of this thesis. The challenge of optimization is the solution of the highly non-linear equations. The conventional equation of Cassie and Mayr equations are used respectively in order to utilize the Browne's theory for the prepared HTS Arc model [59].

The accuracy of the model substantially depends on the exactness of the parameters. The HTS arc model parameters calculation demands intricate analysis for both physical and structural data of HTS breaker arc model. MATLAB based Genetic Algorithm (GA) tool is used in order to determine the parameters of HTS arc model and ANSYS model is used in ANSYS workbench for the breaker size optimization. Different result of the parameters is then used in order to minimize the RRRV of the HTS arc model. Calculated voltage and currents are used to draw out the parameters. In the HTS arc model, the parameters are mostly two types:

i) Direct parameter: like near-zero arc conductance, post-arc current magnitude etc. which are from the empirical parameters.

ii) Indirect parameter: several arc parameters like time constants, cooling power, arc current and arc time etc,

In order to optimize the parameters, the nonlinear behavior of the HTS arc model is described as:

$$\frac{1}{g}\frac{dg}{dt} = \frac{1}{\tau}\left(\frac{ui}{P} - 1\right) = \frac{1}{\tau_0 g^{\beta}}\left(\frac{ui}{P_0 g^{\alpha}} - 1\right) \quad (4.3)$$

where g is the arc conductance (Siemens). The integral equation is known as:

$$g = \int \left(\frac{i^2(t)}{P(R)\tau(R)} - \frac{g}{\tau}\right)dt \quad (4.4)$$

$$R = \int \left(\frac{R}{\tau(R)} - \frac{v^2(t)}{P(R)\tau(R)}\right) dt \quad (4.5)$$

In the equation *i(t)* and *v(t)* are arc current (Ampere) and arc voltage (kV) respectively, while *R* for the arc resistance, *t* is the arc time constant (seconds) and *P* is the arc power loss (Watts).

Again, the equation for the constant of arc time is:

$$\tau = \tau(R) = \tau_0 R^{\alpha} \quad (4.6)$$

and for the loss of power it is:

$$P(R) = P_0 R^{\beta} \quad (4.7)$$

where *α* and *β* are constants of the arcs. The constants impact the conductance dependency of *P* and *t* respectively [60- 61].

Table 3: Optimized Parameters

Optimized Parameters	**Arc model Parameters**		
	Values	***Parameters***	***Values***
Rated breaking (I_{HTS}/I_{SC})	10/5	Rated Frequency	50Hz
Short Circuit breaking current	1200A	Over travel	4±1 mm
Rated short circuit making current	1500 A	Average closing speed	0.6~1.2 m/s
Stroke	7-9	Peak (kV)	550

In Table 3, different optimized parameters of arc model and ANSYS model are listed. The wide range of arc parameters shows the actual state of prospective HTS circuit-breaker.

The electrical behavior of the HTS circuit breaker can be predicted through the HTS arc model. But Browne's HTS arc models in MATLAB shows some limitations particularly for the complex physical operations within the HTS breaker model. Therefore for better outcomes, ANSYS Maxwell package is used to simulate complex actions in this analysis.

In reality, the arc resistance raises from zero to almost no-limit in milliseconds(ms) during the current interruption. The RRRV grows around the HTS circuit breaker contacts right after current interruption. A very small amount of current can still circulate around the contacts.

4.1.5 Transient analysis

The switching phenomena is regarded as one of the fundamental features of the circuit breaker which relates to the voltage level transformation. These phenomena are described as the fault current through the HTS arc model. It happens concerning the HTS breaker contacts prior to the current interruption. The non-zero resistance of the arc model is a concern in this regard. The arc also occurs around the contacts of the HTS circuit breaker. The arc voltage and current throughout the zero-value are simultaneously instantaneous. In cryogenic chamber, the arc is cooled off rapidly. As long as the current experiences current zero, the HTS circuit breaker can interrupt the current.

The arcing time is very important for analyzing the arc quenching behavior of HTS breaker arc model. For this calculation, the limitation index for fault current is used as:

$$a = \frac{(I_{sc1})i - (I_{sc2})i}{(I_{sc1})i}\% \tag{4.8}$$

where I_{SC1} and I_{SC2} are fault currents before and after HTS breaker respectively. For the study of arc-circuit interaction, the arc model simulates the nonlinear behavior and the minuscule time constants.

Switching Transient

Following peak ratings of the recovery voltage often need to be observed for the performance of AC high voltage circuit breakers: i. Peak TRV in kV ii. Time to Peak of TRV in μs and iii. RRRV in kV. These ratings are dependent on its different shapes as well. Three fundamental TRV features are often found as: i. Cosine waveform ii. Triangular TRV waveform iii. Exponential cosine TRV waveform.

TRV functionalities of a circuit breaker are also important in order to improve the short circuit current phenomena as it is known that TRV relies much on the short circuit level of a network [12].

TRV in a breaker is usually evaluated by the following equations:

$$V_{CB} = V_L + V_s \tag{4.9}$$

$$V_L = d(1 - K)\sqrt{\frac{2}{3}}E_{max} \tag{4.10}$$

$$V_s = 2K(T_L - T_d) \tag{4.11}$$

where T_d is the TRV-time delay, $T_L = \frac{V_L}{R_L}$ is the time to peak. Also $R_L = \sqrt{2}\omega I_L Z$ is used where I_L is the fault current, Z is the surge impedance of line, E_{max} is the rated maximum voltage K is the ratio of fault current to rated short-circuit current [62].

In this section, simulation configuration, system specification and modelling of equipment with an HTS Transformer with fault interruption are discussed for the same AC voltage of 11 kV. 1 MVA 11kV/415V HTS Transformer ratings [63] are used in this study.

RRRV Improvement

The waveforms of the TRV for HTS breaker arc model is calculated when a fault appears immediately after HTS transformer. The comparison is also identified under fault conditions as shown in Figure 13.

The HTS arc model is integrated in a circuit using convenient technique and RRRV is used as a function of the arc length. In Figure 13 , at t = 0 s, the circuit breaker contact separation starts. The computed RRRV is shown in Figure 13 (a). For this experiment, the power transformer is linked with the HTS circuit breaker. The time delay used is very low. A modified conventional TRV parameter is chosen.

In Figure 13 (b) and (c) it is clearly shown that the RRRV is reduced than Figure 13 (a). However, normal switching of breaker arc model experienced numerous difficulties.

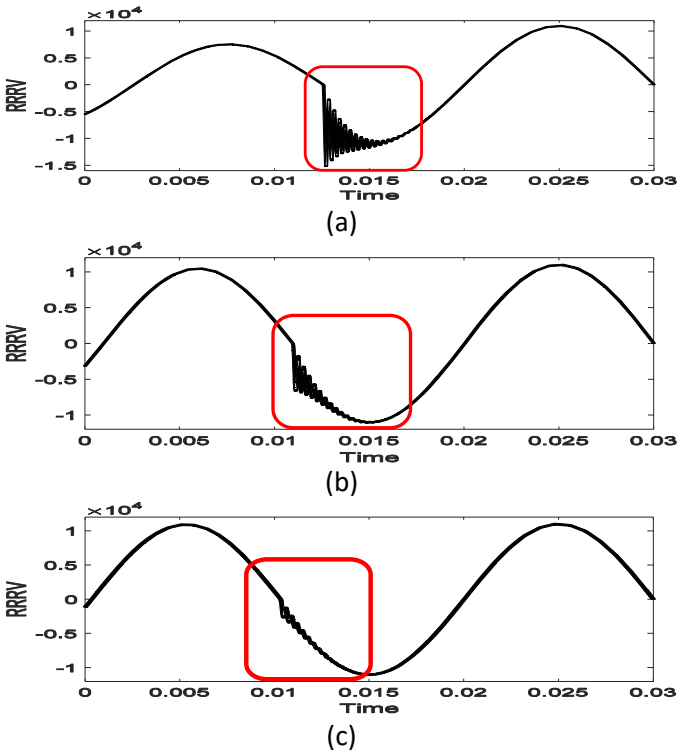

Figure 13. RRRV reduction by different optimized value (a) High RRRV in fault current (b)-(c) Improved RRRV result of HTS breaker arc model for fault

To summarize, it is found that normal switching of arc model cannot address the capacitance or inductive effect due to stored electric charge and its effect on fault current. In Section 4.2, the arc model is applied for further studies of RRRV analysis with controlled switching (CFI method) of arc model.

4.2 CONTROLLED SWITCHING OF HTS ARC MODEL

In this section, controlled switching of HTS arc model is investigated. The steps for this experiment are shown in Figure 14. In this particular study, it is assumed that the fault is located at the circuit-breaker terminal. For the controlled switching calculation, the mathematical expression of RRRV is developed across the HTS arc model. Then corresponding RRRV is investigated for limiting inductance and capacitance values.

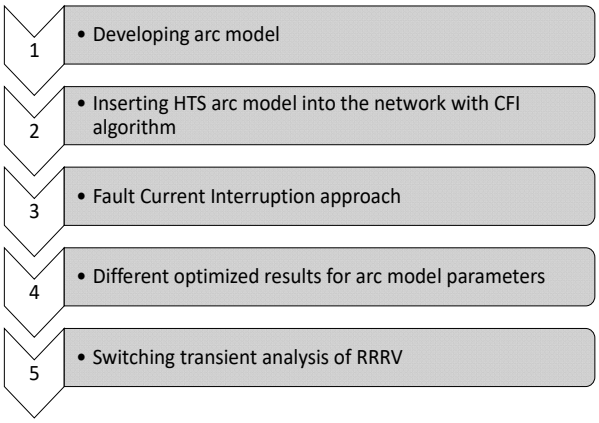

Figure 14: Steps for analysis of RRRV of HTS breaker arc model

4.2.1 Controlled Fault Interruption (CFI) Algorithm

The application of controlled switching of breaker arc model following the basic principles of Controlled Fault Interruption (CFI) is a known method for applications like energization or de-energization of power transformers. The primary goal of CFI is to synchronize the opening/closing of HTSCB's arcing contacts regarding a focused current zero and to achieve a steady arcing time for HTSCB. The result will be controlled by the restriction of a minimum viable arcing time before the focused current zero. The fundamental operating principle of HTS arc model for CFI is illustrated in Figure 15. For simplicity, only the theory for the opening part

of HTSCB's contacts is discussed in Figure 15. It also demonstrates tripping command in CFI mode of HTS arc model for a single phase fault current.

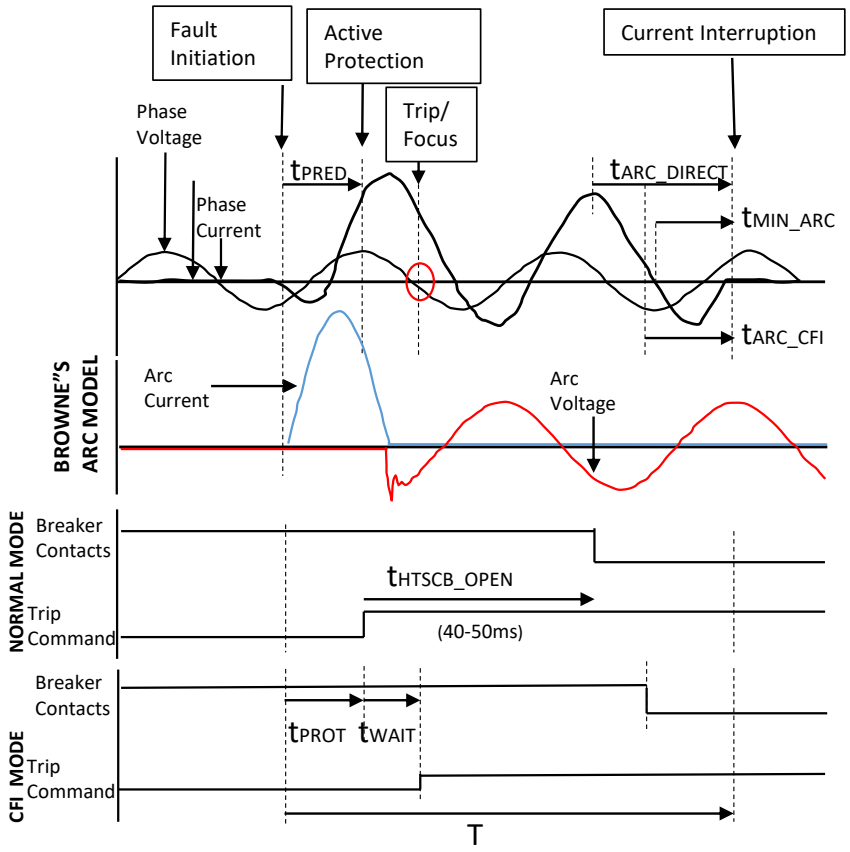

Figure 15: Basic theory of CFI

CFI method interrupts the arcing in order to achieve the quickest feasible arcing time. As shown in Figure 15, t_{PRED}= the system predicts about tripping, t_{HTSCB_OPEN}= HTSCB's contacts apart time, t_{MIN_ARC}= minimum arc time for interruption at first current zero, t_{ARC_DIRECT} =the direct arc time, t_{ARC_CFI}= an arc time for CFI method, t_{WAIT}= waiting time, t_{PROT} = protection response time. T= total fault clearing time. Predicting the current zero time of interruption should be accurate. It is noticeable, in Figure 15 t_{MIN_ARC} is considerably shorter than tARC_DIRECT. In CFI, arcing time will be near to minimum and t_{ARC_CFI} needs to be marginally larger than the expected t_{MIN_ARC}. For CFI, trip command of

HTSCB is also delayed after t_{PRED}. The sequence of controlled switching of breaker model with respect to phase voltage zero is a comprehensive process. Initially, the circuit breaker is set to open as shown in Figure 15. In normal switching mode, the contacts of HTSCB opens without focusing phase zero (anywhere in 0-360 electrical degrees). While in CFI mode, the contact of HTSCB will "focus" for a nearby phase zero to make the interruption. The operation happens instantaneous with respect to the phase voltage. In Figure 15, the objective is to match the opening/closing of HTSCB's contact near any phase voltage zero. Consequently, a “potential” phase voltage zero should be determined as a “focus” where opening/closing command of the HTSCB can be matched. Determining the “focus” phase voltage zero should have: i. previous phase voltage zero ii. HTSCB's predicted circuit breaker closing operation time (from Browne’s HTS arc model). Once "focus" point is decided, the updated operating time for CFI mode will be acknowledged. Thus, HTSCB's opening/closing request is delayed accordingly until a matched operation is reached.

4.2.2 HTS Arc model with HTS transformer in network

This is the same step already discussed as section 4.1.2. In normal condition, the flux reaches its highest value at $\pi/2$ angle or at one-fourth cycle. No flux should be associated to the HTS core before the supply is switched on. The flux value reaches to a higher value depending on the switching of HTS arc model.

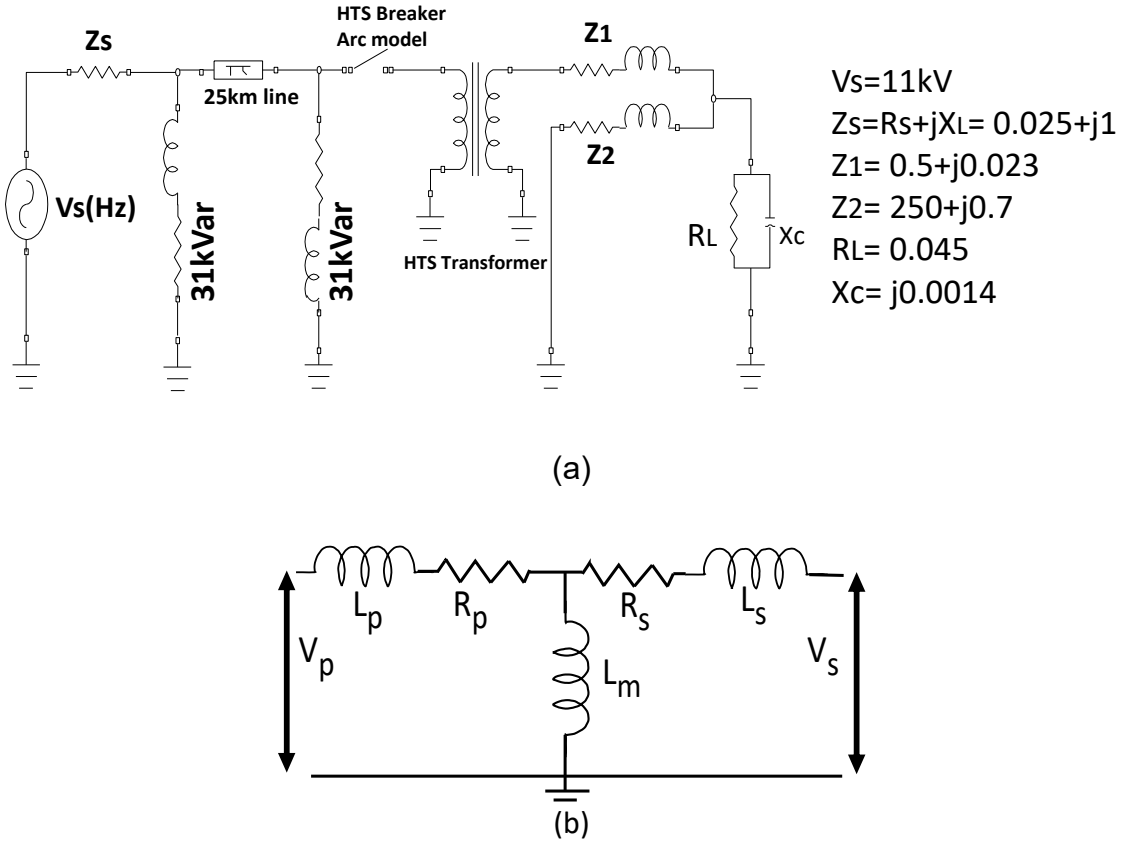

Figure 16: (a) Equivalent circuit of a network for HTS transformer (b)HTS transformer internal circuit

The HTS transformers block performs efficiently as it is developed to meet the mechanical reliability of insulation and windings system. In Figure 16 (b) , R_p and R_s are primary side resistance and secondary side resistance of HTS transformer respectively. $L_P$and L_s represent the leakage reactance of primary and secondary side of HTS transformer respectively. L_m presents the inductance of the HTS core while V_p and V_s are the terminal voltage of phase to the ground from primary side and secondary side respectively. Primary side voltage is found from Figure 16(b) as:

$$V_p = V_m \sin(\omega t + \theta) \tag{4.12}$$

$$V_p = i_\varphi R_p + \frac{N_1 d\emptyset_L}{dt} = \frac{N_1 \emptyset_L . R_p}{L_1} + \frac{N_1 d\emptyset_L}{dt} \quad (4.13)$$

where N_1 is number of turn, $\emptyset_L$ is core flux, θ is the voltage-phase at $t = 0$, $i_\varphi$is magnetizing current, L_1 is inductance in primary side.

$$\emptyset_t = (\emptyset_m cos\theta \pm \emptyset_r) e^{\frac{-R}{L}} - \emptyset_m \cos(\omega t + \theta) \quad (4.14)$$

where $\emptyset_r$ is residual flux and $\emptyset_m$ is maximum flux and. In Equation (5) At $\theta = \pi/2$ it is found:

$$\emptyset_t = \emptyset_r e^{\frac{-Rt}{L_m}} + \emptyset_m \sin(\omega t) \quad (4.15)$$

where residual flux magnitude, $\emptyset_r$ has some transient flux values and arc-time constant $\tau_1 = \frac{L_1}{R_p}$. The maximum of magnetizing current is obtained as below:

$$i_{\emptyset m} = \frac{(2\emptyset_m + \emptyset_r - 2.22\ A_i)}{\mu_0 A_t} \quad (4.16)$$

where A_i is area of HTS core, A_t is the area of the HTS core along winding and μ0 is air permeability. From equation (4.16) it is clear that $i_{\emptyset m}$ is directly proportional to the flux value corresponding to the magnetizing inrush current value of $\frac{B}{H}$ value can be minimized by adjusting the value of phase angle of the voltage at the time of switching.

4.2.3 Fault current interruption approach

The simulation is performed for 11kV HTS breaker arc model in order to examine the arc model ability to interrupt a fault with CFI method. The short circuit current Isc is line breaker current for a fault applied near HTS transformer line. There are some requirements that need to be followed for CFI method at fault condition in AC breakers [4]. The requirements for this system are described as: i. Finding the target current zero times having realistic precision (approx. ±0.5 ms) ii. Finding

the ‘focus’ current zero time (starting from 0.5 cycle) iii. Recognized steady circuit breaker opening time iv. Recognizing steady minimum arcing time. Requirement no. i and ii are the limitation of the control algorithm. Requirement no iii and iv are controlled from the characteristics of the HTSCB. Any substantial calculation response time limitations aren’t considered in the modified CFI algorithm. As this is really incomprehensive if CFI algorithm of HTS arc model needs a number of cycles to find the ‘Focus’ point. In CFI algorithm, the synchronizing control of arcing time is important in order to achieve a successful tripping of HTS arc model. The simplified flow chart of modified CFI process is shown in Figure 17. If the CFI method fail to arrive at a feasible ‘focus’ point, then a decision must be taken. The decision based on minimal operating time and waiting time help to permit the control scheme and to seek a viable solution. Otherwise it will defer tripping of HTS arc model for minimal operating time.

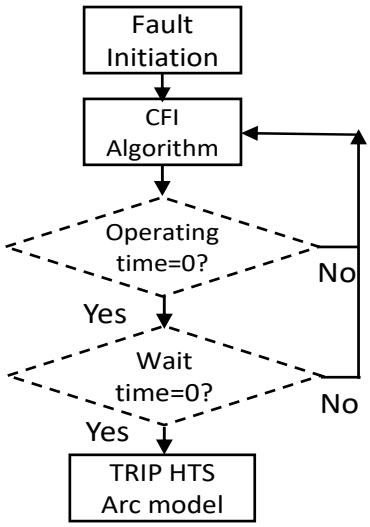

Figure 17: Simplified flow chart of CFI process with HTS breaker arc model

4.2.4 Different optimized results for arc model parameters for CFI

The arc equation and characteristic are determined in Chapter 3 as a non-linear function. The challenge of optimization is the solution of the highly non-linear equations. The conventional equations of Cassie and Mayr are used respectively in order to utilize the Browne's theory for the prepared HTS Arc model. The optimization of arc energy, loss of power and arc time in order to minimize the RRRV of the system is discussed in this section.

Parameter fitting of dynamic arc equations

The accuracy of the model substantially relies on the precision value of the parameters [59- 61]. The accuracy can be maintained either by model prediction method [64], [65],[66] or by optimization of parameters. HTS arc model parameters calculation demands intricate analysis for both physical and structural data of HTS breaker arc model. MATLAB® based Genetic Algorithm (GA) tool is used here in order to determine the parameters of HTS arc model. The different result of the parameters are then used as a way to minimize the RRRV of HTS arc model. First, calculated voltage and currents are used to draw out the parameters. In the HTS arc model, the parameters are mostly two types: i) Direct parameter: like near-zero arc conductance, post-arc current magnitude etc. which are from the empirical parameters. ii) Indirect parameter: several arc parameters like arc time constants, arc current, energy and loss of power etc, In order to optimize the parameters, the nonlinear behaviour of the HTS arc model are described as:

$$\frac{1}{g}\frac{dg}{dt} = \frac{1}{\tau}\left(\frac{ui}{P} - 1\right) = \frac{1}{\tau_0 g^{\beta}}\left(\frac{ui}{P_0 g^{\alpha}} - 1\right) \tag{4.17}$$

$$\frac{dg(t)}{dt} = \frac{g(t)}{\tau}\left(\frac{u(t)i(t)}{P} - 1\right) \tag{4.18}$$

where *g* is the arc conductance (Siemens), *α* and *β* are constants of the arcs, *P* is cooling power (Watts). For simplification of calculation some terms can be written as:

$$F_g(t) = \frac{dg(t)}{dt},\ F_f(t) = Xf_1(t) + Yf_2(t) \tag{4.19}$$

where $X = \frac{1}{\tau P}$, $f_1(t) = u(t)i(t)$, $Y = \frac{1}{\tau}$, f2(t)=g(t), $P = \frac{Y}{X}$ and the function can be written as:

$$F = \sum\nolimits_k [F_g(t_s) - F_f(t_s)]^2 \tag{4.20}$$

$$F = \sum\nolimits_s [F_g(t_s) - (Xf_1(t_s) - Yf_2(t_s)]^2 \tag{4.21}$$

where ts is time steps for CFI where u(t) and i(t) values are recorded. The values of the parameters are recorded in microsecond range with 20 second interval. Since the parameters are time-dependent variable. In equation (4.21), the values of *X* and *Y* which limit the values of *F* can be calculated as follows:

$$X = \frac{\sum_s \left(f_2(t_s).F_g(t_s)\right).\sum_s \left(f_2(t_s).F_g(t_s)\right) - \sum_s \left(f_1(t_s).F_g(t_s)\right).\sum_s f_2(t_s)^2}{[\sum_s (f_2(t_s).f_1(t_s))]^2 - \sum_s f_2(t_s)^2.\sum_s f_1(t_s)^2} \tag{4.22}$$

$$Y = \frac{\sum_s \left(f_2(t_s).F_g(t_s)\right).\sum_s (f_1(t_k))^2 - \sum_s \left(F_g(t_s).f_1(t_s)\right).\sum_s f_2(t_s)(f_1(t_s))}{[\sum_s (f_2(t_s).f_1(t_s))]^2 - \sum_s f_2(t_s)^2.\sum_s f_1(t_s)^2} \tag{4.23}$$

For full-cycle algorithm, if the convention of s sample is written as samples 0, 1, 2,….s-1. Then in exponential form the HTS arc model can be written as:

$$\begin{bmatrix} V_{s-1} \\ V_{s-2} \\ \vdots \\ V_0 \end{bmatrix} = \begin{bmatrix} \sin\theta_{s-1} & \cos\theta_{s-1} \\ \sin\theta_{s-2} & \cos\theta_{s-2} \\ \vdots & \vdots \\ \sin\theta_0 & \cos\theta_0 \end{bmatrix} \begin{bmatrix} V_0\cos\theta_s \\ V_0\sin\theta_s \end{bmatrix} + \begin{bmatrix} e_{s-1} \\ e_{s-2} \\ \vdots \\ e_0 \end{bmatrix} \tag{4.24}$$

It is regarded as time series data of thousand samples and sampled data are used in the Least Squares algorithm matrix calculation. Using Least Square estimation, noise can be eliminated as follows:

$$\begin{bmatrix} \sum_{j=0}^{s-1} sin^2\theta_j & \sum_{j=0}^{s-1} sin\theta_j cos\theta_j \\ \sum_{j=0}^{s-1} sin\theta_j cos\theta_j & \sum_{j=0}^{s-1} cos^2\theta_j \end{bmatrix} \begin{bmatrix} V_0 \cos\theta_s \\ V_0 \sin\theta_s \end{bmatrix} = \begin{bmatrix} \sum_{j=0}^{s-1} sin\theta_j V_0 \\ \sum_{j=0}^{s-1} cos\theta_j V_0 \end{bmatrix} \quad (4.25)$$

Following the same process, half-cycle Fourier algorithm will result in following equations for L^{th} focused current-zero:

$$V_p^L = \frac{2}{s} \sum_{j=L-s+1}^{L} V_j cos\theta_j \quad (4.26)$$

$$V_s^L = \frac{2}{s} \sum_{j=L-s+1}^{L} V_j sin\theta_j \quad (4.27)$$

Again, the integral equation of HTS arc model can be written for optimization as:

$$g = \int \left(\frac{i^2(t)}{P(R)\tau(R)} - \frac{g}{\tau}\right) dt \quad (4.28)$$

$$R = \int \left(\frac{R}{\tau(R)} - \frac{u^2(t)}{P(R)\tau(R)}\right) dt \quad (4.29)$$

In the equation *i(t)* and *u(t)* are arc current (Ampere) and arc voltage (kV) respectively, while *R* for the arc resistance. The equation for the constant of arc time is:

$$\tau g = \tau f = \tau(R) = \tau 0 R\alpha \quad (4.30)$$

Again, arc power in total is calculated as:

$$P_{tot} = P_{rad1} + P_{loss} + P_{axial} - P_{rad2} + P_{net} \quad (4.31)$$

where P_{rad1} is power loss due to radiation as the particles hit the wall of arc chamber of HTSCB, P_{loss} is the power loss due to the turbulence of arcing, P_{axial} is power loss for axial mass flow, P_{rad2} for radial mass flow and P_{net} is the net power of the arc. For HTS Arc model, the losses are calculated as:

$$P_{rad1} = l_{arc}.r_{arc}.T_{arc}^4.\ 2\pi.\sigma_B \tag{4.32}$$

$$P_{loss} = (h_{enth1} - h_{enth2})l.r_{arc} = P_0 R^{\beta} \tag{4.33}$$

$$P_{axial} = h_{enth1}.m_{axial} \tag{4.34}$$

$$P_{rad2} = h_{enth1}.m_{radial} \tag{4.35}$$

$$P_{net} = \frac{d}{dt}(\rho_{arc}.h_{enth1}.V_{arc}) - p_{arc}.V_{arc} \tag{4.36}$$

where l_{arc}, r_{arc}, , ρ_{arc}, p_{arc} ,T_{arc}, V_{arc} are length, radius, mass density, pressure, temperature and volume of the arc respectively. σ_B is Stefan Boltzmann's constant, h_{enth1} and h_{enth2} are enthalpy of the inner and outer surface of the arc chamber. The constants impact the conductance dependency of *P* and *t* respectively.

Parameter Extraction routine

Summary of the program logic written in MATLAB® is described in Figure 18. As shown in Figure 18, the primary assumption is offered for the four indirect parameters. The method has default primary speculation for all the parameters (by enduring lower value). Then, arc conductance and its rate of change are calculated after primary speculation. The conductance are then calculated along with its derivative. The modified Cassie-Mayr equation is used for a system identification problem. The estimation of linear and nonlinear parameter is used in this regard.

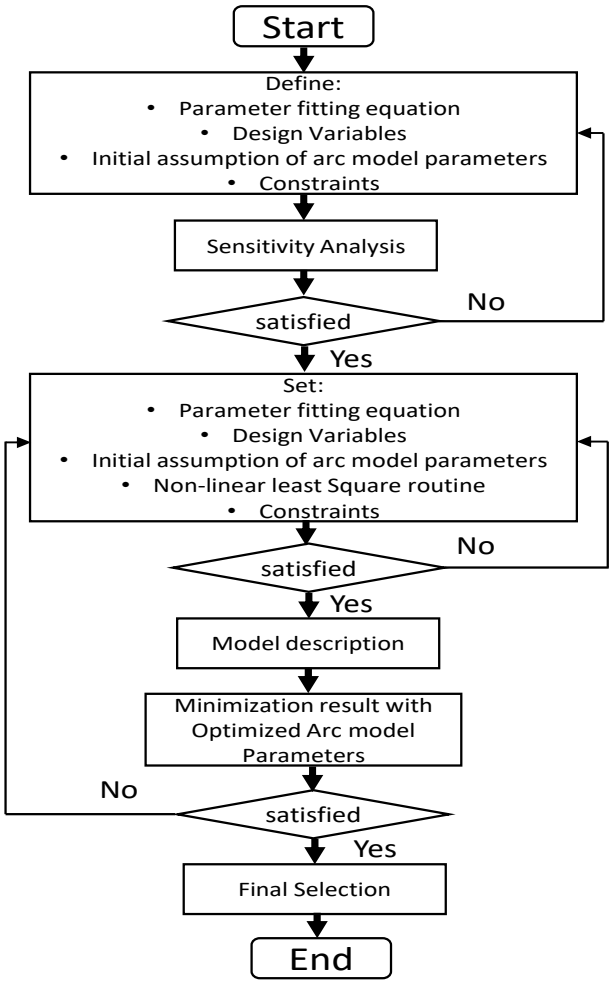

Figure 18: Flowchart of optimization routine

The modified Cassie-Mayr equation is rearranged to a system identification problem of linear and nonlinear parameter estimations. The Nonlinear Least Square Optimization built-in function by MATLAB® is utilised. The process iterates trying to find a global minimum. Finally, the optimized parameters of the modified Cassie- Mayr equation are extracted.

Optimized Model Parameters

The discussion here refers to Browne's HTS arc model. In Table 4, several optimized parameters of arc model are shown. The wide range of arc parameters shows the actual state of prospective HTSCB.The parameters are calculated for every half cycle.

Table 4: Optimized Parameters for CFI Interruption

Optimized Parameters	**Arc model Parameters**		
	Values	***Parameters***	***Values***
Rated breaking (I_{HTS}/I_{SC})	10/5	Rated Frequency	50Hz
Short Circuit breaking current	1200A	Average closing speed	0.6~1.2 m/s
Rated short circuit current (peak)	600	Peak (kV)	550

Table 5: Determination of Arc Parameters

Case	1	2	3	4
Optimization	Clearing time	Arc Energy	Clearing time	Arc Energy
Accuracy	Moderate $\pm$1 ms	Moderate	High $\pm$1 ms	High

Table 6: Model Parameters

Case	P_0	U	τ_g	τ_f
Optimization Result	154563.63	11.5235k	$1.0x10^{-6}$	$3.0x10^{-6}$

Determination of arc parameters and optimized model parameter are shown in Table 5 and Table 6 respectively.

4.2.5 Switching Transient Analysis of RRRV for CFI

The switching phenomena is regarded as one of the very fundamental features of the circuit breaker which relates to the voltage level transformation. These phenomena are described as the fault current through the HTS arc model. It happens concerning the HTS breaker contacts prior to the current interruption. Hence, the non-zero resistance of the arc model is a concern in this regard. The arc also occurs around the contacts of the HTS circuit breaker. The arc voltage

and current throughout the zero-value are simultaneously instantaneous. As long as the current experiences current zero, the HTSCB can interrupt the current.

Case-1: Terminal fault with Capacitance effect on RRRV

The short-circuit current reaches its highest value for terminal faults. In this case, the condition is experienced with the interruption of HTS arc model and compared with the current limiting index. In Figure 19, equivalent loop circuit for single-phase HTS arc model is shown. U_s is the source power and the peak value is $U_{pk}\sin(\omega t + \gamma)$ and Urms is the root mean square (rms) value, L_s, R_s and $Z_s = C_s$ is the source side inductance, resistance, and capacitance respectively. $Z_L = C_L$ is the load side capacitance and γ = phase angle on phase voltage when fault initiated.

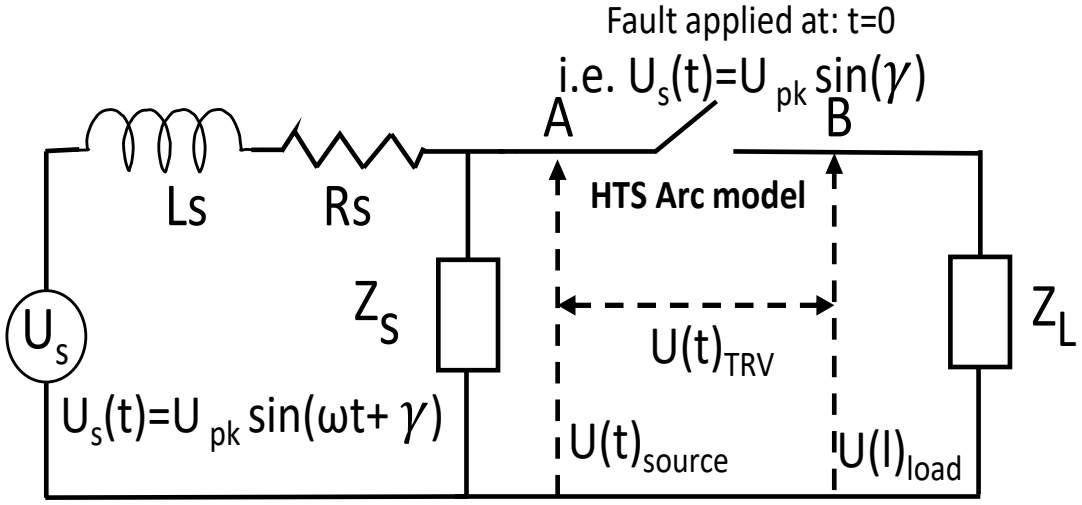

Figure 19: equivalent loop circuit for singl phase HTS arc model

The arcing time is crucial for analysing the arc quenching behaviour of HTS breaker arc model. For this calculation, the current limitation index for fault current is used as:

$$a = \frac{(I_{sc1})i - (I_{sc2})i}{(I_{sc1})i}\% \qquad (4.37)$$

where I_{SC1} and I_{SC2} are fault currents before and after HTSCB. For the study of arc-circuit interaction, the arc model simulates the nonlinear behaviour and the minuscule time constants. The steady RMS value of short-circuit current for the terminal fault is expressed as:

$$I_{sc2} = \frac{U_{pk}\sin(\omega t + \gamma)}{\sqrt{R_s^2 + (\omega L_s + \omega L_f)^2}} \tag{4.38}$$

Where $\omega = 2\pi f$ is the angular frequency of power source, f= 50Hz, L_f = field inductance due to meissner effect, Vs (t) = V_{pk} sin $(\omega t + \gamma)$ and fault appear at t=0 i.e. Vs (t) = V_{pk} sin (γ). To illustrate the relative impact of both the driving source voltage phase angle of fault initiation, and the system transient response time constant, the following (simplified) model for a single phase fault circuit is used. Assuming no pre-fault load current and a constant system fundamental frequency; fault is applied at time t = 0 on the driving source phase voltage. Solving via Laplace transformation will result in a fault current described by equation (4.39) below:

$$i_F(t) = I_F.[\sin(\omega.t + \gamma - \varphi) - \sin(\gamma - \emptyset).e^{(\frac{-t}{\tau})}] \tag{4.39}$$

where peak value of steady-state fault current, $I_F = \frac{U_{pk}}{\sqrt{(\omega^2 {L_s}^2 + {R_s}^2)}}$, t= time, $\omega = 2\pi f$, f = power system (fundamental) frequency, R= fault resistance, L = fault inductance, $\tan(\emptyset) = \frac{\omega L_s}{R_s}$, where ∅ is power factor angle during short-circuit situation, establishing by L_s and R_s, the time constant of the transient component of fault current, $\tau_s = \frac{L_s}{R_s}$. C_s and C_L are capacitors connected in parallel with HTSCB. Voltage around Cs and CL (i.e U_A and U_B) reach their peak values at U_{Apk} and U_{Bpk} at the instant while the arc current passes zero.

$$U_{Apk} = U_{Bpk} = \sqrt{2}I_{ss}L_s = \frac{\sqrt{2}U_{pk}\sin(\omega t + \gamma)L_s}{\sqrt{R_s^2 + (\omega L_s)^2}} \quad (4.40)$$

The voltage equation is governed by the second order equation (4.41) as fault shows at *t=0* i.e. $V_s(t) = V_{pk}sin(\gamma)$ and I_{ss} is the total fault current in the loop. Also, the TRV can be considered constant value during fault as Vs varies very little during short arc timing.

$$U_0 = U_{Apk} + L_s C_s \frac{d^2 U_{Apk}}{dt^2} + R_s C_s \frac{dU_{Apk}}{dt} \quad (4.41)$$

In equation (4.41), the resistance, Rs regarded as very small value. Therefore, U_A will vary in an oscillatory shape. In equation (4.41), substituting $U_{Apk} = Ae^{mt}$, $\frac{dU_{Apk}}{dt} = mAe^{mt}$, $\frac{d^2U_{Apk}}{dt^2} = m^2Ae^{mt}$ and removing the forcing function, the equation stand as:

$$L_s C_S m^2 + R_S C_S m + 1 = 0 \quad (4.42)$$

$$m = \frac{-R_s C_s \pm \sqrt{R_s^2 C_s^2 - 4L_s C_s}}{2L_s C_s} \quad (4.43)$$

This becomes a complicated system to solve the under fault condition. In particular, when the value of the square root is negative and complex values are turned out. Applying Laplace transforms for the domain of Figure 19 RLC network circuit analysis will solve the second order equation (4.42) to find the circuit behaviour for terminal fault effect. The complex transient condition of s domain analysis for Figure 19 is re-written in equations (4.44) and (4.45).

$$\frac{U_0}{S} = U_{Apk} + L_s C_s S^2 U_{Apk} + R_s C_s S U_{Apk} \quad (4.44)$$

$$U_{Apk} = \frac{U_0}{s(L_s C_s S^2 + R_s C_s + 1)} \quad (4.45)$$

Again, t_{pk} is the time when TRV, U_{Apk} grows as first peak. If T_1 and T_2 are the oscillation period of the capacitor voltage in the source side and HTS breaker arc model respectively and $T_2<T_1$ then,

$$t_{pk} = \frac{T_2}{2} = \pi\sqrt{2L_sC_s} \tag{4.46}$$

RRRV of HTS arc model is defined as:

$$RRRV_{HTS} = \frac{V_{AB}}{t_{pk}} \tag{4.47}$$

$$RRRV_{HTS} = \frac{V_{Apk}}{t_{pk}} = \frac{U_0}{s(L_sC_sS^2 + R_sC_s + 1)\pi\sqrt{2L_sC_s}} \tag{4.48}$$

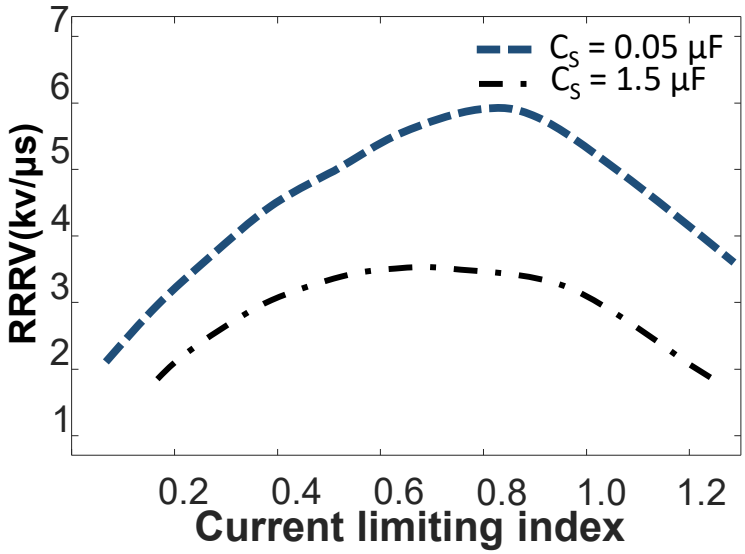

Figure 20: RRRV vs current limitation index with terminal fault Cs =0.05 μF and 1.5 μF

This computational analysis is carried for: Us= 11kV, Ls= 10mH, Rs= 0.1 Ω, According to equations (4.37) and (4..48), the graph for RRRV and current limitation index, a are shown in Figure 20. It is seen if the value of the RRRV also increases and soon have a drop down. The reason is the arc chamber is pressurized by the RRRV after arcing. When rate of recovery near contact distance is quicker than the RRRV, it can be considered as a successful

interruption. The very first 5–10μs of the recovery phase region is known as recovery region. The region after 40 μs of interruption is known as the dielectric region. Whenever RRRV is quicker near contact distance, then there is a high chance of HTSCB breakdown. In Table 7, an overview of successive restrike current amplitudes is recorded.

Table 7: Overvoltage at the time of Restrike (limited numbers)

Case	RRRV- 1st	RRRV - 2nd	RRRV- 3rd	RRRV - 4th
Loop Voltage (pu)	1.5845	1.6684	1.8959	1.9143
Restrike current (A)	255.65	267.27	284.76	287.35
Closing time (sec.)	0.016	0.018	0.021	0.022
Phase Voltage (pu)	1.9374	2.1852	2.8734	2.9634

This is worthwhile to check the limiting inductance effect on RRRV for HTS arc model along with capacitance effect which is discussed in the following section.

Case-2: Out of phase fault with limiting inductance effect on RRRV

An inductance with HTS arc model terminal is used for this study. Following peak ratings of the recovery voltage often need to be observed for the performance of AC high voltage circuit breakers [62]. The mathematical expression of TRV is calculated in this section in order to express the RRRV as a function of different circuit parameters. Then, the influence of limiting inductance and fault current on RRRV is theoretically determined for an out of phase fault. TRV in a breaker is usually evaluated by the following equations:

$$V_{CB} = V_L + V_s \tag{4.49}$$

$$V_L = d(1-K)\sqrt{\frac{2}{3}}E_{max} \tag{4.50}$$

$$V_s = 2K(T_L - T_d) \tag{4.51}$$

where T_d is the TRV-time delay, $T_L = \frac{V_L}{R_L}$ is the time to peak. Also $R_L = \sqrt{2}\omega I_L Z$ is used where I_L is the fault current, Z is the surge impedance of line, E_{max} is the rated maximum voltage K is the ratio of fault current to rated short-circuit current.

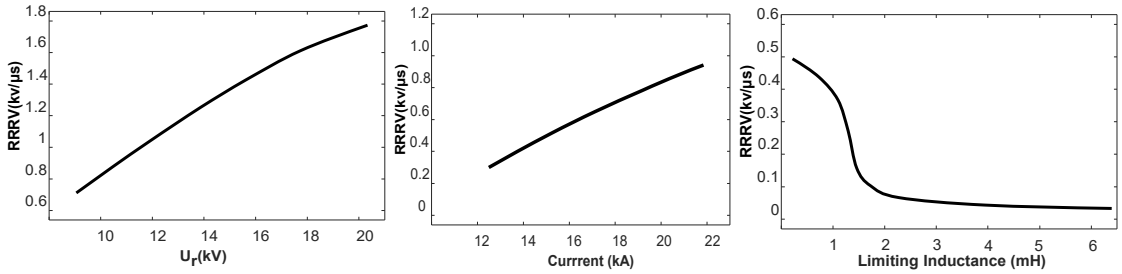

(a) (b) (c)

Figure 21: Variation of RRRV for (a)out of phase fault (b)the function of fault current magnitude and (c) limiting inductance

At *t = 0* sec., the circuit breaker contact separation starts. The computed voltage and RRRV are shown in Figure 21 for out of phase fault, fault current and limiting inductance. The calculated values of U_r and RRRV obtained in a simplified way. For the circuit of Figure 19, the waveform for different parameters is determined for theoretical expression of RRRV. The peak value of RRRV can be determined from the slope of the Figure 21(a) and Figure 21(b). For the minimum TRV-time delay, RRRV reaches its peak value of 1.7 Kv/μs. From the results, it is found that the value of limiting inductance has the influence on RRRV of HTS breaker arc model. On the basis of the mathematical equations (4.48), (4.50) and (4.51), the expression of RRV as a function of limited current can be written as:

$$RRRV_{HTS} = \ 1.2\ \frac{V_{AB}}{t_{pk}} \tag{4.52}$$

The factor 1.2 determines the tangent slope for the waveform of TRV. the dependence of RRRV on limiting inductance is shown in Figure 21 (c). The value

of RRRV decreases significantly for increasing the small value of limiting inductance. t_{pk} is the time where TRV shows its highest value of V_{AB}. In Table 8, numerous results during the second restrike are shown for both out of phase and terminal fault.

Table 8: Overvoltage during second Restrikes

Rated Voltage, U_r	Fault type	TRV Peak value U_0	Time t3 µs	Time delay ms	RRRV= u0/t3 kV/ µs
11kV	Terminal	28.4	28.4	18	0.21
	Out of phase	18.2	18.4	9	0.32

As mentioned in section 4.2.1, arcing time will be near to minimum and t_{ARC_CFI} needs to be marginally larger than the expected tMIN_ARC. Hence, as shown in Table 9 fault case number 3 is a successful case of CFI. In Case numbers 1 and 2 minimum operating time of 0.5 second is achieved instead.

Table 9: CFI results (limited numbers)

Time Segments	t_{PROT}	t_{OPEN}	t_{MIN_ARC}	t_{ARC_CFI}	
Fault-1	15ms	22ms	12ms	10ms	X
Fault-2	15ms	22ms	12ms	10ms	X
Fault-3	15ms	22ms	12ms	8ms	✓

4.3 CONCLUDING REMARKS

The normal switching used in Section 4.1 fails to address the capacitance or inductive effect due to stored electric charge and its effect on fault current. Therefore, in Section 4.2, the arc model is applied for further studies of RRRV analysis with controlled switching (CFI method) of arc model.

Section 4.2 describes the simulation results of the fault arc for two different scenarios. The HTS arc model simulation results presented in this section for RRRV show very promising prospect for reducing the post-arc current for HTS

application. The arc characteristics for current zero measurements also ensure successful interruption of the experimental setup. The model also helps to develop the future TRV for HTS breaking applications. The result of RRRV for the transformer fed fault case indicates the benefits of HTS arc model during the interruption. The proposed CFI algorithm for HTS arc model with 'focus' current zero therefore, is believed to determine the 'focus' time before ± 0.5 ms in real life application.

CHAPTER 5- APPLICATION OF CONTROLLED SWITCHING OF HTS ARC MODEL FOR DIFFERENT FAULT PROBLEMS

In this chapter, Controlled Fault Interruption (CFI) mode application with HTS arc model is used for two different problems. The theory is used to mitigate the residual flux of HTS Transformer at first. The residual flux mitigation method for HTS transformer is demonstrated with CFI mode at first in section 5.1. The results show the usefulness of the calculation method. It reveals that the calculation can estimate the polarity of the residual flux accurately.

Then, a fault detection algorithm is developed in order to detect and minimize the post-arc current of HTS arc model in section 5.2. THD is calculated under various working situations for HTS arc model's calculated voltages. The simulation shows the transient behaviors of HTSCB during opening condition. The results also show the efficiency of the suggested process by predicting the faulty condition of HTSCB mechanism.

This chapter is based on the following articles:

[1] **A. Ullah**, T. T. Lie, K. Gunawardane and N. K. C. Nair, " Mitigation of Residual Flux for High-Temperature Superconductor (HTS) Transformer by Controlled Switching of HTS Breaker Arc Model" 2017 IEEE ISGT, Auckland, 2017, pp. 1-6.

[2] **A. Ullah**, T. T. Lie, K. Gunawardane and N. K. C. Nair, " Failure Detection Algorithm for High-Temperature Superconductor (HTS) Breaker Arc Model" 2017 IEEE ISGT North America, USA, 2018.

5.1 MITIGATION OF RESIDUAL FLUX FOR HTS TRANSFORMER

AC circuit breaker's controlled switching is a popular method to reduce dielectric and thermal stresses during switching of transformers, transmission lines, reactor and shunt capacitors. The magnitude of inrush current often reaches five to nine times of rated magnetizing current and thus it affects the network stability. Particularly, it affects the superconductivity of HTS transformer. Moreover, residual flux is developed in HTS transformer due to high inrush current. The amount of flux may increase to a very high value that has direct impact to have a very high transient inrush current. This section of the thesis presents inrush current mitigation phenomena in a single-phase HTS transformer by controlled switching of HTS breaker arc model. The inrush current phenomenon is modelled for a single-phase HTS transformer. The inrush current is mitigated by the reclosing of a new type of arc model named HTS breaker arc model and the residual flux also minimized. The calculating method is established on the investigation of fast switching timing and characteristics of the HTS breaker arc model.

5.1.1 Different switching methods and CFI

Typically, three different approaches are followed to mitigate magnetic inrush in any power transformers.

(i) The residual fluxes can be ignored by shutting at peak of voltage. The phenomena can overcome a reasonable degree of inrush current.

(ii) By shutting the load side voltage while prospective flux is equal to residual flux. Residual flux is measured by integrating load side voltages.

(iii) By controlled switching of the breaker. The Residual flux needs to be locked to its least probable degree during every cycle through controlled de-

energization. The method needs to be accompanied by controlled energization of HTS transformer. To the extent that prospective flux needs to be identical to the residual flux.

Other than these three methods Pre-Insertion Resistors (PIR) has also been used to mitigate inrush currents for transformers. Methods (ii) or (iii) are well-known method in order for mitigating inrush to a extremely decreased level. On load side Method (i) and (ii) needs supplemental voltage measurements. Method (iii) is chosen for this experiment among three methods for its efficiency, simplicity, and uncomplicated practical application.

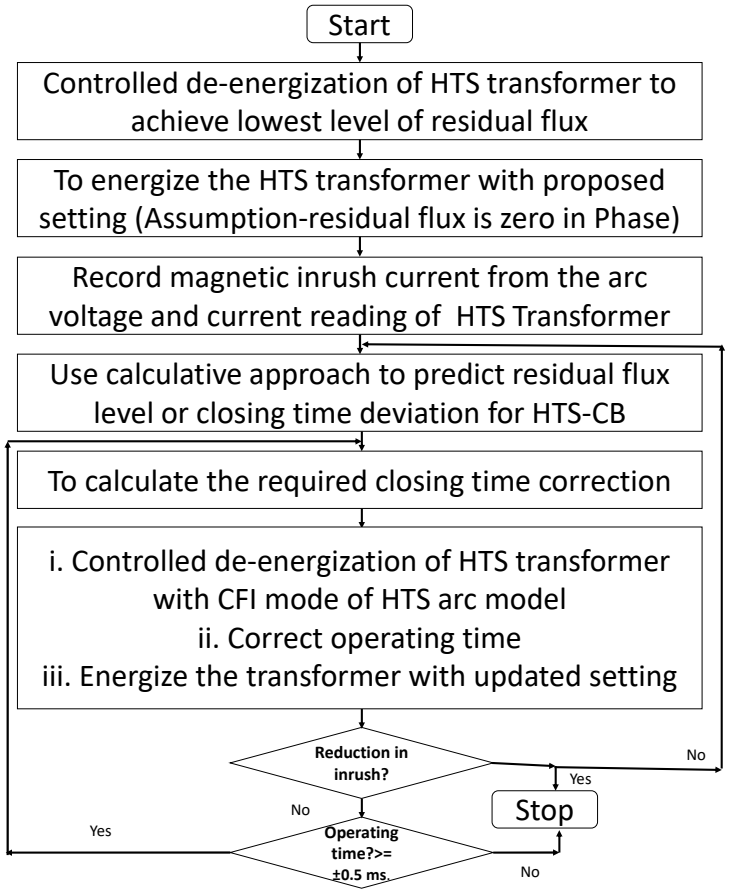

Figure 22: Modified Methodology of mitigating residual flux with CFI

The proposed procedure is conveniently comprehended by block diagrams demonstrated in Figure 22. In very first step, residual flux in the phase is counted as zero. At the time of initial energization operation inrush current is recorded.

For next stages, the closing times for HTS breaker arc model is fixed by the optimum value of 1ms in order to reduce residual flux. An implementation of the large correction value in the phases may result into a misleading outcome. The high inrush current with faulty correction value would detrimentally affect HTS transformer's superconductivity. Afterward, transformer needs to be de-energized again in a controlled way. The phenomena will be accompanied by re-energization using adjusted and updated settings. Inrush current can still be identified as increasing. In that case, the entire method needs to commence again and the operating time requires to be decreased more until ideal mitigation impact is obtained. During each energization attempt, controlled de-energization needs to perform earlier than the controlled energization procedure.

The energization of 11kV HTS transformers often results for high inrush currents. Consequently, it imposes substantial thermal stresses on HTS transformers and associated circuit breakers. The controlled switching of AC circuit breakers is a popular method to overcome the inrush current. Though, some uncertainties in the measurement of circuit breaker's operating time are found in [67]. CIGRE is noted to have potential research works regarding the need of HVAC circuit breakers with controlled switching controller [68-69].The method helps to reduce dielectric and thermal stresses during switching of shunt reactors and capacitors or transformers. Controlled switching features significant financial advantage along with several technical benefits. The performance of HTS breaker arc model has been used in this research to investigate its controlled switching. This is vital to get a steady operating time of HTS circuit breaker or breaker arc model throughout the operations in order to attain the similar amount of inrush current

and residual flux level. Usually, most of the modern era breakers present outstanding operating time regularity within ±0.5 ms.

5.1.2 Residual flux calculation using CFI

The residual flux of HTS transformer relies on three issues: (i) the winding connection (ii) the structure of HTS transformer and (iii) power factor angle. As power factor angle is a changing value, the result should observe before switching off the HTS transformer.

As per the law of Faraday, core flux is acquired through the integration of induction voltage. The HTS breaker contacts are assumed to be separated when the transformer opens. In HTS breaker the arc blows out in cryogenic chamber till the current becomes zero. Subsequently, the current will turn to zero completely.

Primary voltage side's blow out angle is considered as identical to the power factor angle. The HTS core flux can be found then as per the equation of the flux and the voltage. Following the arcing, residual flux becomes weaker. The residual flux is infected by load features and power storage as well. After maintaining all these factors residual flux will be kept at a steady value. The HTS transformer linked to bus-bar doesn't have any voltage reading of opening phase if the phase is blow out. Due to HTS winding connections and core structure, the fluxes will be altered. The flux will attenuate and will reach a steady value. Finally, the analysed result satisfies the law of Faraday.

The residual flux density is expected to reduce after first cycle resulting from losses. It is a damping function of transformer losses. The new value of residual flux density, B_r(new), is introduced as

$$B_{r(new)} = B_{r(old)} - [B_{mp}.\frac{K_3.R}{X_s}(2.(sin\theta - \theta cos\theta))] \quad (5.1)$$

where K_3 is the correction factor inrush-decay R is the total resistance of system resistance and transformer winding resistance. The calculations are replicated to analyse the high values of the subsequent cycles [70].

5.1.3 Mitigating inrush current

There are two major ways of mitigating inrush current: (i) by finding the best switching time (delay or advance of reclosing time of breaker) and (ii) by controlled switching method. Best switching timing is searched in this section.

The simulation result shows the existence of high inrush current produced resulting from saturation of HTS transformer.

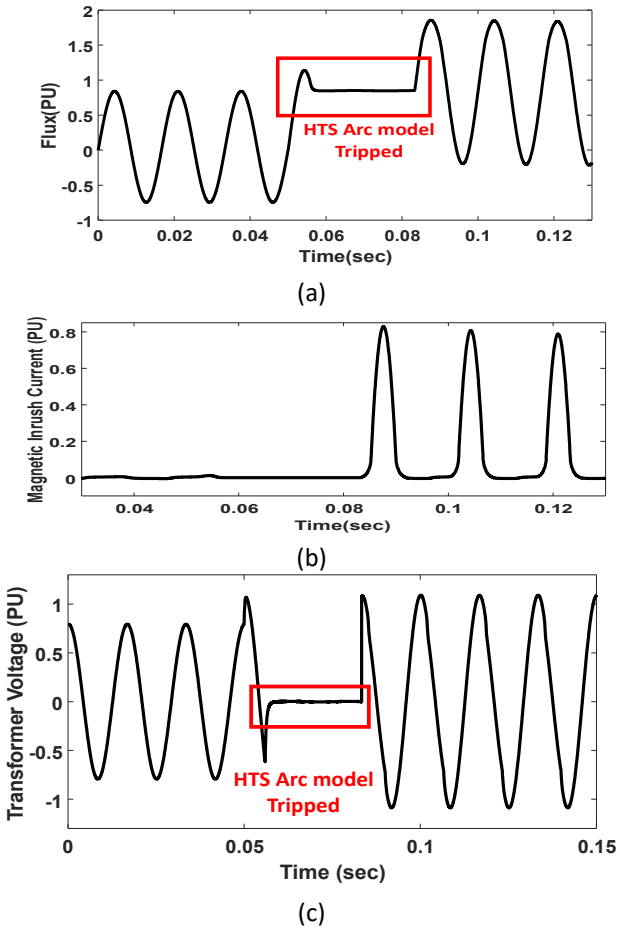

Figure 23: (a)Flux (PU) (b) Magnetizing current and excitation current (c) Transformer voltage

In the beginning, the HTS breaker arc model opens at t = 3 cycles (0.05 sec.), then it recloses at t = 5 cycles (0.09 sec.). The high inrush current values with controlled switching of HTS arc model is demonstrated in Figure 23. The inrush current is mitigated in great extent. This feasible method can mitigate the inrush current value to nominal value from six to ten times lower.

There is a significant level of inrush current reduction observed during the simulation. It varies within the range of 1-1.3 per unit (pu) or close to 1.8 pu considering different parameters of HTS breaker arc model. The residual flux decreases if the operating time of breaker is remarkably steady. However, the inrush current is not likely to be reduced lesser than HTS transformer's full load current with the applied method. Although marginal residual fluxes can be obtained with controlled de-energization. The results show the transient varied nearly 11% from the nominal voltage within the time period of 3 cycles. The calculated values are listed in Table 10.

Table 10: Calculated Values at Mitigating condition

Energization of HTS transformer Phase voltage		Overvoltage (within permissible limits)	
Calculated minimum value [p.u]	0.95	Phase Voltage [p.u.]	0.95
Reference voltage limit for transient [p.u.]	0.91	Magnetizing flux [p.u.]	1.98
Minimum/ permissible value [p.u.]	0.93	Magnetizing Current [p.u.]	3.4
Restoration time [ms]	45	Restoration time [ms]	45

In Table 10, the short-circuit condition highlights the high values for energization of HTS transformer due to mitigated inrush current. The transient results depend on short circuit voltage transient limit which is allowed value of 0.94 pu. The

situation of 1.0 pu inrush current peak permission is investigated for similar scenario in this subsection. The practical specifications for the tolerable deviations is identified for this scenario. The HTS core is led to saturation when transient inrush currents take place. Consequently, magnetic flux reaches its peak following energisation. For this scenario, the method and operating time need to find again.

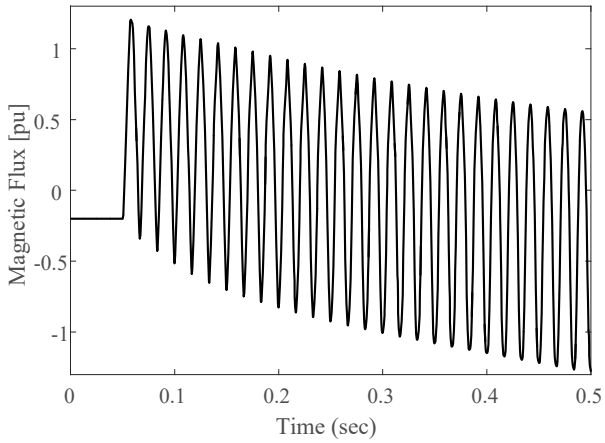

Figure 24: Magnetic flux result after energization with acceptable tolerances of 1pu maximum inrush current peak

In Figure 24, magnetic flux result after energization for this scenario is shown. Acceptable tolerances of 1pu maximum inrush current peak is applied. It is found that the tolerable values vary for positive and negative values of residual flux. It means that the magnetic flux doesn't attain steady state condition for this scenario. The result nonetheless maintains an offset value in the beginning as a result of small damping of the system. If the delay is increased to 7 to 10 cycles, it does not bring significant improvement. The inrush current can still be driven below the full load current ratings of HTS transformer. In all cases, the operating time needs to be lessened until the desired mitigated result is obtained.

5.2 FAULT DETECTION ALGORITHM WITH CFI METHOD

This section of the thesis provides a failure detection algorithm for evaluating the faulty operation for a High-Temperature Superconductor Circuit breaker (HTSCB) operation. The simulation of HTSCB is achieved using an HTS arc model. The arc model is used to define the transient behavior of HTSCB after each operation. The transient signals resulting from electric arc comprise numerous harmonics. The total harmonic distortion (THD) index is regarded in diagnosing the circuit breaker (CB) operating mechanism. The simulation of arc model and corresponding signal analyses are performed in MATLAB® environment. The calculating method is established on the investigation of fast switching timing and characteristics of the HTS breaker arc model.

5.2.1 Different detection techniques

There are a number of detection approaches existing for CBs. A brief summary of different existing detection techniques for the specific condition of the circuit breaker is described in this section. A steady monitoring period is described as a non-stop sequential sampling about circuit breaker's condition. Data collection, analysis, investigation and processing periods possibly does not produce real-time solutions. As the processing periods are not always recorded with time, analysis of different artificial intelligence techniques like neural networks, fuzzy logic and expert system measurements are gathered from these continuous or periodic monitoring methods. By applying historical or statistical information the mentioned techniques can interpret the recorded data [71]. A monitoring technique relating to Vacuum Circuit Breakers (VCB) is documented to be diagnosed online [72]. The noticeable failures can be identified and located by the monitoring technique. The method is based on electrical rating measurement,

sensor data, communication methodologies and computer analysis. Parameters like temperature, the resistance of contact area, contact's electrical stress tolerance, coil and line currents and condition of the operating system can be diagnosed [72]. Ref. [73] reports about a constant vibration study of CB analysis with over thousand vibration samples. The samples are accumulated in normal operation and from the operating system of different SF6 CBs. The samples are assessed at the time of individual closing or opening procedure. Then frequency and time variation is determined by comparisons with signatures. It is checked if the vibration results are reliable enough to withstand both mechanical and electrical stresses throughout normal or faulty condition. Then, the method is trusted to deliver beneficial diagnosis information [73]. Ref. [74] suggested a different method with Artificial Neural Networks (ANNs). The method accepts dynamic characteristics of the mechanism using simulation. It is demonstrated that predefined types of mechanical problems for breakers can be determined proficiently by the method [74]. In addition, Ref. [75] reports about a distributed system that facilitates CB maintenance and asset supervision. It works with an architecture determined by server and client to send meaningful data from the CB servicing engineers to operators working on the site in order to diagnosis CB condition. Then, the profile is translated as an index during tripping time [75]. A data mining approach for the evaluation of CB data is reported as well. This approach uses data from trip coil as well. The data creates the base of a decision making algorithm. The algorithm works for CB' when routine trip test runs [76]. There are some more instances by using the approach of close and trip coil current signatures. In these approaches, the most productive features of coil current is identified initially. Then, the anomalies of the features are recorded and compared with healthy CB data. Afterward, the anomalies of features are

categorize using absolute values. Finally, failure detection is accomplished [77]. Ref. [78] reports about overvoltage failure of VCB and its disastrous malfunctioning via simulations contemplating numerous re-ignitions of a VCB model [78]. The application of the fuzzy logic principle, analytical hierarchy method and certain reasoning of CB is proposed in [79]. One other research studies the improvement of a monitoring algorithm which is real-time. The algorithm is carried out for monitoring trip coil of a CB assembly. It suggests the maintenance activities when in faulty condition. The suggested method determines the abnormal conditions, identifies the reasons, and states feasible solutions for the CB trip coil assembly [80]. Another instance of contact force monitoring for VCB is also reported in [81]. It is shown that the detection of the contact separation is feasible and touch moments can also be recorded by applying numerous signal processing methods and designed force sensors. The closing velocity, opening velocity and the open gap is figured out with the move of each phase by utilizing measured contact separation and touch moments indirectly [81]. One more technique is recommended to analyse the faulty situations of SF6 CB. The features are first observed in by control circuit signals. Then the signals are co-related with the features for target analysis. The method claimed to cover nearly 60% of CB defects. Besides, a data-mining technique is also used to categorize the captured data with preceding enlisted data in order to figure out the healthy or faulty condition of CBs [82]. Lastly, another protocol is determined by the fuzzy-probabilistic technique. The technique can identify CB operating mechanism and can utilize its close and trip coil current signatures to present a convenient condition evaluation technique [83]. A brief summary of the techniques is described from [84]. A contribution on another technique determined by HTS arc model is described in this subchapter. The analysis can

help evaluating the operating mechanism of CBs from the arc voltage calculations.

5.2.2 Process of the algorithm

Short Time Fourier Transform (STFT)

The failure detection algorithm is designed in order to do the harmonic analysis of HTSCB using STFT. A condition evaluation algorithm for HTS arc model is discussed in this section. The algorithm is competent in order to recognize the failure variation in the system. According to the algorithm result, the system operator can decide about the servicing of the HTSCB. The working situation of HTSCB can be analyzed from the developed voltage around it by the algorithm. Arcing of a breaker functioning comprises essential details about the condition of the breaker. The information can be applied in this suggested evaluation algorithm. After arcing two important information is found from arc model: i) arc voltage and ii) transient recovery voltage (TRV). TRV is part of arcing voltage when it is quenched. The algorithm is carried out in a flowchart in Figure 25.

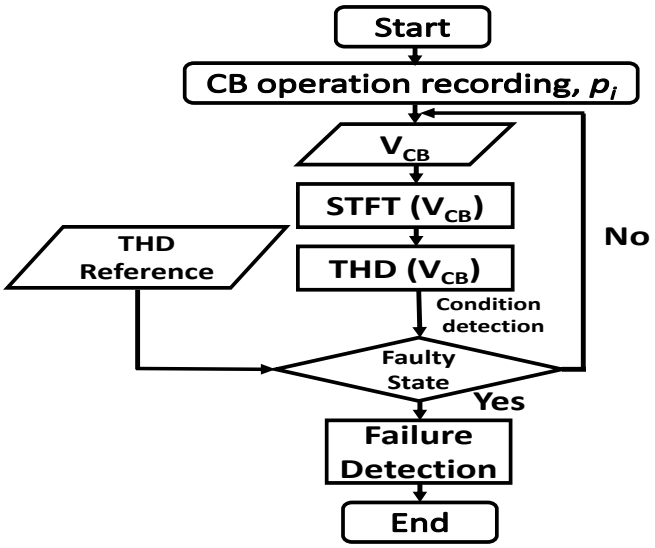

Figure 25: Outline of proposed failure detection algorithm

The flowchart is described mainly in three steps:

1) The arcing voltage needs to be evaluated for minimum two cycles with a proper rate of sampling.

2) STFT is applied then as a way to attain the frequency content of the assessed signal. In STFT, a non-zero window function with a short duration of time travels via the time domain and also is multiplied by the signal under transformation simultaneously.

3) THD is then applied as a directory for HTS arc model. The live voltage THD of the CB normal operation can be measured and then compared to the reference THD. Failure detection performs based on THD deviation value. If the pre-specified tolerance limit is surpassed, then, the failure recognition algorithm is carried out. Otherwise, the procedure starts from the beginning by voltage measurement. There can be unsuccessful operation because of arcing restrikes and it can delay the procedure of HTSCB.

The Fourier transform is applied to each multiplication pair to build a two-dimensional expression of the signal. The numerical formula of the STFT is described as:

$$STFT\{x(t)\}(\tau,\omega) \equiv X(\tau,\omega) \tag{5.2}$$

$$STFT\{x(t)\}(\tau,\omega) = \int_{-\infty}^{\infty} x(t)\omega(t-\tau)e^{-j\omega t}dt \tag{5.3}$$

In equations (5.2) and (5.3), x(t) is the chosen signal for transformation, X(τ,ω) is fundamental for Fourier Transform of *x(t)ω (t-τ)* and *ω(t)* is used as a window function. The window function is typically a Gaussian or Hann window centered

near zero. For the classification of *ω(t)*, the area of the window function can be expressed as:

$$\int_{-\infty}^{\infty} \omega(\tau)d\tau = 1 \tag{5.4}$$

$$x(t) = x(t)\int_{-\infty}^{\infty} \omega(t-\tau)d\tau = \int_{-\infty}^{\infty} x(t)\omega(t-\tau)d\tau \tag{5.5}$$

Considering continuous Fourier transform:

$$\mathrm{X}(\omega) = \int_{-\infty}^{\infty} x(t)e^{-j\omega t}dt \tag{5.6}$$

$$X(\omega) = \int_{-\infty}^{\infty} [\int_{-\infty}^{\infty} x(t)\omega(t-\tau)d\tau]e^{-j\omega t}dt \tag{5.7}$$

$$X(\omega) = \int_{-\infty}^{\infty}\int_{-\infty}^{\infty} x(t)\omega(t-\tau)e^{-j\omega t}d\tau dt \tag{5.8}$$

As shown in Figure 25, THD is then applied as directory of HTS arc model after STFT is applied as a way to attain frequency content of assessed signal.

THD variation

THD is a measurement that gives the information about the distortion of a voltage or current due to harmonics in the signal. A lower value of THD is an important aspect in power systems. THD reference value is calculated using the following expression:

$$THD = \frac{\sqrt{{V_2}^2 + {V_3}^2 + {V_4}^2 + \cdots}}{V_1}\mathrm{x}100\% \tag{5.9}$$

The adjustment leads to variations on harmonics of the signal. Hence, the THD works as a monitoring parameter. The THD of the signal is defined as following equation (5.10)

$$THD_t = \frac{\sqrt{\sum_{h=2}^{H} I_h^2}}{I_1} \times \mathrm{x}100\% \tag{5.10}$$

where, I_h is the rms value of fundamental harmonic components. The average THD_t for over one-cycle can be expressed as:

$$THD_{avg,t} = \frac{1}{N} \tag{5.11}$$

To calculate the THD of the signature signal, the STFT is applied to the measured signal at first which provides its frequency contents. Then, the THD can be computed by cancelling out the fundamental frequency which is 50 Hz in this study. Practically, this process could be performed using a THD analyzer or a notch filter.

5.2.3 Operation on re-striking effect

A simple short line fault (SLF) has been simulated for this test. Transient analysis is used in order to introduce the HTS arc model equations. A single-phase system is simulated which has an AC voltage source of 11 kV. For HTS arc model, arcing parameters are used. τ_m = 4 μs; τ_c = 12 μs; P_0 = 2 MW; v_0 = 5 kV. The voltage across HTS arc model recorded for two cycles of the 50 Hz fundamental frequency. The developed voltage across the CB after opening operation can be considered which includes arcing effects at the early stage of the CB life span.

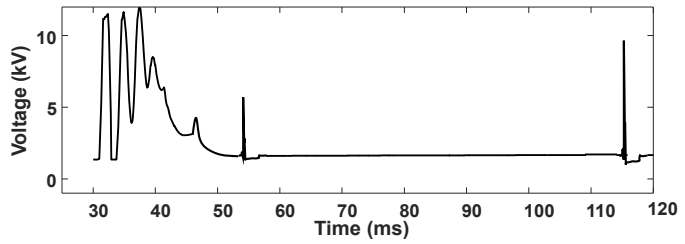

(a)

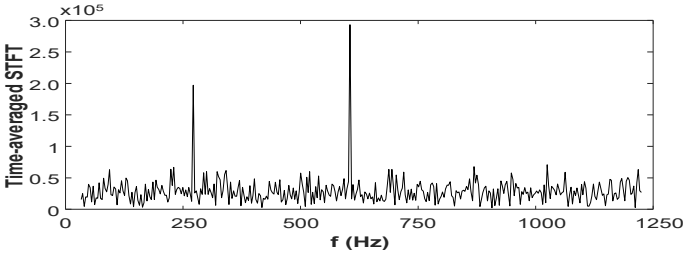

(b)

Figure 26: (a) Measured voltage with re-strikes across arc model (b) corresponding calculated STFT of the CB voltage

In Figure 26, measured voltage with re-strikes across arc model and its corresponding calculated STFT of the CB voltage is shown.

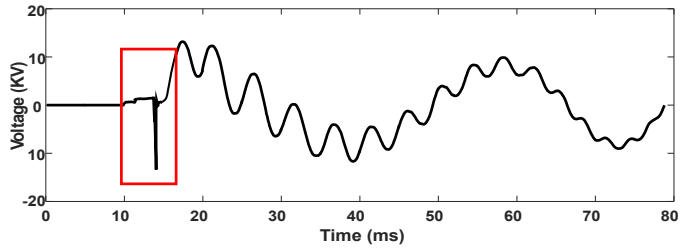

(a)

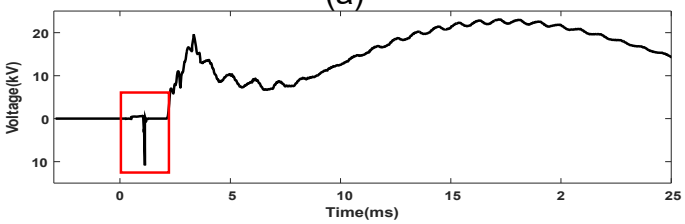

(b)

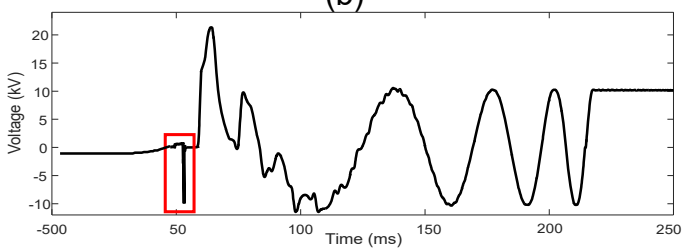

(c)

Figure 27: The CB measured voltage after faulty operation with one re-strike under scenario 1 to 3 respectively

In Figure 27, the CB measured voltage after faulty operation with one restrike is shown. In scenario1, for a fixed load, distributed generation is varied and the fault is applied. In scenario 2, for fixed distributed generation, the load is varied and the fault is applied. In scenario 3, for a random event, the distributed generation and load is varied and the fault is applied. In Figure 28, measured CB voltage after faulty operation with multiple restrike under different operating condition obtained using the fault detection algorithm are shown.

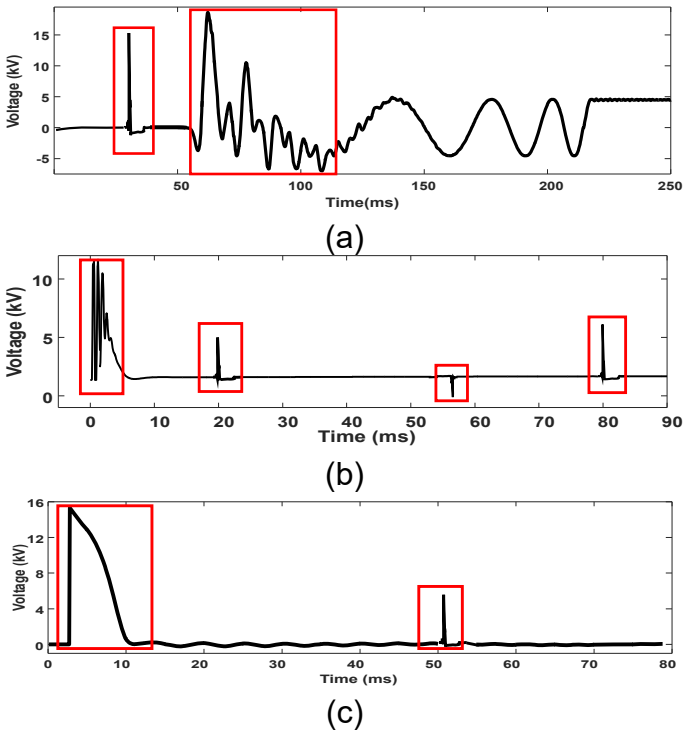

Figure 28: The CB measured voltage after faulty operation with multiple restrike under scenario 1 to 3 respectively

5.3 CONCLUDING REMARKS

In Section 5.1, the simulation and calculation studies are carried out for energizing 1 MVA 11kV/415V HTS transformers during short circuit condition. Throughout the energizing of the transformers, the HTS breaker arc model is switched off for the time when the voltage crosses the zero point. The situation highlights the increased value of inrush current. Magnetizing flux is proportional

to the value of inrush current. The calculation has some deviation as the breaker model is developed with some realistic assumptions. With the proposed calculation method, inrush currents could be restrained to a lower level along with residual flux. It is found the transient voltage raises to 1.03 pu, during HTS transformer's energization. The overvoltage limit hence has a vivid impact of inrush current in HTS transformer. The variation of operating time can still be readjusted with future modified HTS breaker arc model. For future experiments, the arc model with CFI method can be investigated for broad-area systems protection or in SCADA/ EMS central systems.

In Section 5.2, the THD deviation threshold value needs to be precisely defined based on arc parameters and network specifications. THD analyzer or a notch filter can be used in practice in order to perform THD operation. The CB operating voltage should be calculated for a minimum of two cycles of its basic frequency to obtain the best results out of signal analysis constraints. The algorithm can be applied practically with proper accessories and in smart grid with real-time platforms.

CHAPTER 6- DESIGN AND EXPERIMENTAL VALIDATION OF ARCING PHENOMENON IN CRYOGENIC ARC CHAMBER

In this chapter, Computational Fluid Dynamics analysis (CFD) in ANSYS CFX is used to analyse the flow fields in cryogenic arc chamber. Furthermore, two-dimensional Finite Element Method (FEM) numerical solution analysis in ANSYS Maxwell also used to observe the magnetic field in cryogenic arc chamber. The analysis shows that the significant geometrical parameters of arc chamber and breaker contacts need to be optimised to improve the performance of HTSCB. The detailed analysis of flow separation, losses, its origin and minimized electrical field strength in short circuit condition help the design to improve its flow field and efficiency. Finally, the CFD and experimental result are compared in validation chapter.

6.1 DESIGN METHODOLOGY

It is essential to analyze the magnetic field of proposed HTS breaker model in order to improve its dynamic efficiency. Finite Element Method (FEM) is an effective strategy for dealing with the complex electric field with significant accuracy. The FEM software package, ANSYS Maxwell is chosen as an analytical tool in this research in order to conduct static and transient calculations of HTS circuit breaker. The magnetic field distributions of arc quenching chamber, magnetic forces and thermal model are evaluated using FEM analysis. The purpose of this analysis is to execute static and transient computation of magnetic forces and field in HTS circuit breaker. The circulation of the equivalent electric field analysis of the HTS arc quenching chamber is also studied.

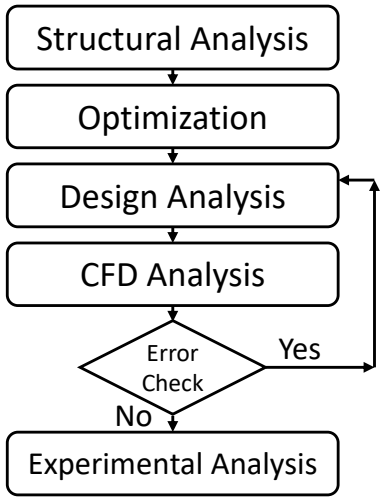

Figure 29: : Flow chart of the HTS breaker design

Figure 29 shows the breakdown of the major phases of the research work. The methodology is to carry on a structural analysis to evaluate the performance of the breaker. The optimization of breaker parameters leads to the main design thereafter. As part of the process, the influence of breaker parameter optimization on CFD analysis and experimental analysis is also discussed.

6.2 STRUCTURE AND MECHANISM (DESIGN MODELLER)

The structure of HTSCB is designed with high interrupting capability. The method of arc control in prospective HTS breaker will differ from oil, vacuum or air-break circuit-breakers. The oil breaker performs by flushing out the 'combustion' products of the arc. The Vacuum Circuit Breaker (VCB) is very common, particularly for medium ranges of voltage, due to its excellent efficiency. The vacuum breaker works by controlling the arc medium while the air-breaker operates by controlling the re-striking voltage wave. In arc quenching analysis of HTS breaker model, the cryogenic medium is used in interruption chamber during the separation of the arc contacts. Cryogenic chamber is designed with the pressurized reservoir. So that vibrational and optical disturbance can be minimized due to the suppression of liquid nitrogen during arcing [85].

An HTS pull-rod (CSL-26/120.3 type [86]) links the contacts of the interruption chamber. The contacts inside the HTS breaker can be designed as butt type, spiral type or Axial Magnetic Field (AMF) type contact with HTS bulk material. The moving contact can move only a short space from the fixed contact while opening. When the contacts first separate in mid-cycle, an arc is driven and the current continues to flow.

Figure 30 shows a cross-sectional draw of such an interruption chamber of an HTSCB. A cryogenic chamber in cold cndition is important part of HTSCB. Due to the cold medium, there should be no gas dielectric to break down like other usual circuit breakers during arc re-striking. The moveable and fixed contact functions are designed to perform inside the cold chamber. Interruption of nominal currents in the range of tens of amperes to 2~2.5 kA can occur here. The chance of growing a new arc should be very less as the environment is very cold

medium. Consequently, the arc should not restrike. HTSCB contacts are suitable for repetitive use as contactors.

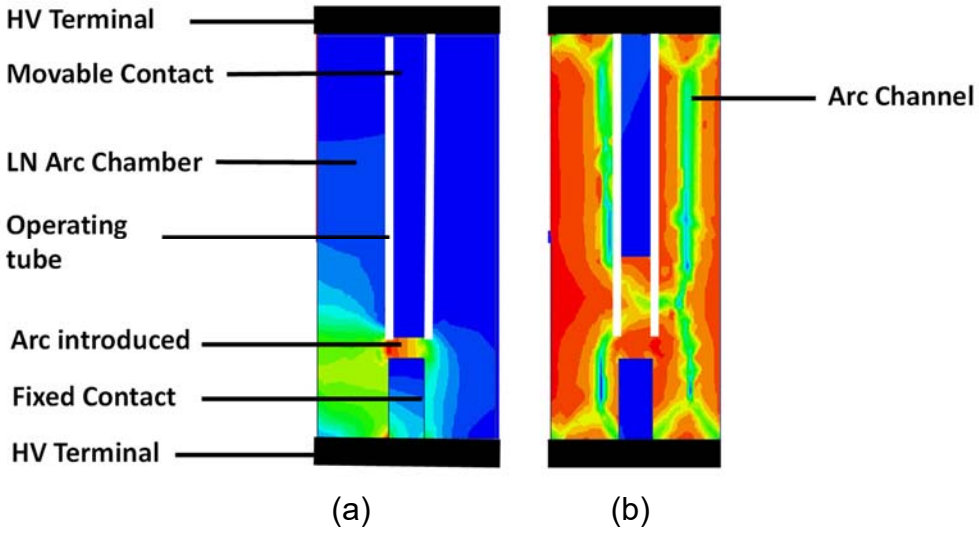

Figure 30: Geometry of HTS breaker (a) arc in mid cycle (b) current-zero arc extinguish

In a VCB, when the operating linkage reaches a certain level specified by the manufacturer, the whole vacuum interrupter element must be replaced. The proposed HTSCB offers the advantage of replacement of its cold medium. Moreover, liquid nitrogen can work as an insulator as it is not electrically conductive. As nitrogen is non-polar gas, it will behave as non-conductive. The same scenario is used while using liquid nitrogen cooling studies in computer modelling.

6.3 FUNCTIONAL EQUATIONS

The mass, momentum and energy conservation equations of the HTS breaker model are solved with the ANSYS CFX solver in Chapter 7. The functional equation of Continuity or the conservation of mass equation is as:

$$\frac{\partial \rho}{\partial t} + \frac{\partial y}{\partial z}(\rho V_z) + \frac{1}{r} \cdot \frac{\partial}{\partial}(\rho V_r) = 0 \tag{6.1}$$

The functional equation of Axial Momentum is as:

$$\rho . \frac{\partial V_z}{\partial x} + \rho V_z \frac{\partial V_z}{\partial z} + \rho V_r \frac{\partial V_z}{\partial r} = \left(- \frac{\partial P}{\partial z} + \frac{1}{r} \frac{\partial}{\partial r} [\eta + \eta_l] r \frac{\partial V_z}{\partial r} \right) \tag{6.2}$$

where ρ is the cold medium density, V_z and V_r represents the axial and radical velocity respectively. As for other terms η and η_l are molecular and turbulent viscosity correspondingly and finally P is pressure.

The functional equation of Energy is as:

$$\sigma E^2 - U + \frac{1}{r} . \frac{\partial}{\partial r} [k + k_t] . r \frac{\partial T}{\partial r} = \left(\rho \frac{\partial h^0}{\partial t} + \rho V_z . \frac{\partial h^0}{\partial z} + \rho V_r . \frac{\partial h^0}{\partial z} \right) \tag{6.3}$$

where $k_t$the turbulent thermal conductivity and h0 is the total enthalpy and and σ is the electrical conductivity.

The functional equation of Ohm's Law is as:

$$I = E \int_0^r 2\pi\sigma dr \tag{6.4}$$

where current is proportional to the conductance, G of the proposed model. In addition, assuming the steady state voltage gradient E is pre-set voltage value. Other terms are known as the finite rate of energy loss is N, energy storage capacity is Q and the arc time constant is θ, where $\theta = \frac{Q}{N}$. The equation for energy can be integrated from the value of zero to the arc radius which is accurate enough for the realistic application purpose so it is not necessary to include the other equations anymore.

An HTS arc model is used initially to find the characteristic of arc current, arc voltage, conductivity value and before, after and during current zero of arc breaking. The equations for energy of HTSCB in the contact opening process are

solved in this regard. The equation for different interrupting phases are given in (6.5), (6.6) and (6.7):

$$\text{Before Current Zero: } W_{i.j} = \frac{G_{i,j}}{\left(\sum_{k=1}^{n} G_{i,k}\right)^2} i^2(t) - W_{con} \tag{6.5}$$

$$\text{After Current Zero: } W_{i.j} = \frac{\left(\sum_{k=1}^{n} G_{i,k}\right)^2}{G_{i,j}} u^2(t) - W_{con} \tag{6.6}$$

$$\text{During Current Zero: } W_{i.j} = \sigma_{i,j}(T,P) S_{i,j} L_{i,J} E_{i,j}^2 - W_{con} \tag{6.7}$$

where $G_{i,j}$ is the conductivity value of HTS, $\sum_{k=1}^{n} G_{i,k}$ is the total conductivity value and $i(t)$ is the instant interrupting current and W_{con} is the convection value. $G_{i,j} = \sigma_{i,j}(T,P) S_{i,j}/(L_{i,J})$ and $\sigma_{i,j}(T,P)$ represents the cold medium conductivity. The conductivity depends on the function of T and P the distribution of $\sigma_{i,j}(T,P)$. Other components like the chamber area temperature, arc length, electric field, and AC loss also depends on the variation of conductivity.

6.3.1 Boundary conditions

FEM is used to analyze the nonlinear magnetic field of the HTS breaker. Hysteresis and Eddy current losses have been ignored to avoid the static field complexity. The boundary equation is described as:

$$\begin{cases} \nabla \times \nabla \times A = -J \\ \nabla \times \upsilon \nabla \times A = 0 \\ \nabla \times (\nabla \times A - B) = 0 \end{cases} \tag{6.8}$$

where J represents the current density of exciting current, υ symbolizes the reluctivity, A is arbitrary integral constant and B presents the flux density. For the domain of HTSCB 2D Navier-Stokes vector equation for cold medium are chosen under Local Thermodynamic Equilibrium (LTE) condition. The equation can be written as follows:

$$\rho\left(\frac{\partial u}{\partial t}\right) + \frac{\partial}{\partial t}(\rho\varphi) + \nabla(P\vec{v}\varphi - \nabla\emptyset) = 0 \tag{6.9}$$

where ρ is the density and P is pressure, u is axial velocity and v is the radial velocity. For the ANSYS Fluent model, boundary condition of no-slip is placed to most of the domain walls. It is used for outer walls as well. The heat transfer system works as automatic convection. 5-7 W/ m2K is used as the heat transfer coefficient for the HTS breaker walls. The ambient temperature outside arc chamber is selected as 290K with an average temperature of 77K at the walls.

6.4 MESH FACTS

The mesh of the geometry is important in order to address the precise value for the temperature and the velocities near the wall. Furthermore, fine grid near the arc chamber wall and contacts are also important. Initially, the structured or unstructured mesh choices with prismatic features are used alternatively near the arc chamber wall. Tetrahedral features are used around the contacts. Tetrahedral features throughout the chamber are identified as better when mesh sizes are lessened to a compact size of similar sizing.

The unstructured mesh ultimately generates nearly thirty-five thousand nodes and nearly thirty thousand wedges. For arc chamber dimensions the mesh length scale was within a specified value of 1~2.5 mm, until mesh become independent. Finally, a mesh size of 1.483 mm is determined for entire geometry. Prismatic features have also been used to the arc chamber wall. The process verified an ample of elements close to the arc chamber wall. It was found that below 2 mm, mesh independency was achieved.

In Figure 31, refinement of mesh for the arc chamber of HTS breaker is shown step by step. Initially, in Figure 31 (a) long edges of the breaker cylinder are

chosen. The edges are then refined by edge-split in Figure 31b) and Figure 31 (c). In Table 11, Mesh Specification for the components is included.

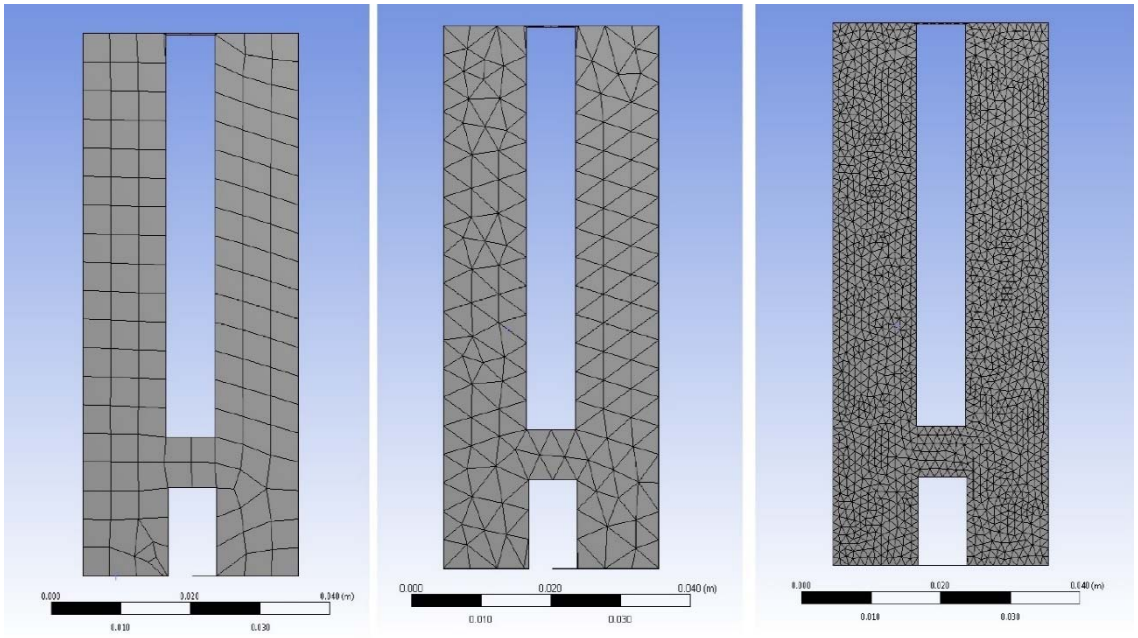

(a) (b) (c)

Figure 31: Refinement stages of mesh for the arc chamber of HTSCB

Table 11: Mesh Specification for the components

Domain	Number of nodes	Heat Dissipation Rate (w)
Arc chamber wall	8,58,054	15
Moveable contact	9,56,346	18
Fixed contact	2,38,615	17

6.5 OPTIMIZED MAGNETIC FIELD ANALYSIS

In order to find the optimized critical magnetic field strength the conventional conservation equations [87] can be used. The equations are used for momentum, mass and energy making use of the Euler's equations. Various electromagnetic terms like magnetic forces in the energy transfer equations are dealt in [87].

Simplified Maxwell's equations are used for the calculation of electric and magnetic fields. The metallic erosion is not taken into account.

It is found earlier in Chapter -3, that the arc for HTSCB acts as a non-linear resistance. As the non-linear arc characteristic has been defined earlier, therefore liquid nitrogen ionization is factored into the non-linear characteristics of Local Thermodynamic Equilibrium (LTE) regarding the pressure and temperature for electric field analysis. Furthermore, the flux through the chamber walls regarded as the typical feature of HTS arc chamber. The entire simulation is processed through two-dimensional Magnetic Field Analysis (using the ANSYS Maxwell). The HTS breaker FEM model is used to demonstrate the uniformity of electric field and flow field at cryogenic temperature. The optimized values of breaker parameters are shown in Table 12.

Table 12: The initial optimized values of breaker parameters

Rated current (A)	250 A	Rated Frequency	50Hz
Rated breaking (I_{HTS}/I_{SC})	10/5	Rated voltage	11kV
Short Circuit breaking current	1200A	Average closing speed	0.6~1.2 m/s
Rated short circuit making current (peak)	570A	Average opening speed	1.2~1.5 m/s
Rated short-time withstand-current (3 sec.)	680A	Peak (kV)	30
Close/open contact time	<50ms	Stroke	7-9
Clearance between contact	8±1 mm	Total Mass	3.7kg
Allowable maximum contact erosion	3 mm	Moving distance	15mm
Moveable contact	160~200mm	Arc chamber initial temperature	77K
Fixed contact	80~90 mm	Outlet pressure	6.92 bar
Arc Chamber length	400 mm	Exit pressure	11bar
Contact radius	12.7mm	Exit temperature	65~68 K
Overtravel	4±1 mm	Pressure rise	37~40 Pa
Mass flow rate	0..05 kg/s	Heat flow rate	37-39 CFM
Arc chamber pressure	15 bar	Contact Gap distance	330-450 mm

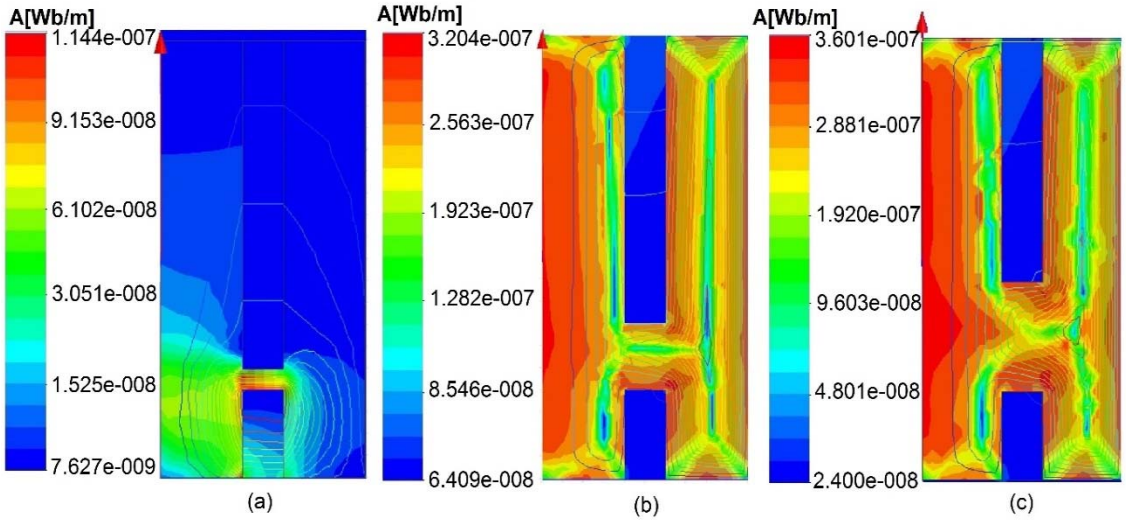

e

Figure 32: 2D view for Magnetic flux distribution of HTSCB interruption [(a) Phase-1 (Arc introduced), (b) Phase-2 (mid-cycle), (c) Phase-3 (Current Zero arc extinguish) at 40ms, 42ms and 44ms respectively]

The FEM-model for investigating electromagnetic characteristic is shown in Figure 32. The results are significant in order to examine the magnetic field of HTS breaker for dynamic performance and effective control strategy. In Figure 32 (a), the arc is introduced at 40 millisecond Figure 32 (b) shows the mid-cycle flux distribution scenario at 42 millisecond with greater contact distance than Figure 32 (a). Finally, in Figure 32 (c), current zero arc extinguishing scenario is demonstrated at 44 millisecond. These stage wise demonstrations shows the flux distributions at the different position of opening contact. The near zero magnetic field advantage of Messner-Ochsenfeld theory [20] is visible from this discussion. The magnetic flux distribution of HTS breaker in different interrupting phases illustrated with arc duration of 6.45 milliseconds.

In order to derive the arc force at ideal time period the fundamental arc force equation is calculated as $F_{arc} = \frac{\mu_{hts} I^2}{8\pi}$ where, μ_{hts} is the magnetic permeability of HTS. The equation of arc force changing rate is as:

$$\frac{dF_{arc}}{dt} = \frac{d}{dt}\left(\frac{\mu_{HTS} I^2}{8\pi}\left(1 + 2ln\left(\frac{R_{fc}}{R_{mc}}\right)\right)\right) \quad (6.10)$$

where R_{fc} is the radius of the fixed contact and Rmc is the radius of moveable contact.

The arc force on different phases of HTS breaker is demonstrated in Figure 33. The illustration shows that the raise of arc force between 40-46 milliseconds. The change of arc force varies by nearly 10% from first and last phase position. In between the forces reach to its peak value.

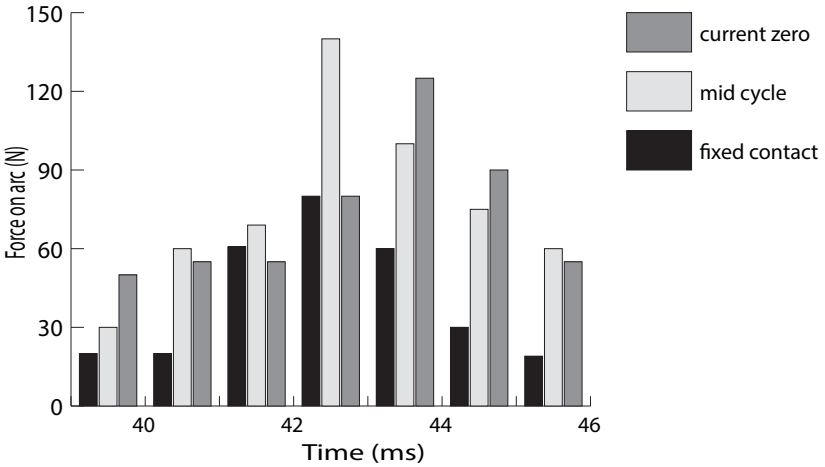

Figure 33: arc force rate comparison for diferent cases of HTS breaker model (case-1: arc force at fixed contact, case-2: arc force at mid cycle, case-3: arc force for moveable contact at current zero)

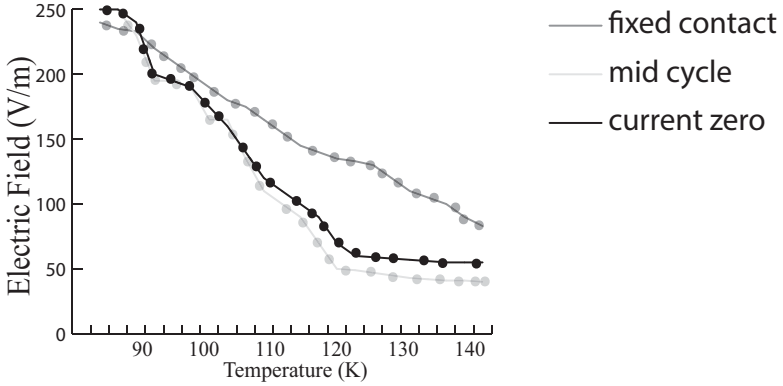

Figure 34:The electric field reduction with increase of temperature for HTS breaker model (at 40-46 millisecond)

Figure 34 shows the variation of temperature up to 140 K at 0.1MPa. Initially, no deviation is recorded. As long as the arc force becomes dominant, the temperature increases as well. The electric field strength affiliated to the steadiness of arc generation is calculated from prior field analysis. The electric field reduction rate is usually different from other typical field reduction as in the case of SF_6. As SF_6 product are changeable with the pressure of gas. As further enhancement to this modelling assessment, improved cross-sectional study of HTSCB sets are investigated in following sections.

6.6 COMPUTATIONAL FLUID DYNAMICS (CFD) SIMULATION APPROACH

CFD study is used to optimize the flow field because of the experimental difficulties of high temperatures and high costs of experimental setup. The HTS breaker model with fixed and opening contact is studied by CFD simulations. The numerical solution is carried out using the ANSYS Fluent. The entire computational domain is kept under same conditions as mentioned in section III. Three different interruption phases of HTS breaker are considered with variable temperature distributions. The contour result of velocity for the contact parts is investigated here with whole arc chamber in order to predict heat performance of HTS breaker. The parameters for inside body of arc chamber is kept fixed and the contact positions are changed. The mesh is much refined in order to review the results with the HTS breaker model. The heat dissipation values are recorded from the HTS breaker model experimental setup. It is also found that liquid nitrogen generates force on the arc chamber walls and recirculate in the arc chamber.

6.6.1 Convergence concern

The continual results are obtained from a well converged simulation model. During the simulation when iterations continue and the scalar values do not change, subsequently it can be reported that the solution is converged. Convergence criteria should ensure that the results have less impact on simulation result. An equation of representing the rate of convergence can be described with the ratio of $\frac{R_n}{R_{n-1}}$, where R_n and R_{n-1} is the normalized log residual at time step n and n-1 respectively. Various convergence tolerances are investigated such as 10^{-7} for energy, 10^{-5} for flow and 10^{-8} for energy. The edges of the contacts of HTS breaker are found as generating heat uniformly.

6.6.2 Flow field analysis

A detailed flow field analysis is carried out in order to discover the numerous areas of loss generation and to calibrate it. The field variables such as the contour of velocity, velocity vectors, velocity magnitude, pressure, particle variables, particle ID can be calculated from the computational domain analysis. The contour results are then used to determine the regions of loss generation and minimize it. Computational domain of one region is kept identical for the analysis.

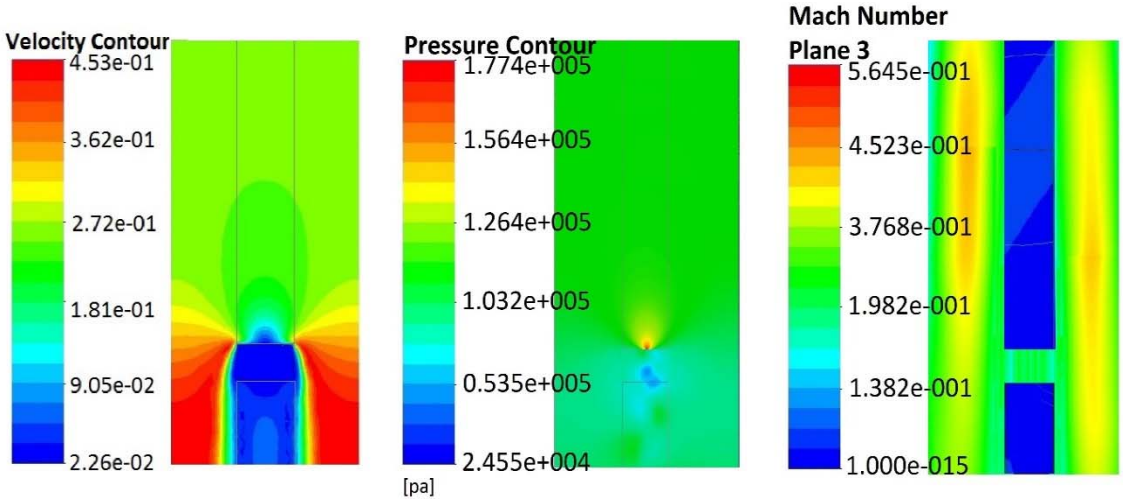

(a) (b) (c)

Figure 35: (a) Plot of temperature contours (contours of velocity vs velocity magnitude) and (b) pressure contour (pressure of velocity vs velocity magnitude) (c) Mach Number for heat distribution of HTS breaker model at 40milli second

Figure 35 presents the velocity vector, mach number and total pressure distribution at mid-span of arc breaking. The velocity vectors, mach number, total pressure, and total entropy are plotted to analyse the flow characteristics within arc chamber.It is found that the liquid nitrogen flow accelerates through the contacts with a drop in total pressure along the surface of the arc chamber. The contact position for 40 milliseconds after interruption and its contour velocity is as shown in Figure 35 (a). The heat distribution is located symmetrically as shown in Figure 35 (a) on two sides of the contacts. The temperature contour distributions are found identical with dimensions through the first stage of the release of arc on the contact gaps. When the arc is sensed, the separation of contacts occurs. During the separation, the center parts initially recorded high temperature of 140 K, while the wall was still maintaining cryogenic temperature. With time progression the wall temperature also reaches up to 140 K. The flow angle contour at the major edges of the contacts exhibits slight deviation from the optimum flow angle which impacts the flow structure within the arc chamber.

The CFD simulation study results nicely predict the liquid nitrogen pressure drop under different arcing temperature. Inlet velocity of arc chamber has also been measured with CFD simulation. The partial differential equations of HTS breaker model are discretized in order to implement the finite volume solutions for pressure-velocity coupling. The same Navier-Stokes vector (equation (6.9) for cold medium is used under LTE condition for Pathline and Velocity inspection. In the vector velocity, the cryogenic chamber has shown relatively impede velocity and slow wave property as quenching medium than the similar event using other dielectrics as it is shown in

Figure *36*.

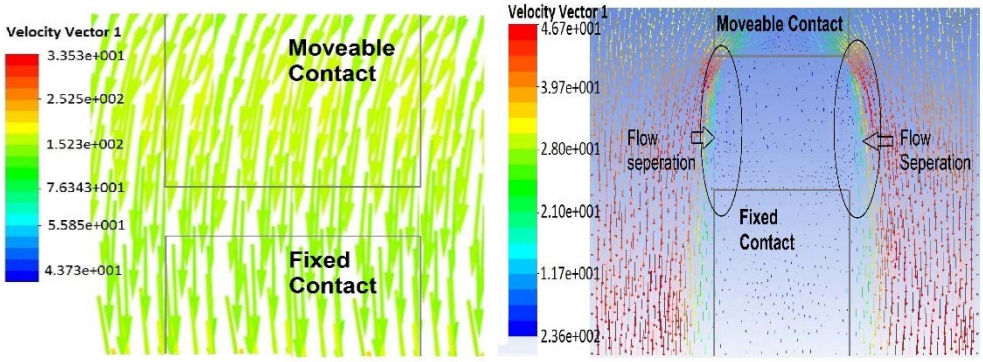

(a) (b)

Figure 36: (a) Plot of velocity contours [Vectors of velocity VS velocity magnitude] (for P=1 bar, T=77-140 K, Standard initialization, 149 iterations) in normal condition (b) Velocity vector plots in arc chamber after arcing.

The velocity vector plots of Figure 36 represented the effect of moveable contact on the growth of arc and the flow distribution in arc chamber. Figure 36 (a) and Figure 36 (b) shows the flow is mostly uniform. As seen from the velocity vectors (Figure 36 (a) and Figure 36 (b)) the flow always maintain the same direction and pushes the fixed contact. This has a considerable impact on the performance of

the HTSCB. In general, the contacts splits the flow and influence the flow acceleration as downstream.

Table 13 : Velocity in arc chamber

No	1	2	3	4	5	Average
Consumed time (s)	3.54	4.34	4.89	3.37	4.28	4.08
Velocity (ms^{-1})	0.16	0.15	0.21	0.17	0.19	0.18

The total arc chamber length is 400mm. The average velocity of liquid nitrogen in the arc chamber during arcing can be calculated. This is actually the consumed time for the liquid nitrogen to flow from the top area to the arcing area during arcing. In Table 13, the consumed times for liquid nitrogen to flow through the arc chamber is shown. The data is taken with random positions in arc chamber. From Table 13, the average velocity in the arc chamber is found as 0.18 ms^{-1}.

6.6.3 Pathlines

The temperature reduces slowly with the time once the arc is quenched. The breaker contact generates higher conduction rates. The heat is diminished in the arc chamber in a reliable trail. Hence, it is worthwhile to investigate the pathline of CFD. When the arc chamber is explored for pathlines, the top part of contact gap shows adequate free route for liquid flow. The cold medium circulation is predicted to travel to the underside area for the movement of contacts. Consequently, the downward flow of liquid nitrogen will make the fixed contact less hot as estimated from the simulation.

The impact of cold medium movement can be observed from the pathline distributions of Figure 37(a). In Figure 37(b), magnetic flux density during arcing near contact area is shown.

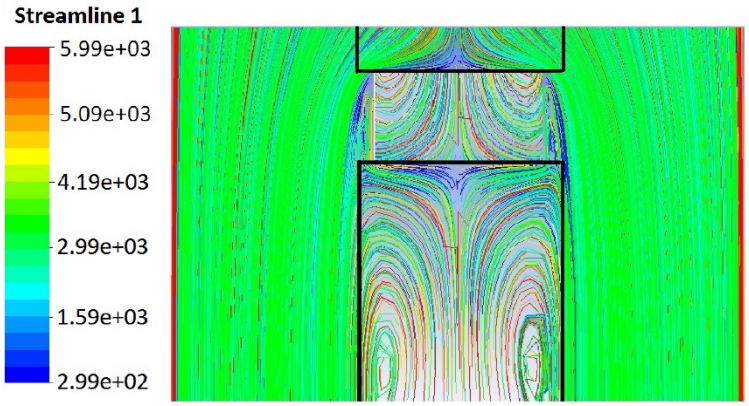

(a)

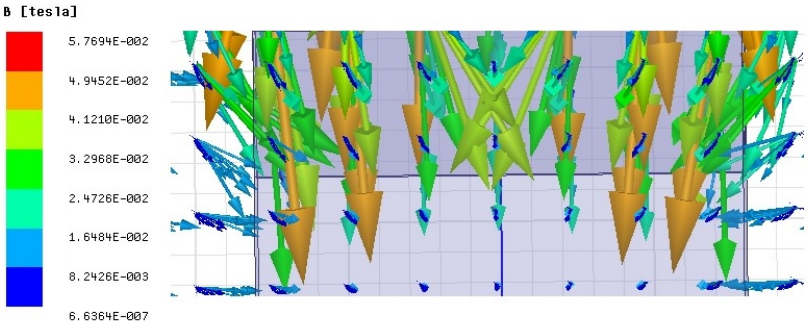

(b)

Figure 37: (a) Pathlines for interior body (particle variables vs particle ID) for the contact gap of HTS breaker (b) Magnetic flux density during arcing near contact gap area

On the lower sides of the contact gap, cold medium pathlines come back close to contact gap striking the HTS contacts of fixed contact. The cold medium flow grows highly efficient at this section of the HTS breaker. The HTS contacts had its superconductor stage holding during the whole arcing process, even though the thermal resistance is not substantially changing. The cold liquid flow path works fine to transfer the heat inside the arc chamber. For different heat transfer area then the thermal resistance of the contacts is not significantly transformed. The circulation of pathlines flow inside arc chamber can be spotted from Figure 37. The simulation study result presents the circulating areas inside arc chamber. The arc chamber wall is then carried out for Velocity distribution.

6.6.4 Entropy contour

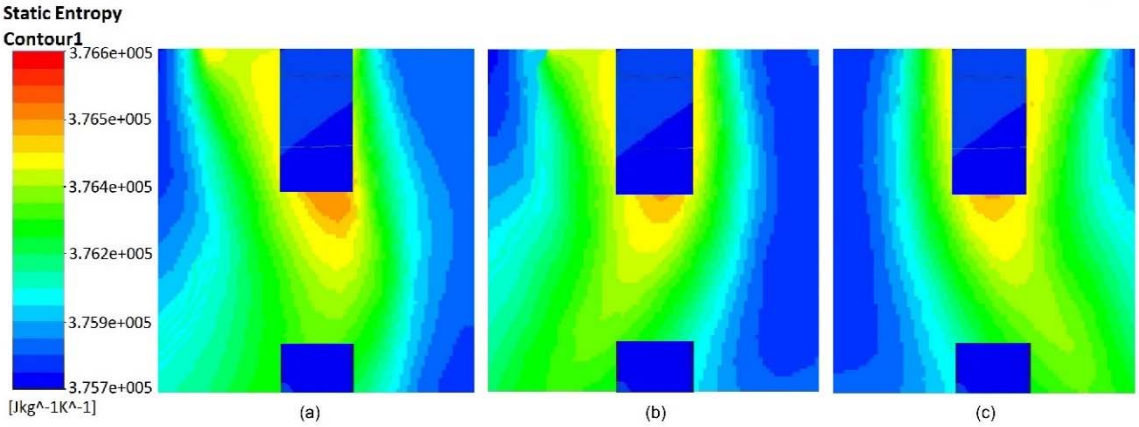

Figure 38: Entropy contour in arc chamber passage after arc switching

The entropy plots illustrate the entropy developed during the formation and distribution of arcing (Figure 38(a), Figure 38 (b) and Figure 38 (c)). The Entropy plots in Figure 38 (b) shows that the arc passage moves with the moveable contact. From the pressure contour (Figure 38 (b) it was found the pressure was high at moveable contact. This high-pressure stress consequence the dominance of the arc inertia force in arc chamber.

In Figure 38 (b) during the initiation of arcing for contact gap, the center is seen as hot spots in Figure 38 (a), Figure 38 (b) and Figure 38 (c), it shows the end part of arcing in entropy contour. As a result, the heating source goes along to the nearness of the base center of HTSCB.

Table 14: Entropy loss coefficients in different components of HTSCB

Component	Entropy loss coefficient
Fixed Contact	0.592
Moveable Contact	1.573
Arc Chamber	0.834

The moveable contact accelerates the fluid and directs it towards fixed contact. The entropy loss coefficient of different component is shown in Table 14. It is

seen that the flow distortions in arc chamber has a significant influence on the loss.

6.7 VALIDATION OF ARC MODEL

6.7.1 Experimental set up

The proposed HTSCB phenomenon is tested to investigate its arcing time for different current interruption cases. The interruption can be made for a very restricted number of times as large power experiments are costly. The verification of the study is carried out with respect to time with the comparison result of the experimental setup and HTS arc model. The test circuit is shown in Figure 39. It has three major sections: (1) arc circuit (2) liquid nitrogen arc chamber and (3) measurement unit. In section-1 of Figure 39, an arc circuit with 700-1200 ampere arc source is used to provide high peak current within millisecond range. The circuit is attached for producing the arc at the source side of the HTSCB. Section-2 of Figure 39 is the liquid nitrogen arc chamber where the arcing happens. The HTS contacts are submerged into LN and the moveable HTS contact is travelled 10-25mm with the help of a tension spring. The moveable contact is an HTS pull-rod (CSL-26/120.3 type) and the fixed contact is made of Yttrium barium copper oxide (YBCO) which is attached to the center of the base plate of the cryogenic arc chamber. In section-3 of Figure 39, the numerical values of the measurement results are recorded in measurement unit. 1252C RCD meter is used to measure the arcing time. 34972A-Data logger switch unit and USB 2404 series measurement computing are used to measure numerous temperature and pressure reading.

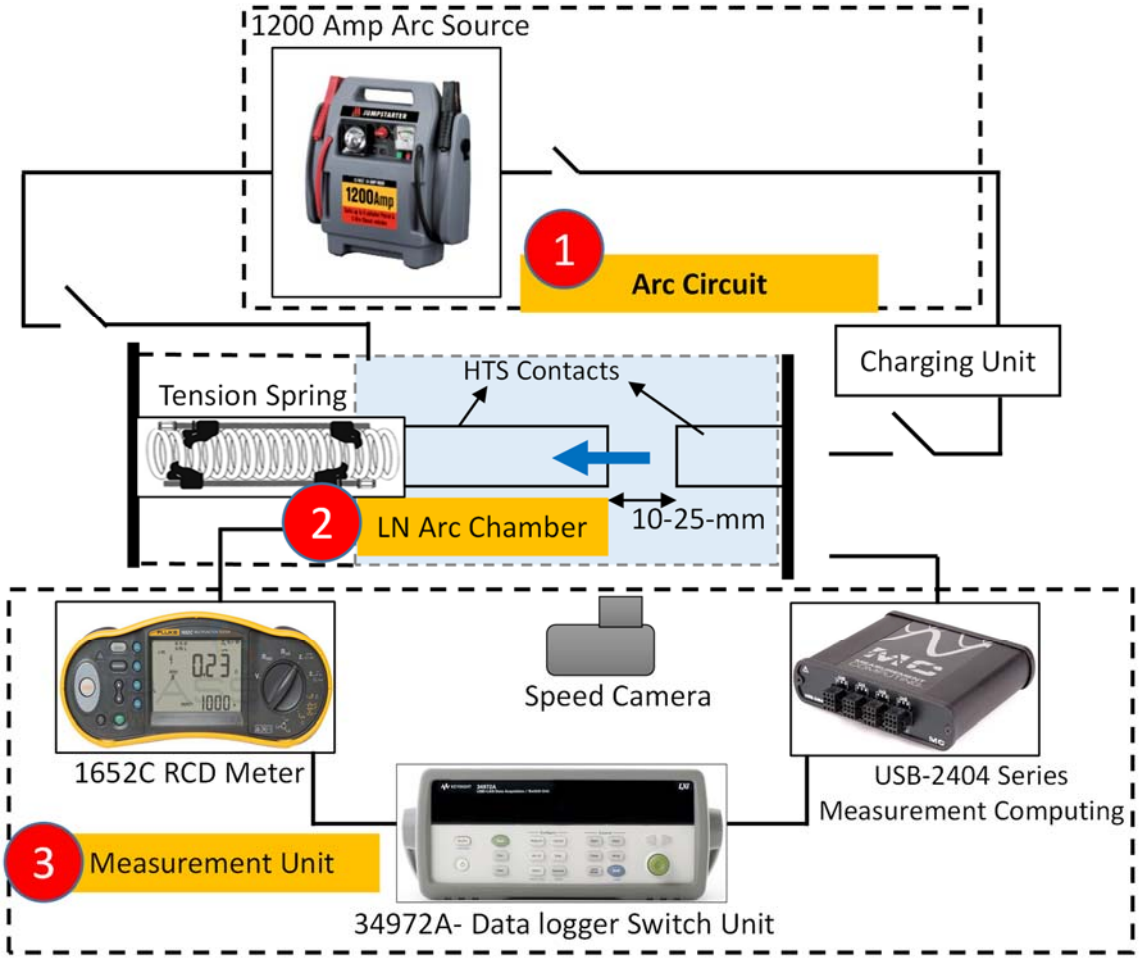

Figure 39: Test object configuration and overview of experimental set-up for arc phenomena captured with thermographic speed camera in cryogenic arc chamber

Figure 40(a) shows the experimental set up used for the CFD validation in a cryogenic arc chamber. Figure 40(b) shows the moveable and fixed contact used with tension spring and operating tube. This test setup is not an automated system. The experiments are carried out in a small closed domain with single heat resource. The fixed contact is attached to center of the base plate of th cryogenic arc chamber. The atmospheric air is passed around the arc chamber which is heated inside. Consequently, the water drops are observed in arc chamber wall. During arcing, the bottom and top surface temperatures are measured using thermocouples at different points.

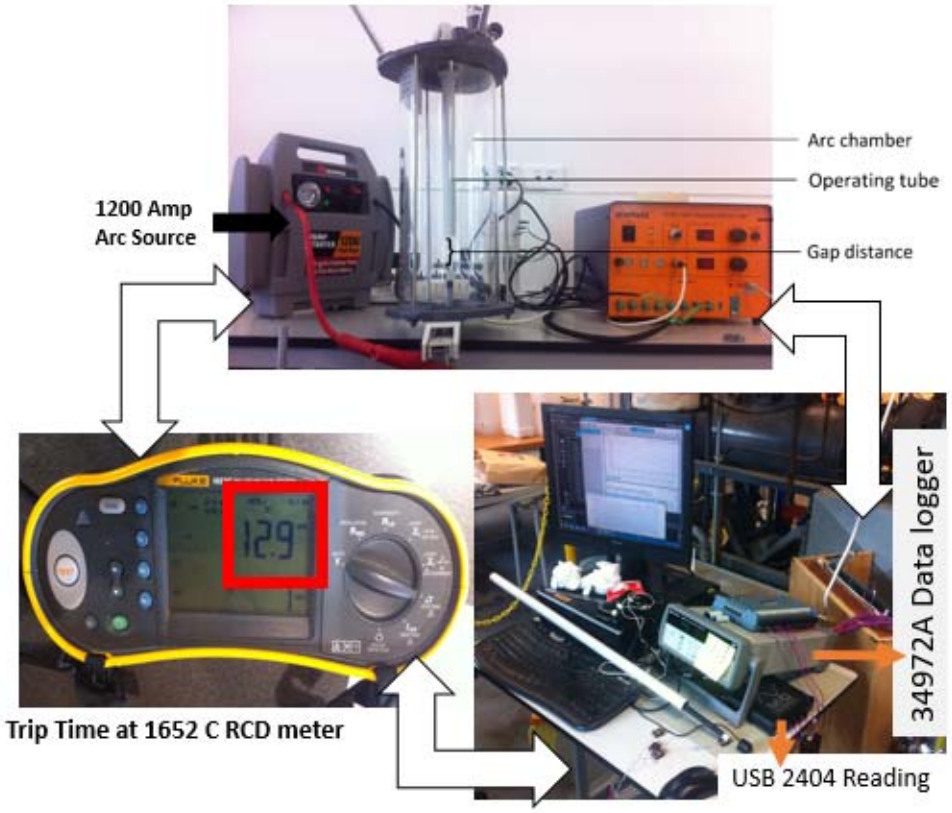

(a)

(b)

Figure 40: (a)Experimental Set-up for Superconducting contact in cryogenic arc chamber (b) Moveable and fixed contact with tension spring and operating tube

In the experiment, the center and edges of arc chamber walls are anticipated to be less hot than the present simulations estimated. It is also observed that the top section of the HTS breaker has lower temperature in comparison to center part. This is on account of liquid nitrogen flow within the arc chamber. The side part of moveable contact is also recorded a lower temperature. The cooling of arc chamber becomes less effective near the side part where the arc is introduced. The conduction rate is found larger in HTS-HTS joint rather than

copper-copper joint for the contacts. The heat is generated from the bottom of moveable contact. In Figure 41, arc phenomena in the cryogenic chamber is shown with the thermographic view. The change of color indicates the temperature changing of temperature change during arcing.

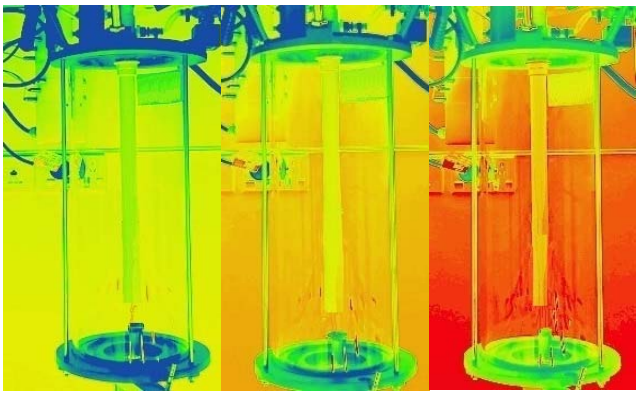

Figure 41: Arc phenomena captured with thermographic camera in cryogenic arc chamber

6.7.2 Experimental result

In Figure 42 (a) four test results out of eighty shots from the experimental set up are plotted. Two results are compared with HTS arc model's simulation arc result in Figure 42 (b). It is found that the arc current test result waveforms have similarity with arc model's arc current wave form in same phase.Though there is difference in ramp rate.

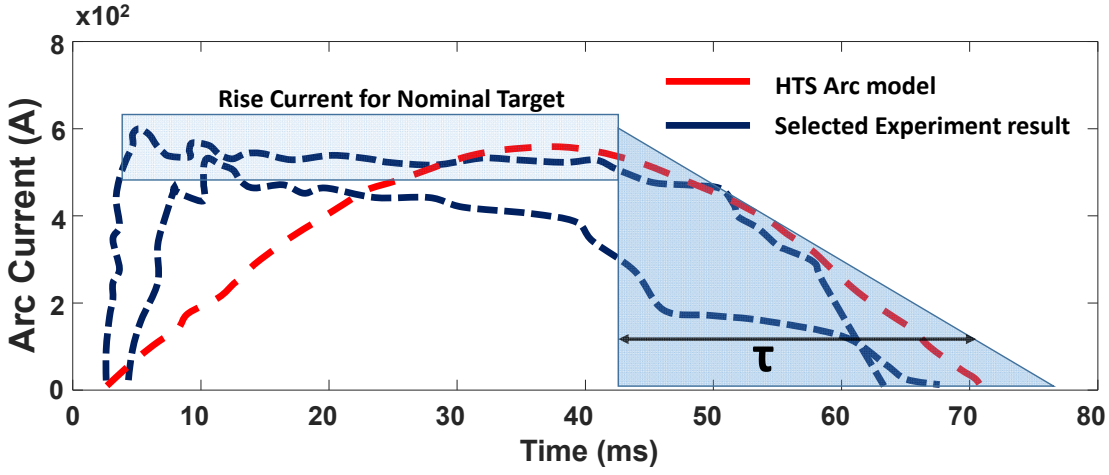

(a)

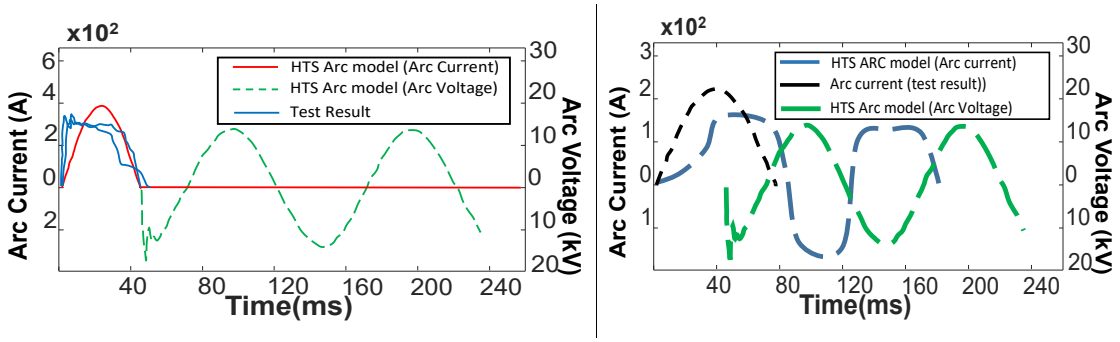

(b) (c)

Figure 42: (a) Test results from experimental set up (b) selected test result comparison (in phase) (c) selectd test result comparison (out of phase)

In the experimental result the arc timing varied from 50 to 80 milliseconds, while in simulation result it was much consistent near 50 to 60 milliseconds. For some cases, the fault currents are found out of phase as shown in Figure 42(c). A big deviation for fault current is observed between the results. For the same fault current of 700A, the current was recoded up to 800A in HTS arc model simulation result. The precision for arcing timing is expected to develop during real-time implementation of arc model.

Table 15: Arc characteristic in experimental model

Arc peak (A)	Post arc current peak (A)	Rate of post-arc current (A/ μs)	Number of test	Number of failure	Out of phase
300	5	2.7	20	4	3
350	15	2.1	20	6	5
400	12	3.3	20	6	6
550	18	4.1	20	8	5

In Table 15, the arc characteristic reading for the experimental model is listed. The overview experiment results have shown stability of minimum arcing times showing important potential for HTSCB design optimization. Although, 25-30% of the shots are recorded as failure attempt and another 20-25% of the shots are recorded as out of phase. This is the limitation of the test bed scheme. Moreover, theoritically an arc peak of 700A can not be recorded with current probe in

osciloscope. In reality, 600A current peak wasn't achievable to record in oscilloscope reading.

6.8 CONCLUDING REMARKS

In section 6.7.2, HTS black box arc model is reviewed for a test bed scheme in order to develop a better understanding about interruption behavior of HTSCB. The transient behaviors of test bed result are studied in order to verify the developed arc model. The results from both simulation and experimental studies were in agreement in terms of the shape of the output waveform. The proposed model can be trusted to behave fairly accurately. The future research will be focused on identification of different failure scenarios and their reasons using intelligent methods. Automatic classification algorithms can be effective in order to achieve this goal.

CHAPTER 7- CONCLUSION

This chapter presents the concluding remarks of the thesis and discusses some recommendations for the future investigation.

7.1 SUMMARY AND CONCLUSION

HVAC breakers are the major elements in the advancement of multi-terminal HVAC grids. The study performed in this thesis has included both simulation and experimental work. The output(s) of the experimental works are presented as input(s) to the simulation models. The investigation conducted in this thesis has aimed two important features of an HVAC breaker: pre and post arcing effect. This section summarises the results and provides a comparative analysis at various stages of research.

The design of ultra-fast breaker with high consistency requires a multi-physics simulation model. HTS arc models with a diverse degree of complexity meet the requirements to some extent. Different underlying assumptions of the arc model parameters are chosen in this thesis in order to minimize its complexity and yet to preserve the high accuracy. The developed first-order arc model can be used to accurately simulate the breaker characteristics within a reasonable arc time. A parameter sweeping analysis has been carried out to find the range of high peak current and to increase the efficiency of arc model. The sweep value of parameters and the average arc resistance also demonstrates the advantage of dealing with the non-linear arc models.

As for the application of the arc model, it is used to find the characteristic of TRV for different current zero scenarios and to mitigate the residual flux problem of HTS transformer. A fault detection algorithm based on the arc model is also

developed covering different constraints and objective function. The study also has aimed to improve the arcing time and reduce the inrush current for HTS machine. Thus a novel arc model has been developed.

One downfall of the research is the longer simulation time of developed breaker and arc models. A computing algorithm is executed in order to minimize the simulation time. Nevertheless, a model with minimized computation time has the risk of less accuracy.

The research about proposed HTSCB design is accomplished in this thesis. The HTS arc model is investigated with the initial set of parameters. The thesis illustrates the HTS arc model with the setup parameters and executes the fault operational activities in a regular distribution network. The experimental test shows that the results of the black box arc model are in close proximity to experimental ones.

To conclude, the accomplished work presented in this thesis is another attempt for further HTS research trends. Different analysis of short-circuit current, inrush current analysis and residual flux mitigation of HTS transformer with HTSCB are conducted in the study. Different analytical methods are applied for the studies. The thesis signifies step by step in depth procedure for each study. Nevertheless, the research has scope to be further investigated and developed.

7.2 SUGGESTIONS FOR FUTURE WORK

Development Scope in Simulink model: Development of HTS arc model are well deserved. Firstly, the model must be integrated with other alternative models of HTS machines. Secondly, HTS arc model has limitations similar to other usual arc models. It is known that the differential model of Mayr's and Cassie are more

applicable for merely few micro-seconds near current zero. Future advancement of HTS model can be validated throughout the total current interruption time. The application of HTS arc model demands to be tested for more advanced and complicated networks as well.

Thirdly, the HTS transformer model is inserted in sample case study network. There are scopes to include the load loss fraction of HTS transformer. The comparison study of the performance for loss with or without arc model in that case would be interesting.

Lastly, the effect of the parameters of HTS arc model is investigated around constrained number of ranges. Significantly bigger computational steps for future investigation is well deserved as well.

Different short circuit conditions: It will be interesting to investigate HTS arc model with different sample networks and with various kinds of short circuit situations. The simulated sample network with the arc model and the calculation for fault voltages and currents and its impact on HTS transformer for individual fault categories needs to be investigated. The benefit of HTSCB insertion in network could be experienced by way of real power reduction management. The calculated short-circuit voltage and current values need to drop within the standard set by the utility issues in that case.

Inrush current: The study discussed in this thesis demonstrated that the peak values of inrush current could maximize several times than the rated current value. The residual flux has been attempted to be mitigated by controlled switching method of HTS arc model. The inrush current force on energized winding of HTS transformer can still survive for few seconds. A power network

system characteristic study should have greater influence on resultant inrush current. This possible phenomena can be investigated in future study.

Switching on RRRV: The numerical arc model with fault detection algorithm discussed in Chapter 4 finds the RRRV values for short circuit condition. Some streamline assumptions is found to impact the model's accuracy significantly. The comparison and outcome on the application of introduced model for two different types of switching is analyzed. The findings from different switching scenarios of HTS arc model demands further investigation for various distribution network conditions as well.

HTSCB with FCL: The findings from the analysis can lead the research to further investigation on the HTSCB with FCL for various distribution network conditions. An analysis for HTSCB with FCL conductor can be an interesting investigation. Development of HTSCB with FCL should prevent the limitations more conveniently. The FCL can minimize the chance of any heat increase in LN arc chamber. The event can reduce the arcing growth as well. Other HTS materials should also be explored for the same objective. Thus, elaborate analysis can be established as the application of the HTSCB with FCL conductor. The current design of the HTSCB has not been viable enough to endure the long term existing fault duration of arcing current over 1600 A.

Others: It is assumed earlier that HTS material of HTSCB can bring the advantage of similar material contact resistance for other HTS machines. An in depth of analysis of contact resistance advantage should be investigated as well. The contacts inside the HTS breaker can be designed as butt type or spiral shape or cup shape or Axial Magnetic Field (AMF) type contact with HTS bulk material.

The improved arc model in short line fault interruption should be analyzed to find different analysis of HTS breaker to compare with normal breaker. The analysis can be performed with respect of Mean Time to Failure (MTTF), Mean Time to Maintenance (MTTM), Mean Time to Repair (MTTR) etc .

REFERENCES

[1] J. L. Tallon, R. G. Buckley, P. W. Gilberd, M. R. Presland, I. W. M. Brown, et al., Nature 333 (1988) 153-156.

[2] J. L. Tallon, R. G. Buckley, M. R. Presland, US Patent 6686319 (2004).

[3] Stuart C. Wimbush, Large Scale Applications of HTS in New Zealand, Physics Procedia, Volume 65, 2015, Pages 221-224, ISSN 1875-3892, http://dx.doi.org/10.1016/j.phpro.2015.05.125.

[4] Bednorz, J. George, and K. Alex Müller. "Possible highTc superconductivity in the Ba− La− Cu− O system." *Zeitschrift für Physik B Condensed Matter* 64, no. 2 (1986): 189-193.

[5] Funaki, Kazuo, Masataka Iwakuma, Kazuhiro Kajikawa, Masanori Hara, J. Suchiro, Takehiro Ito, Yasuyuki Takata et al. "Development of a 22 kV/6.9 kV single-phase model for a 3 MVA HTS power transformer." *IEEE transactions on applied superconductivity* 11, no. 1 (2001): 1578-1581.

[6] Iwakuma, Masataka, Kazuo Funaki, Kazuhiro Kajikawa, Hideki Tanaka, Takaaki Bohno, Akira Tomioka, Hisao Yamada et al. "AC loss properties of a 1 MVA single-phase HTS power transformer." *IEEE transactions on applied superconductivity*11, no. 1 (2001): 1482-1485.

[7] Lewis, Clive, and Jens Muller. "A direct drive wind turbine HTS generator." In *Power Engineering Society General Meeting, 2007. IEEE*, pp. 1-8. IEEE, 2007.

[8] Fukui, Satoshi, Jun Ogawa, Takao Sato, Osami Tsukamoto, Naoji Kashima, and Shigeo Nagaya. "Study of 10 MW-class wind turbine synchronous generators with HTS field windings." *IEEE Transactions on Applied Superconductivity* 21, no. 3 (2011): 1151-1154.

[9] Maguire, J. F., F. Schmidt, S. Bratt, T. E. Welsh, J. Yuan, A. Allais, and F. Hamber. "Development and demonstration of a HTS power cable to operate in the long island power authority transmission grid." *IEEE Transactions on Applied Superconductivity* 17, no. 2 (2007): 2034-2037.

[10] Yumura, H., Y. Ashibe, H. Itoh, M. Ohya, M. Watanabe, T. Masuda, and C. S. Weber. "Phase II of the Albany HTS cable project." *IEEE transactions on applied superconductivity* 19, no. 3 (2009): 1698-1701.

[11] Xin, Ying, Weizhi Gong, Xiaoye Niu, Zhengjian Cao, Jingyin Zhang, Bo Tian, Haixia Xi et al. "Development of saturated iron core HTS fault current limiters." *IEEE Transactions on Applied Superconductivity* 17, no. 2 (2007): 1760-1763.

[12] Leung, E., B. Burley, N. E. al Chitwood, H. Gurol, G. Miyata, D. Morris, L. Ngyuen et al. "Design and development of a 15 kV, 20 kA HTS fault current limiter." *IEEE transactions on applied superconductivity* 10, no. 1 (2000): 832-835.

[13] McConnell, B. W., S. P. Mehta, and M. S. Walker. "HTS transformers." *IEEE Power Engineering Review* 20, no. 6 (2000): 7-11.

[14] Mehta, Sam P., Nicola Aversa, and Michael S. Walker. "Transforming transformers~ superconducting windings" *IEEE spectrum* 34, no. 7 (1997): 43-49.

[15] Nanato, N., T. Ohzawa, S. Murase, and S. B. Kim. "Simple measurement of the AC transport current loss for HTS conductors using an active power detection method." Cryogenics 46, no. 9 (2006): 672-675.

[16] Golubov, Alexandre Avraamovitch, and M. Yu Kupriyanov. "Anomalous proximity effect in d-wave superconductors." *Journal of Experimental and Theoretical Physics Letters* 67, no. 7 (1998): 501-507.

[17] Sykulski, J. K., R. L. Stoll, A. E. Mahdi, and C. P. Please. "Modelling HTc superconductors for AC power loss estimation." *IEEE Transactions on magnetics* 33, no. 2 (1997): 1568-1571.

[18] Sykulski, J. K., R. L. Stoll, A. E. Mahdi, and C. P. Please. "Modelling HTc superconductors for AC power loss estimation." *IEEE Transactions on magnetics* 33, no. 2 (1997): 1568-1571.

[19] Larbalestier, David, Alex Gurevich, D. Matthew Feldmann, and Anatoly Polyanskii. "High-Tc superconducting materials for electric power applications." Nature 414, no. 6861 (2001): 368-377.

[20] Meissner, Walther, and Robert Ochsenfeld. "A new effect when superconductivity occurs." *Natural sciences* 21, no. 44 (1933): 787-788

[21] Smith, G. J., J. A. Alexander, A. B. Buyrn, and J. A. Alic. "High temperature superconductivity: Prospects and policies." *Futures* 21, no. 3 (1989): 235-248.

[22] Bardeen, John, Leon N. Cooper and John Robert Schreieffer. “Theory of superconductivity” *Physical Review* 108, no 5 (1957):1175.

[23] Kunzler, John E., Ernest Buehler, FSL al Hsu, and Jack H. Wernick. "Superconductivity in Nb 3 Sn at high current density in a magnetic field of 88 kgauss." *Physical review letters* 6, no. 3 (1961): 89.

[24] Khare, Neeraj, ed. *Handbook of High-Temperature Superconductor*. CRC Press, 2003.

[25] Bhattacharya, Raghu N., and M. Parans Paranthaman, eds. High temperature superconductors. John Wiley & Sons, 2011.

[26] Mahseredjian, Jean, Michel Landry, and B. Khodabakhchian. "The new EMTP breaker arc model." In Proc. IPST, pp. 22-26. 1997.

[27] Xi-xiu, Wu, Li Zhen-Biao, Tian Yun, Mao Wenjun, and Xie Xun. "Investigate on the simulation of black-box arc model." In *Electric Power Equipment-Switching Technology (ICEPE-ST), 2011 1st International Conference on*, pp. 629-636. IEEE, 2011.

[28] Paithankar, Yeshwant G., and S. R. Bhide. *Fundamentals of power system protection*. PHI Learning Pvt. Ltd.,pp278-280, 2010.

[29] Garzon, Ruben D. *High voltage circuit breakers: design and applications*. CRC Press, 2002.

[30] J. Slepian, Extinction of an a.c. arc, Transactions AIEE, 47, p. 1398, 1928.

[31] Tang, Hong. "A Strategy for Opening Loop Disconnects" PhD diss., University of Manitoba, 1998.

[32] D. C. Prince and W. F. Skeats, The oil blast circuit breaker, Transactions AIEE, 50, pp 506-512, 1931

[33] F. Kesselring, Untersuchungen an elektrischen Lichtogen., (in German), ETZ., 55,92, 1932.

[34] A. M. Cassie, Arc rupture and circuit severity: **A** new theory, Internationale des Grands Reseaux Electriques'a Haute Tension (CIGRE), Paris, France, Report No. 102,1939.

[35] 0. Mayr, Beitrage zur Theorie des Statisghen und des Dynamishen Lichtbogens, (in German), Archiv fur Electrotechmk, 37, 12,588-608, 1943

[36] T. E. Browne, Jr., A study of arc behavior near current zero by means of mathematical models, AIEE Transactions, 67: 14 1-143, 1948.

[37] T. E. Browne, Jr., An approach to mathematical analysis of a-c arc extinction in circuit breakers, AIEE Transactions, 78, (Part 111): 1508- 15 17, 1959.

[38] J. Urbanek, The time constant of high voltage circuit breaker arcs before current zero, Proc. IEEE, 59: 502-508, April, 1971.

[39] W. Reider and J. Urbanek, New Aspects of Current Zero Research on Circuit Breaker Reignition. A Theory of Thermal Non Equilibrium Conditions, CIGRE, Paper 107, Paris, 1966.

[40] R. Amsinck, “Verfahren zur Ermittlung der das Ausschaltverhalten Bestimmenden Lichtbogenkenngrö□en,” *ETZ-A*, vol. Bd. 98, no. H. 8, pp. 566–567, 1977.

[41] A. Hochrainer, “Study of Arcs in Breakers with the Help of a Cybernetic Model and Under the Influence of Turbulence,” Cigre, Report 13-10, 1972.

[42] K. Zückler, “Untersuchungen zum Dynarnischen Verhatten von Schalterlichtbögen,”ETZ-A, vol. Bd. 99, no. H. 9, pp. 546–548, 1978.

[43] O. Mayr, “Beitrage zur Theorie des Statischen und des Dynamischen Lichthogens,” Archiv für Elektrotechnik, vol. Band 37, no. Heft 12, pp. 588–608, 1943.

[44] U. Habedank, “Application of a new arc model for the evaluation of short-circuit breaking tests,” IEEE Trans. Power Del., vol. 8, no. 4, pp. 1921–1925, Oct. 1993.

[45] P. H. Schavemaker and L. van der Sluis, “An improved Mayr-Type arc model based on current-zero measurements,” IEEE Trans. Power Del., vol. 15, no. 2, pp. 580-584, Apr. 2000.

[46] H. Wu, L. Yuan, L. Sun, and X. Li, “Modeling of Current-Limiting circuit breakers for the calculation of short-circuit current,” IEEE Trans. Power Del., vol. 30, no. 2, pp.652-656, April 2015.

[47] A. Ahmethodžić, M. Kapetanović, K. Sokolija, R. P. P. Smeets, and V. Kertész, “Linking a Physical Arc Model with a black Box Arc Model and Verification,” IEEE Trans. Dielectr. Electr. Insul. , vol. 18, no. 4, pp. 1029-1037, Aug. 2011.

[48] S. Nitu, C. Nitu, C. Mihalache, P. Anghelita, and D. Pavelescu, “Comparison between model and experiment in studying the electric arc,” J. Optoelectron. Adv. Mater., vol. 10, no. 5, pp. 1192–1196, May 2008.

[49] Comber, M. G., L. E. Zaffanella, and J. J. La Forest. "Corona loss ."*Transmission Line Reference Book* 345 (1982).

[50] Bizjak, Grega, Peter Zunko, and Dusan Povh. "Circuit breaker model for digital simulation based on Mayr's and Cassie's differential arc equations." IEEE Transactions on Power Delivery 10, no. 3 (1995): 1310-1315.

[51] Simulink® is a block diagram environment for multidomain simulation and Model-Based Design. It supports simulation, automatic code generation, and continuous test and verification of embedded systems. https://au.mathworks.com/products/simulink.html

[52] Hott, Roland. "Materials aspects of high-temperature superconductors for applications." arXiv preprint cond-mat/0306442 (2003).

[53] D. Djurek, Z. Medunić, A. Tonejc, and M. Paljević, "PbCO3·2PbO+Ag2O and PbCO3·PbO+Ag2O (PACO) systems: route for novel superconductors," Physica C: Superconductivity, vol. 351, p. 4, March 2001.

[54] R. Wesche, High-Temperature Superconductors: Materials, Properties, and Applications. Boston/Dordrecht/London: Kluwer Academic Publishers, 1998.

[55] B. W. McConnell, S. P. Mehta, and M. S. Walker, "HTS transformers," Power Engineering Review, IEEE, vol. 20, pp. 7-11, 2000.

[56] M. A. Abdul Rahman, T. T. Lie and K. Prasad, "The Effects of Short-Circuit and Inrush Currents on HTS Transformer Windings," in *IEEE Transactions on Applied Superconductivity*, vol. 22, no. 2, pp. 5500108-5500108, April 2012.

[57] M. A. Abdul Rahman, T. T. Lie and K. Prasad, "Computation of the Thermal Effects of Short Circuit Currents on HTS Transformer Windings," in IEEE Transactions on Applied Superconductivity, vol. 22, no. 6, pp. 5501211-5501211, Dec. 2012

[58] M. A. Abdul Rahman, T. T. Lie and K. Prasad, "Performance analysis of HTS transformer with fault current limiting properties on short circuit current," *Applied Superconductivity and Electromagnetic Devices (ASEMD), 2011 International Conference on*, Sydney, pp. 54-57, NSW, 2011

[59] Lotfi, Abbass. "Identification of KEMA arc model parameters in high voltage circuit breaker by using of genetic algorithm." In Power and Energy Conference, 2008. PECon 2008. IEEE 2nd International, pp. 1515-1517. IEEE, 2008.

[60] Darwish, Hatem A., and Nagy I. Elkalashy. "Universal arc representation using EMTP." IEEE Transactions on power delivery 20, no. 2 (2005): 772-779.

[61] Orama-Exclusa, Lionel R., and Bienvenido Rodríguez-Medina. "Numerical arc model parameter extraction for SF6 circuit breaker simulations." In Proc. *International Power System Transients Conference* (IPST). 2003.

[62] Bahirat, Himanshu, Muhammad Ali, and K. K. Praveen. "Effects of Transient Recovery Voltages on Circuit Breaker Ratings." Instructor (2008).

[63] A A Rahman, “Distribution Network Modelling and Analysis of the Application of HTS Transformer” PhD dissertation, Faculty of Designs and Creative Technologies, Auckland Uni of Technology (AUT), 2012

[64] Samet, H., Golshan, M.E.H.: ‘Employing stochastic models for prediction of arc furnace reactive power to improve compensator performance’, IET Gener. Transm. Distrib., 2008, 2, (4), pp. 505–515

[65] Samet, H., Mojallal, A.: ‘Enhancement of electric arc furnace reactive power compensation using Grey-Markov prediction method’, IET Gener. Transm. Distrib., 2014, 8, (9), pp. 1626–1636.

[66] Samet, Haidar, and Aslan Mojallal. "Enhancement of electric arc furnace reactive power compensation using Grey–Markov prediction method." *IET generation, transmission & distribution* 8, no. 9 (2014): 1626-1636.

[67] Ebner, A. "Determination of acceptable closing time scatter and residual flux measurement uncertainty for controlled switching of transformers." In *Proceedings of the 16th international symposium on high voltage engineering*, pp. 1-6. 2009.

[68] Controlled switching 0f HVAC circuit breakers: guide for application lines, reactors, capacitors, transformers: Part-I. ELECTRA 183, Cigré Working Group A3.07; April 1999. p. 43–73.

[69] Controlled switching 0f HVAC circuit breakers: planning, specification and testing of controlled switching systems. ELECTRA 197. Cigré Working Group A3.07; August 2001. p. 22–33.

[70] Controlled switching of HVAC circuit breakers: guide for application lines, reactors, capacitors, transformers: Part-II. ELECTRA 185. Cigré Working Group A3.07; August 1999. p. 37–57.

[71] *IEEE Guide for the Selection of Monitoring for Circuit Breakers*, IEEE Std. C37.10.1, Dec. 2000.

[72] S. Ma, J. Wang, “An Approach for Intelligent Detection and Fault Diagnosis of Vacuum Circuit Breakers,” *IEEE Trans. on Dielectrics and Electr. Insulation*, vol. 9, no. 2, pp. 226–229, Apr. 2002.

[73] H. K. Høidalen, M. Runde, “Continuous Monitoring of Circuit Breakers Using Vibration Analysis,” *IEEE Transactions on Power Delivery*, Vol.20, No. 4, pp. 2458–2465, Oct. 2005.

[74] M. Rong, X. Wang, W. Yang, S. Jia, “Mechanical Condition Recognition of Medium-Voltage Vacuum Circuit Breaker Based on Mechanism Dynamic Features Simulation and ANN,” *IEEE Transactions on Power Delivery*, Vol. 20, No. 3, pp. 1904–1909, Jul. 2005.

[75] B. Stephen, S. M. Strachan, S. D. J. McArthur, J. R. McDonald K. Hamilton, “Design of trip current monitoring system for circuit breaker condition assessment,” *IET Gener. Transm. Distrib.*, Vol. 1, No. 1, pp. 89–95, Jan. 2007.

[76] S. M. Strachan, S. D. J. McArthur, B. Stephen, J. R. McDonald, A. Campbell, “Providing Decision Support for the Condition-Based Maintenance of Circuit Breakers

Through Data Mining of Trip Coil Current Signatures," *IEEE Transactions on Power Delivery*, Vol. 22, No. 1, pp. 178–186, Jan. 2007.

[77] A. A. Razi-Kazemi, M. Vakilian, K. Niayesh, M. Lehtonen, "Circuit-Breaker Automated Failure Tracking Based on Coil Current Signature," *IEEE Trans. on Power Delivery*, Vol. 29, No. 1, pp. 283–290, Feb. 2014.

[78] S. Kam, S. Nielsen, G. Ledwich, "A Systematic Review of a Statistical Vacuum Circuit Breaker Model for Condition Monitoring," *IEEE Trans. on Dielect. and Electr. Insulation*, Vol. 20, No. 2, pp. 620–627, Apr. 2013.

[79] P. Lin, J. Gu, M. Yang, "Intelligent maintenance model for condition assessment of circuit breakers using fuzzy set theory and evidential reasoning," *IET Gener. Transm. Distrib.*, Vol. 8, No. 7, pp. 1244–1253, Jul. 2014.

[80] S. S. Biswas, A. K. Srivastava, D. Whitehead, "A Real-Time Data-Driven Algorithm for Health Diagnosis and Prognosis of a Circuit Breaker Trip Assembly," *IEEE Transactions on Industrial Electronics*, Vol. 62, No. 6, pp. 3822–3831, Jun. 2015.

[81] J. Tang, S. Lu, J. Xie, Z. Chengb, "Contact Force Monitoring and Its Application in Vacuum Circuit Breakers," *IEEE Transactions on Power Delivery*, Vol. PP, No. 99, pp. 1–1, Apr. 2015.

[82] A. A. Razi-Kazemi, M. Vakilian, K. Niayesh, M. Lehtonen, "Data Mining of Online Diagnosed Waveforms for Probabilistic Condition Assessment of SF6 Circuit Breakers," *IEEE Transactions on Power Delivery*, Vol. 30, No. 3, pp. 1354–1362, Jun. 2015.

[83] A. A. Razi-Kazemi, "Circuit breaker condition assessment through a fuzzy-probabilistic analysis of actuating coil's current," *IET Gener. Transm. Distrib.*, Vol. 10, No. 1, pp. 48–56, Jan. 2016.

[84] Feizifar, Behnam, and Omer Usta. "Condition monitoring of circuit breakers using arc models and failure detection algorithm." In *Smart Grid and Cities Congress and Fair (ICSG), 2017 5th International Istanbul*, pp. 32-36. IEEE, 2017.

[85] Takayoshi, S., W. Kokuyama, and Hiroshi Fukuyama. "The boiling suppression of liquid nitrogen." Cryogenics 49, no. 5 (2009): 221-223.

[86] http://www.cansuperconductors.com/uploads/2/1/2/9/21298520/csl_datasheetv2.pdf (accessed on October'2017)

[87] Ph. Robin-Jouan, N. Kairouani, ''Numerical and Experimental Analysis of the Propagation of Hot Arc Plasma in High Voltage Circuit-breakers'', Proc. Conf. Gas Discharges and Their Applications, Liverpool, UK, Vol. 1, pp. 103106, 2002.

[88] Majka, Michal, Janusz Kozak, and Slawomir Kozak. "HTS Tapes Selection for Superconducting Current Limiters." *IEEE Transactions on Applied Superconductivity* 27, no. 4 (2017): 1-5

[89] Maruyama, Osamu, Tetsutaro Nakano, Tomoo Mimura, Toshiya Morimura, Takato Masuda, Tomohiro Takagi, and Masashi Yagi. "Fundamental Study of Ground Fault Accident in HTS Cable." *IEEE Transactions on Applied Superconductivity* 27, no. 4 (2017): 1-5.

[90] Lee, Seung Ryul, Jong-Joo Lee, Jaeyoung Yoon, Yoen-Woog Kang, and Jin Hur. "Protection Scheme of a 154-kV SFCL Test Transmission Line at the KEPCO Power Testing Center." *IEEE Transactions on Applied Superconductivity* 27, no. 4 (2017): 1-5.

[91] Takagi, Tomohiro, Masashi Yagi, Shinichi Mukoyama, Kazuo Watanabe, Tomoo Mimura, Osamu Maruyama, and Tetsutaro Nakano. "Basic Study on Ground Fault Characteristics of 275-kV HTS Cable." *IEEE Transactions on Applied Superconductivity* 27, no. 4 (2017): 1-5.

[92] Rebizant, W., K. Solak, B. Brusilowicz, G. Benysek, A. Kempski, and J. Rusiński. "Coordination of overcurrent protection relays in networks with superconducting fault current limiters." *International Journal of Electrical Power & Energy Systems* 95 (2018): 307-314.

[93] Cheng, K. H., H. K. Chiou, T. H. Chiu, C. H. Cheng, C. F. Shih, and T. W. Huang. "The new FCL with HTS for the high-speed communication system." *Microwave and Optical Technology Letters* 59, no. 4 (2017): 964-966.

[94] Ohtaka, Toshiya, Viktor Kertész, and René PP Smeets. "Novel Black-Box Arc Model Validated by High-Voltage Circuit Breaker Testing." *IEEE Transactions on Power Delivery*(2017).

[95] Mürmann, Mario, Alexander Chusov, Roman Fuchs, Alexander Nefedov, and Henrik Nordborg. "Modeling and simulation of the current quenching behavior of a line lightning protection device." *Journal of Physics D: Applied Physics* 50, no. 10 (2017): 105203.

[96] Ash, A. D., A. J. T. Holmes, S. Zheng, S. McIntosh, K. Cave-Ayland, F. Domptail, E. Surrey, N. Taylor, K. Hamada, and N. Mitchell. "Free or confined arc model relevant to the quench hazard of large superconducting coils." *Fusion Engineering and Design* (2017).

[97] Khakpour, Alireza, Steffen Franke, Sergey Gortschakow, Dirk Uhrlandt, Ralf Methling, and Klaus-Dieter Weltmann. "An improved arc model based on the arc diameter." *IEEE Transactions on Power Delivery* 31, no. 3 (2016): 1335-1341.

[98] Andrea, Jonathan, Marc Bournat, Romaric Landfried, Philippe Testé, Serge Weber, and Patrick Schweitzer. "Model of an Electric Arc for Circuit Analysis." In *28th International Conference on Electric Contacts ICEC 2016*, pp. 361-366. 2016.

[99] Wang, Ju-feng, Ping Huang, Wei Guo, Dong Wu, and Qi-liang Liu. "Research and application of a new jet stream arc extinguishing gap lightning protection device." *Electric Power Systems Research* 139 (2016): 161-169.

[100] Mürmann, Mario, Alexander Chusov, Roman Fuchs, Alexander Nefedov, and Henrik Nordborg. "Modeling and simulation of the current quenching behavior of a line lightning protection device." *Journal of Physics D: Applied Physics* 50, no. 10 (2017): 105203.

[101] Vidales, B., S. Weber, R. Schweitzer, D. Torres, and M. Madrigal. "Smart inverter arc fault protection for photovoltaic power systems." In *Environment and Electrical Engineering and 2017 IEEE Industrial and Commercial Power Systems Europe (EEEIC/I&CPS Europe), 2017 IEEE International Conference on*, pp. 1-6. IEEE, 2017.

[102] Hyo-Sang, C.H.O.I., Park, S.Y., Jeong, I.S., Choi, H.W., Kim, J.B., Lee, Y.K., Park, N.A. and Hwang, S.H., Chosun National University. Industry-Academic Cooperation Foundation (IACF), 2017. *Superconducting dc circuit breaker using arcing induction*. U.S. Patent 20170316894A1

[103] Mokhberdoran, Ataollah, Adriano Carvalho, Nuno Silva, Helder Leite, and Antonio Carrapatoso. "Application study of superconducting fault current limiters in meshed hvdc grids protected by fast protection relays." *Electric Power Systems Research* 143 (2017): 292-302.

[104] Xiang, Bin, Licai Zhang, Kun Yang, Yaxiong Tan, Zhiyuan Liu, Yingsan Geng, Jianhua Wang, and S. Yanabu. "Arcing Time of a DC Circuit Breaker Based on a Superconducting Current-Limiting Technology." *IEEE Transactions on Applied Superconductivity* 26, no. 7 (2016): 1-5.

[105] Xiang, Bin, Zhiyuan Liu, Chuanchuan Wang, Zhenle Nan, Yingsan Geng, Jianhua Wang, and Satoru Yanabu. "DC Interrupting with Self-excited Oscillation Based on Superconducting Current-Limiting Technology." *IEEE Transactions on Power Delivery* (2017).

[106] Xiang, Bin, Yaxiong Tan, Kun Yang, Zhiyuan Liu, Yingsan Geng, Jianhua Wang, and S. Yanabu. "Quenched Resistance Effects on a Superconducting Current-Limiting-Type DC Breaker." *IEEE Transactions on Applied Superconductivity* 26, no. 7 (2016): 1-5.

[107] Lee, Hee-Jin, and Seung-Mook Baek. "The Effect of HTS Quench Resistance on DC Transmission System." (2016)